الجمهورية الجزائرية الديمقراطية الشعبية
People's Democratic Republic of Algeria
وزارة التعليم العالي و البحث العلمي
Ministry of Higher Education and Scientific Research

معهد المناجم
University of Larbi Tebessi, Tebessa



جامعة العربي التبسي, تبسة
Institute of Mines

Laboratory of Environment

Order N°: 0441/2021
Defense authorization N°: 079/2025

DOCTORAL THESIS

3rd Cycle Doctoral (D-LMD)

Presented by:

Beddi Abdelraouf

Branch: Electromechanical

Specialty: Electromechanical

Topic

Contribution to the control of a photovoltaic conversion system

Supported, on 24/04/2025, before the jury composed of:

Louafi Messaoud	Professor	University of Larbi Tebessi, Tebessa	President
Hebbir Nacer	Professor	University of Larbi BenM'hidi, Oum El Bouaghi	Supervisor
Serhoud Hicham	Professor	University of Hamma Lakhder El-Oued	Co- Supervisor
Aoulmi Zoubir	MCA	University of Larbi Tebessi, Tebessa	Examiner
Touil Sliman	MCA	University of Hamma Lakhder El-Oued	Examiner

Dedication

To my beloved parents, whose unwavering love and guidance have shaped me into the person I am today.

To my wife, cherished children whose bond and support me have been a source of joy throughout my life.

To my cherished brothers and sisters, whose bond and support have been a source of strength and joy throughout my life.

Moreover, to all those who hold a special place in my heart, your presence and care have enriched my life beyond measure.

Acknowledgements

In the Name of Allah, the Most Compassionate, the Most Merciful,

I begin by expressing profound gratitude to Allah, the Almighty, the ultimate source of sustenance and guidance. With heartfelt appreciation, I acknowledge His unwavering support that enabled me to successfully complete this academic journey.

My sincere and wholehearted gratitude extends to my esteemed supervisor, Prof. Nacer HEBBIR and Dr. Hicham SERHOUD, whose invaluable guidance, meticulous insights, and constructive feedback have been instrumental throughout this endeavor.

I am equally indebted to the distinguished members of the committee, namely Prof Louafi Messaoud, Dr Zoubir Aoulmi, and Dr Touil Sliman for graciously agreeing to assess and evaluate this body of work.

A special acknowledgment is also extended to the dedicated team at the Laboratory of Environment, Echahid Cheikh Larbi Tebessi University. Their steadfast support and the enriching academic environment provided a solid foundation, enabling me to undertake and accomplish this research. Its realization.

Lastly, and of utmost significance, I offer profound gratitude to my small family "wife and children" and grand family “parents, and siblings". Their unwavering belief in me and their encouragement to relentlessly pursue ambition have been the driving force behind my determination to confront challenges head-on.

In conclusion, I am profoundly grateful to all those who have played a part in shaping this academic journey, and I acknowledge their contributions with humility and sincerity.

Abstract:

The aim of this work is to propose a successful contribution to Maximum Power Point Tracking (MPPT) strategies for photovoltaic (PV) Stand-Alone systems; the Conventional Incremental Conductance (CON-INC) algorithm is used as a basis. In order to overcome the disadvantages of the CON-INC method, which include oscillations, imperfect MPPT, and slow MPP tracking. These drawbacks are caused by using a classic INC algorithm with a fixed duty cycle disturbance step. It is not capable of providing the ideal duty cycle, especially when faced with changing weather conditions (temperature and irradiation). Our first proposal involved ensuring Sliding Mode Control's performance by comparing it with the CON-INC. In addition, the optimization of the CON-INC as a reference is divided into two approaches as follows, first a combination-based controller is Fuzzy Logic that is integrated into INC to treat and improve the signal of duty cycle of CON-INC. Secondly, using Particle Swarm Optimization PSO to regulate and compute its gains of PI that integrated into CON-INC. The proposed methods have a better efficiency compared to the CON-INC algorithm, as confirmed by simulation results in different scenarios.

Keywords : Photovoltaic, Boost converter DC-DC, MPPT, Incremental Conductance (INC), Particle Swarm Optimization (PSO), Sliding Mode Control (SMC), Fuzzy Logic (FL)

Résumé

L'objectif de ce travail est de proposer une contribution réussie aux stratégies de suivi du point de puissance maximale (MPPT) pour les systèmes photovoltaïques (PV) autonomes, l'algorithme de conductance incrémentale conventionnelle (CON-INC) étant utilisé comme base. Afin de surmonter les inconvénients de la méthode CON-INC, qui comprennent les oscillations, le MPPT imparfait et le suivi MPP lent. Ces inconvénients sont dus à l'utilisation d'un algorithme INC classique avec une étape de perturbation du cycle de service fixe. Il n'est pas capable de fournir le cycle de service idéal, en particulier lorsqu'il est confronté à des conditions météorologiques changeantes (température et irradiation). Notre première proposition consistait à assurer les performances du contrôle en mode coulissant en le comparant avec le CON-INC. De plus, l'optimisation du CON-INC en tant que référence est divisée en deux approches comme suit, tout d'abord un contrôleur basé sur la combinaison est Logique Floue qui est intégré à l'INC pour traiter et améliorer le signal de cycle de service de CON-INC. Deuxièmement, l'utilisation d'optimisation des essaims de particules (PSO) pour réguler et calculer ses gains de PI qui s'est intégré dans CON-INC. Les méthodes proposées ont une meilleure efficacité par rapport à l'algorithme CON-INC, comme le confirment les résultats de simulation dans différents scénarios.

Mots-clés : Photovoltaïque, Convertisseur Boost DC-DC, MPPT, Conductance Incrémentale (INC), Optimisation des Essaims de Particules (PSO), Mode Glissant (SMC), Logique Floue (FL)

ملخص:

نجحت استراتيجيات تتبع نقطة الطاقة القصوى (MPPT) يهدف هذا العمل إلى تقديم مساهمة النظام الكهروضوئي المستقل (PV)، مع استخدام خوارزمية التوصيل المتزايد التقليدية (CON-INC)كأساس . من أجل التغلب على عيوب طريقة CON-INC، والتي تشمل التذبذبات، MPPTغير الكامل وتتبع MPPالبطيء .خوارزمية INC الكلاسيكية غير قادر على توفير دورة العمل المثالية ، خاصة عند مواجهة الظروف الجوية المتغيرة درجة الحرارة والإشعاع ترجع هذه العيوب إلى إستخدام مع خطوة إضطراب دورة التشغيل الثابتة. كان اقتراحنا الأول هو ضمان أداء التحكم في الوضع المنزلق من خلال مقارنته مع .CON-INCعلاوة على ذلك، ينقسم تحسين CON-INCكمعيار إلى طريقتين على النحو التالي، أولاً، وحدة التحكم القائمة على المجموعة هي Fuzzy Logicوالتي تم دمجها مع INCلمعالجة وتحسين إشارة دورة .CON-INCثانيًا، استخدام Particle Swarm Optimization (PSO) لتنظيم وحساب مكاسب PIالخاصة بها والتي تم دمجها في .CON-INCتتمتع الطرق المقترحة بكفاءة أفضل مقارنة بخوارزمية CON-INC، كما تؤكد نتائج المحاكاة في سيناريوهات مختلفة.

الكلمات المفتاحية:

الخلايا الكهروضوئية ، محول تعزيز DC-DC ، MPPT، التوصيل التدريجي (INC) ، تحسين أسراب الجسيمات (PSO) ، الوضع المنزلق (SMC) ، المنطق الضبابي(FL)

Table of Contents

List of figures

List of tables

List of abbreviations and symbols

General Introduction

I Overview of Photovoltaic Conversion 4

I.1 Introduction 5

I.2 Electricity production in the world 5

I.3 Electricity production in Algeria 7

I.4 The Solar Potential in Algeria 7

I.5 Principle of photovoltaic conversion: 8

I.6 Photovoltaic generator 10

I.6.1 Photovoltaic cell: 10

I.6.2 Modeling of a photovoltaic cell 13

I.6.3 The one-diode model 13

I.6.4 The two-diode model 15

I.7 Constitution of a photovoltaic generator (GPV) 17

I.7.1 Photovoltaic Cell Connection 17

I.7.2 Protection of a photovoltaic generator 18

I.8 Applications of photovoltaic systems 19

I.8.1 Stand-alone application 19

I.8.2 Photovoltaic connect to the grid 20

I.8.3 Hybrid system 21

I.9 Current-Voltage (I-V) characteristic at variable irradiation and temperature 21

I.9.1 Influence of temperature: 21

I.9.2 Influence of irradiation 22

I.10 Power-Voltage (I-V) characteristic at variable irradiation and temperature 22

I.11 Advantages of photovoltaic energy 23

I.12 Disadvantages of photovoltaic energy 24
I.13 Conclusion 24
II Electrical Conversion of Photovoltaic 25
System 25
II.1 Introduction 26
II.2 Architecture of different photovoltaic conversion chains 26
II.2.1 Generator photovoltaic-load connection 26
II.2.2 Generator photovoltaic-Grid connection 28
II.2.3 Generator photovoltaic connected to multi-sources 30
II.3 DC-DC convertor 31
II.3.1 Boost converter 32
II.3.2 Buck convertor 35
II.3.3 Buck-Boost convertor 38
II.4 DC–AC Inverter 39
II.4.1 DC-AC Single Phase 40
II.4.2 DC-AC Three-Phase 41
II.4.3 Inverter off-grid 42
II.4.4 Inverter on-grid 43
II.5 Control of the electrical conversion chain of a PV system 44
II.5.1 Control the DC/DC converter 44
II.6 Conclusion 46
III Techniques MPPT for DC/DC Stand- 48
Alone photovoltaic system 48
III.1 Introduction 49
III.2 The research principal of MPPT 50
III.2.1 Local MPP (LMPP) 50
III.2.2 Global MPP (GMPP) 51
III.3 Challenges facing MPPT techniques 51
III.4 MPPT techniques 53
III.4.1 Classic Methods 54
III.4.2 Modern Methods “Artificial Intelligence” 61

III.5 MPPT based on Sliding Mode Control (SMC) for Stand-Alone System (SAS) "proposed method" 65

III.5.1 SMC MPPT technique 67

III.5.2 Simulation Results and Discussion 69

III.6 CONCLUSION 76

IV Optimization of Incremental 77

Conductance for MPPT of a Photovoltaic Stand-Alone System 77

IV.1 INTRODUCTION 78

IV.2 PV optimization Technique 78

IV.3 Optimization of Incremental Conductance Using Particle Swarm Optimization-Tuned PID Controller for MPPT of a Photovoltaic Stand-Alone System 80

IV.3.1 Particle Swarm Optimization (PSO) algorithm 80

IV.3.2 PSO-Based Tuning of PI Controller 81

IV.3.3 Results and Discussion 84

IV.4 Optimization of Incremental Conductance by combination to Fuzzy Logic Control for MPPT of a Photovoltaic Stand-Alone System 88

IV.4.1 Fuzzification 88

IV.4.2 Rule base 89

IV.4.3 Defuzzification 89

IV.4.4 INC-FLC Controller 90

IV.4.5 Result and Discussion 91

IV.5 Conclusion 95

V General conclusion 96

List of Abbreviations

PV	Photovoltaic
GPV	Generator Photovoltaic
MPPT	Maximum Power Point Tracking
MPP	Maximum Power Point
LMPP	Local Maximum Power Point
GMPP	Global Maximum Power Point
PS	Partial Shading
CON	Conventional
PSC	Partial Shading Condition
P&O	Perturbation and Observation
INC	Incremental Conductance
HC	Hill Clamping
PSO	Particle Swarm Optimization
FLC	Fuzzy Logic Control
SMC	Sliding Mode Control
CSP	Concentrated Solar Power
IEA	International Energy Agency
AM	Air Mass
ASTM	The American Society for Testing and Materials
P-N	Positive-Negative
GaAs	Gallium Arsenide
Ge	Germanium
GaInP2	Indium Gallium Phosphide
CIGS	Copper Indium Gallium Selenide
OC	Open Circuit
SC	Short Circuit
T	Temperature
I	Irradiation
MOSFETS	Metal Oxide Field Effect Transistors

IGBTS	Insulated Gate Bipolar Transistors switches
DC	Direct Current
AC	Alternative Current
S	Switch
D	Diode
PWM	Pulse Width Modulation
THD	Total Harmonic Distortion
ZSI	Z-Source Inverter
FOCV	Fraction Open Circuit Voltage
FOSC	Fraction Open Short-Circuit
ARV	Adaptive Reference Voltage
CV	Constant Voltage
RV	Reference Voltage
PI	Proportional Integral
PID	Proportional Integral Derivative
CSP	Canadian solar module
LTC	Linear Technology Corp
DG	Duralast Gold
NSL	Nature Smart Libraries
SSV	Structure Systems Variable
AI	Artificial Intelligence
Eq	Equation
ITAE	Integral of Time weighted Absolute Error
IAE	Integral of the Absolute Error
ISE	Integral of Square Error
ITSE	Integral Time Square Error
f	The switching frequency of the boost converter
Iout	The output current of the boost converter.
Vout	The ripple output voltage.

List of Figures

Figure I. 1 Consumption the different energy in World by using Data based on BP Statistical Review of World Energy (2022) [9] 6
Figure I. 2 Renewable energy net capacity additions 7
Figure I. 3 Standards for measuring the spectrum of solar energy emitted by the sun, nation of the AM convention 8
Figure I. 4 Solar spectra recorded under several conditions according to the AM convention (source NREL solar spectrum) [18]. 9
Figure I. 5 Structure of a photovoltaic cell. 11
Figure I. 6 I (V) characteristic of a photovoltaic cell 13
Figure I. 7 Electrical model equivalent to a photovoltaic cell one-diode. 14
Figure I. 8 Simplified equivalent electrical model of the photovoltaic cell 14
Figure I. 9 Electrical model equivalent to two diodes of the photovoltaic cell 15
Figure I. 10 Characteristic results of parallel cells group 17
Figure I. 11 Characteristic results of series cells group 18
Figure I. 12 Protect the photovoltaic cell by the bypass and anti-reverse diode 19
Figure I. 13 Autonomous system of photovoltaic 19
Figure I. 14 Grid connected system of photovoltaic 20
Figure I. 15 Hybrid system of photovoltaic 21
Figure I. 16 The Voltage-Current characteristic with different temperatures 22
Figure I. 17 The Current-Voltage characteristic with different irradiations 22
Figure I. 18 The Voltage-Power characteristic with different temperatures 23
Figure I. 19 The Voltage-Power characteristic with different irradiation 23

Figure II. 1 PV systems direct connect to the load 27
Figure II. 2 Structure of PV system connect to the load DC through DC-DC convertor with an algorithm of control 28
Figure II. 3 Structure of PV system connect to the load AC through DC-AC inverter with a controller . 28
Figure II. 4 Structure of PV system connect to the grid 29
Figure II. 5 Structure of PV system connect to the grid by two stage 30
Figure II. 6 Structure of PV system connected to multi-sources 31
Figure II. 7 Basic schematic of DC-DC BOOST Converter 32
Figure II. 8 Schematic of DC-DC BOOST Converter (S closed) 33
Figure II. 9 Schematic of DC-DC BOOST Converter (S open) 34
Figure II. 10 The format of the current and voltage during the switching in boost converter 35
Figure II. 11 Basic schematic of DC-DC Buck Converter 36
Figure II. 12 Schematic of DC-DC Buck Converter (S closed) 37
Figure II. 13 Schematic of DC-DC Buck Converter (S open) 37
Figure II. 14 Basic schematic of DC-DC Buck-BOOST Converter 38
Figure II. 15 Schematic of DC-DC Buck-Boost Converter (S close) 38
Figure II. 16 Schematic of DC-DC Buck-Boost Converter (S open) 39
Figure II. 17 *DC-AC Single Phase* Inverter **Figure II. 18** Control Signals of Inverter 40

Figure II. 19 DC-AC Three-Phase inverter 41
Figure II. 20 Schematic of the topology off-grid inverter 43
Figure II. 21 Schematic of the topology on-grid inverter 44
Figure II. 22 Finding and recovering the Maximum Power Point, a) Variation in irradiation at the level of the GPV, b) Variation in consumption loads, and c) Temperature variation at the level of the GPV. 46

Figure III. 1 Appearing the different MPP types 50
Figure III. 2 Challenges facing MPPT techniques 52
Figure III. 3 Partial shading for PV modules. 53
Figure III. 4 MPPT Techniques 53
Figure III. 5 *P-V curve of the P&O algorithm* [50] 54
Figure III. 6 Flowchart of the Perturbation and Observation (P&O) method 55
Figure III. 7 Flowchart of the Incremental conductance 57
Figure III. 8 Function scheme of ARV-MPPT technique 58
Figure III. 9 Function scheme OVC Method 59
Figure III. 10 Function scheme of SCC method 60
Figure III. 11 Organogram of HC methods 61
Figure III. 12 Three layer feed-forward neural network 63
Figure III. 13 General principles of genetic algorithms 64
Figure III. 14 Flow Chart of the Hybrid Method 65
Figure III. 15 The basic structure photovoltaic system 66
Figure III. 16 The electrical diagram of the boost converter 68
Figure III. 17 The variation of irradiation 70
Figure III. 18 The variation of temperature 70
Figure III. 19 The Voltage-Power characteristic with different irradiation 70
Figure III. 20 The Current-Voltage characteristic with different irradiations 71
Figure III. 21 The Voltage-Current characteristic with different temperatures 71
Figure III. 22 The Voltage-Power characteristic with different temperatures 72
Figure III. 23 Output Current of PV KC200GT arrays 72
Figure III. 24 The output voltage of PV KC200GT arrays 73
Figure III. 25 Power of PV KC200GT arrays 73
Figure III. 26 Dynamic MPPT of PV KC200GT arrays 74
Figure III. 27 The duty cycle of PV arrays by sliding mode control 75
Figure III. 28 The duty cycle of PV by incremental conductance 75

Figure IV. 1 Optimization techniques are commonly used for the output PV system. 79
Figure IV. 2 The random movement of PSO model 81
Figure IV. 3 The process to implementing the PSO algorithm for tuning the PI 82
Figure IV. 4 PSO-Based Tuning of PI Controller 83
Figure IV. 5 Result of optimized sets of PI using different iterations 84
Figure IV. 6 Voltage of PV arrays by using the INC and PSO-INC 85
Figure IV. 7 Output current of PV 85
Figure IV. 8 The output current of the DC-DC converter 86
Figure IV. 9 Power of PV arrays by using the INC and PSO-INC 87

Figure IV. 10 Power of DC convertor by using the INC and PSO-INC 87
Figure IV. 11 Structure of Fuzzy Logic Control 88
Figure IV. 12 MEs for input variables 89
Figure IV. 13 MEs for output variable 90
Figure IV. 14 The proposed optimization of INC-FLC 90
Figure IV. 15 Flowchart to the proposed combination of INC-FLC 91
Figure IV. 16 Variation of temperature 92
Figure IV. 17 Variation of Irradiation 92
Figure IV. 18 Current of PV arrays by using the INC and INC-FLC 92
Figure IV. 19 Voltage of PV arrays by using the INC and INC-FLC 93
Figure IV. 20 Power of PV arrays by using the INC and INC-FLC 93
Figure IV. 21 Power of output DC convertor by using the INC and INC-FLC 94
Figure IV. 22 Voltage of output DC convertor by using the INC and INC-FLC 94
Figure IV. 23 Current of output DC convertor by using the INC and INC-FLC 95

List of tables

Table I. 1 Performances of the different silicon sectors 12

Table III. 1 KC200GT Data Sheet under STC Conditions and internal parameters 66

Table IV. 1 PSO parameters..... 83
Table IV. 2 Optimized sets of PI..... 84
Table IV. 3 FLC rule based..... 89

General Introduction

The means taken on by man in finding sources of energy have evolved with the self-development of man and it differed according to the different periods of development that it experienced, due to there being mutually interactions between the type of civilization and energy sources. Beforehand the industrial revolution, man depended on muscle strength, on animals, or on some natural resources such as the sun, wind and water-falls ....etc. to meet his daily needs, a person has used solar energy since ancient times to dry his clothes and to dry fruits to preserve them, too the wind energy was used and the energy of water-falls was used to grind grain, and other uses.

The Industrial Revolution in the World constituted a major convert point in the style of humans to use energy. It accompanied the industrial revolution increase on mechanical machines where it spread widely, thus the demand for the fuel needed to operate these machines increased.

Renewable energy sources have a significant amount of potential, and they have multiple advantages over conventional energy sources. Many sources, such as solar, wind, geothermal, biomass, and water, are employed to provide renewable energy. They have the capacity to generate huge amounts of electricity over extended periods without producing excessive levels of greenhouse gases. The sun's renewable energy can be used both directly and indirectly. Two different methods are involved in the direct use of solar energy, the first is the solar thermal energy, which burns calories, and the second is the photovoltaic energy, which generates electricity. Photovoltaic (PV) technology is one of the most promising renewable energy technologies. Stand-alone, grid-connected, off-grid and hybrid systems available are configurations [1].

Contributing to photovoltaic system optimization in partially shadowed settings is the aim of this effort. Despite efforts to advance solar cell technology, the electrical efficiency is still not satisfied. Additionally, because it has a significant impact on how much energy a photovoltaic system produces, the partial shadowing (PS) problem has garnered a lot of attention. Statistics in the literature show that, depending on the degree and kind of shading pattern, the power loss caused by the (PS) might range from 10 to 70 % of the system yield. Although the PS phenomenon is a well-defined problem in and of itself, there are many different ways to mitigate it, each with a different level of complexity, performance, and cost trade-off. Researchers typically focus on ways to maximize energy generation from the PV system when the

phenomenon does not occur as, in the majority of circumstances, prediction nor prevention of the PS is possible. System architectures, converter topologies, PV array layouts, and maximum power point tracking (MPPT) methods are a few of these strategies. Despite the improvements that can be made using the first three methods, adding more material makes the system more complex and therefore more expensive. Therefore, the development of MPPT algorithms that can handle the partial shading can result in a good cost-efficiency compromise [2].

Conventional MPPT techniques work well in uniform settings, but when partial shade occurs, their effectiveness suffers. In fact, when the P-V characteristic is multimodal, these approaches such Perturb and Observe (P&O)This thesis' primary goal is to optimize, design and simulate global MPPT techniques based on PV systems under partial shading conditions by using meta-heuristics. To accomplish the research objective, a critical and strategic literature review of MPPT methods was first presented. In this review, several previous works on MPPT used for PV systems were discussed. Furthermore, PV systems are modeled and simulated in both uniform and partial shading scenarios. To accurately study PV systems on partial shading, a high-quality PV module model is necessary. Thus, on the basis of one diode KC200GT, a simple, fast and accurate PV system simulator was selected. Then, Particle Swarm Optimization (PSO) and algorithms-based maximum power point tracking (MPPT) controllers were chosen. and Incremental Conductance (INC) might become imprisoned in an LMPP because they lack the ability to discern between the two types of P-V patterns. There have been numerous global MPPT algorithms developed to address the partial shading problem. The techniques vary in terms of their complexity, the types and numbers of sensors they use, and the tools they use for implementation. The suggested strategy involves treating the tracking of maximum power point as an optimization issue and using meta-heuristics drawn from nature to determine the global maximum [3]. To deal with the multimodal P-V characteristic under shade situations, several academics have begun to focus more on meta-heuristic techniques. These algorithms are considered well suited for a problem of this nature due to their ability to handle multimodal objective function. We have mainly interested at the following meta-heuristics:

Particle Swarm Optimization "PSO" Algorithms, Fuzzy Logic Control "FLC", and the Sliding Mode Control "SMC" are highly efficient with few control parameters, have reliable performance and straightforward structures. For these reasons, this thesis proposes these meta-

heuristic algorithms to develop MPP trackers for PV systems that are exposed to in-uniform irradiance and temperature.

Several simulations for different shading patterns have been run in the Matlab/Simulink milieu to ensure the success of the proposed technique. The outcomes of simulations prove the accurateness of the suggested plan for conversation with the energy available at the photovoltaic panels' output. In addition, the proposed approach performs better in terms of dynamic performance and global search ability when compared to classic Incremental Conductance "INC" method. Their contents outlined as follows:

Chapter I giving an overview on the production of electricity in general and that of renewable in the world and in Algeria. In addition, provides an overview of solar photovoltaic systems including the PV array and modeling. Behavior of the PV systems under varying environmental conditions and partial shading is critically analyzed.

Chapter II provides an extensive review of different parts that make up the PV conversion chain and their modeling. Focusing on the modeling of Boost, Buck, and Boost-Buck converter. In addition, we provide a wide overview on the different topologies that's used in PV systems namely: PV connects to grid "mono-phases and three-phases", off-grid, and multiple sources.

In chapter III, we will present the different MPPT control systems for DC-DC converters. We concentrated on the common types like the P&O, INC, and HC...etc. Moreover, contributing to the improvement of energy conversion is a part of the thesis; when we confirmed in the last of this section, the reliability of proposed sliding mode control on the tracking MPP by comparison with INC appeared.

In the last chapter which contains the second part of the main contributions of this thesis. We will carry out a simulation of a stand-alone system combined from boost converter using two optimization methods. I will start by optimizing the incremental conductance by using the particle swarm optimization algorithm. And then, the incremental conductance will optimize using Fuzzy Logic Control on the next step.

Finally, we conclude this research with a general conclusion and perspectives.

I Overview of Photovoltaic Conversion

I.1 Introduction

Today, a wide part of the world's energy production is provided by fossil sources. The consumption of these sources results in greenhouse gas emissions and therefore an increase in pollution. The exploitation of renewable energies is an essential solution. Among these renewable energies, photovoltaic energy, which is the direct conversion of the energy sent to us by the sun into electricity. Indeed, among other advantages, it uses a renewable, abundant and well-distributed source of energy in the world. It is low cost, clean and environmentally friendly energy [4].

This chapter presents a general theory of renewable energies and mainly solar energy. This chapter's primary focus is on the photovoltaic effect and the operating techniques of the solar cells. We will then describe in the second part the operation of photovoltaic cells, their main characteristics, and the limits of the theoretical model. The chapter concludes with the main uses of photovoltaic systems and how they are operated in various patterns [5].

I.2 Electricity production in the world

Electric power is an indispensable factor for economic development all over the world. Indeed, technological progress in industrialization and in the comfort of modern life explains the increase in its importance [6].

The share of renewables in global electricity generation reached 28.7% in 2021, after modest growth of 0.4 percentage points [7].

The record rise in coal was not matched by global gas generation, which increased by only 1% in 2021. 62% of the world's electricity came from fossil fuels in 2021, up from 61% in 2020—the first year since 2012, that fossil fuel's share has risen [8].

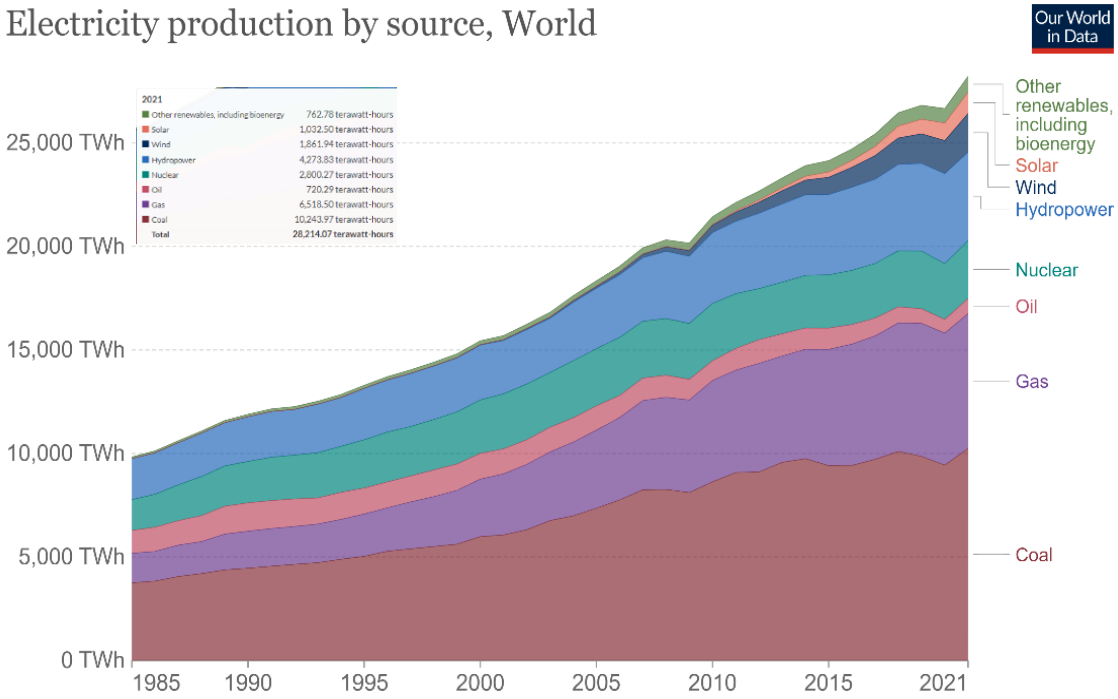


Figure I. 1 *Consumption the different energy in World by using Data based on BP Statistical Review of World Energy (2022)* [9]

In spite of the ongoing supply chain disruptions brought on by the pandemic, delays in building and record-high prices for raw materials and commodities, the amount of renewable capacity added in 2021 increased by 6% and broke another record, reaching nearly 295 GW. This growth is marginally higher than the IEA's estimate last year [10]. Globally, the growth in hydropower installation and solar PV offset the 17% fall in annual wind capacity additions in 2021. In comparison to 2020, the growth of concentrated solar power (CSP) remained steady in 2021. The year-over-year growth of renewable capacity last year was slower than it was in 2020, a year marked by an extraordinary surge as Chinese developers raced to connect projects ahead of the phase-out of subsidies [11].

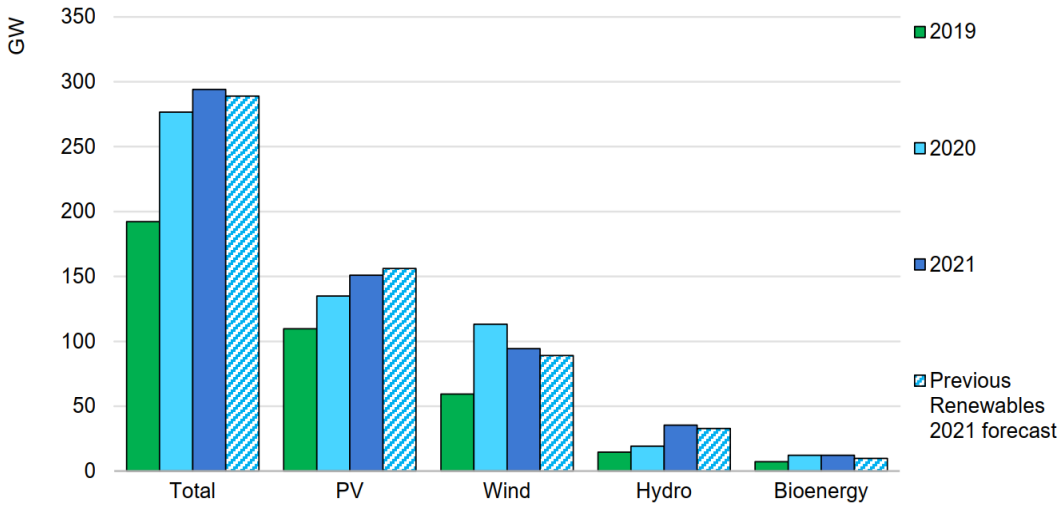


Figure I. 2 Renewable energy net capacity additions

I.3 Electricity production in Algeria

Algeria is set to reach electricity production capacity of 33,000MW by 2022 against the current 21,000MW. Thus, it has achieved multiplied electricity production four times from 6,000 MW in 1999 to 21,000 MW in 2019; In addition, they are committed to commission other projects to reach our 2022 target of 33,000 MW [12]. Moreover, they prepare for the implementation of the program that seeks to provide installation of 22,000 MW of renewable energy by 2030 [13].
Currently SONELGAZ group has generated 400 MW of solar and wind power that has been connected to the national grid. The government also called for tenders for construction of solar photovoltaic power plants with a capacity of 150 MW. In addition, the new plant will contribute to supply the SONATRACH facilities by producing 20 MW additional of electrical energy [14].

I.4 The Solar Potential in Algeria

Due to its geographical location, Algeria has one of the highest solar deposits in the world. With an average of more than 300 sunny days per year, where it exceeds 2000 hours annually and can reach 3900 hours (high plateau and Sahara), Algeria has the potential to become a major player in solar energy production. In most regions of the national, the energy received on a horizontal surface of 1 m^2 per day is approximately 5 KWh, or nearly 2263 KWh/m^2/year in the south and

1700 KWh/m^2/year in the north. In the desert of the Sahara, this potential can be an important factor for sustainable development if it is operated economically [12][15].

I.5 Principle of photovoltaic conversion:

Solar radiation is made up of photons with wavelengths ranging from ultraviolet to infrared. To characterize the solar spectrum in terms of emitted energy, we use the notion AM for "Air Mass". In space outside the Earth's AM0) [16], the energy transported by solar radiation over the distance of sun-earth is 1350W/m² figure I.3. When passing through the atmosphere, solar radiation undergoes a decrease and a modification of its spectrum due to the phenomena of absorption and diffusion in gases. Its value is around 1000 W/m² at ground level, at 90° inclination (AM1) [16].

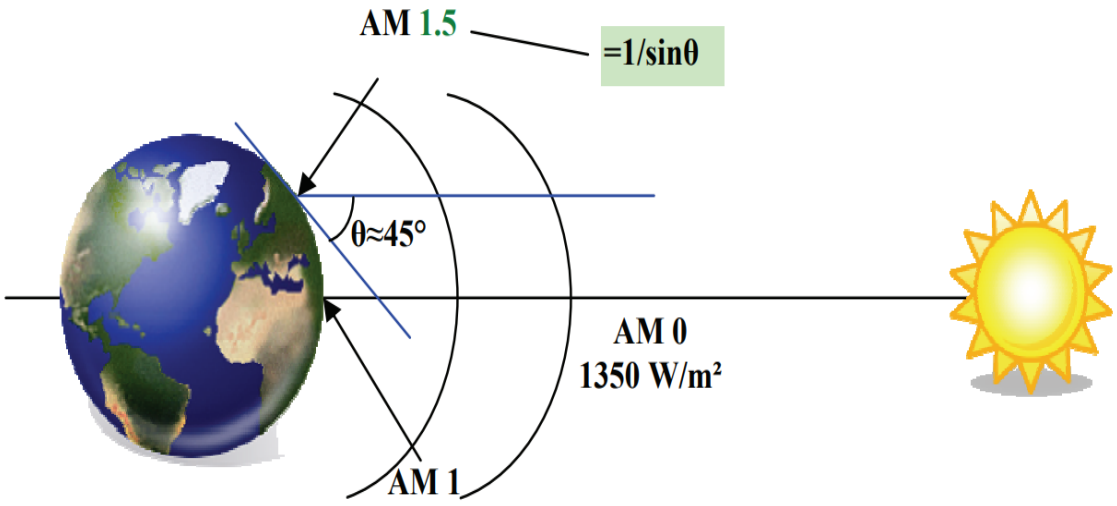


Figure I. 3 Standards for measuring the spectrum of solar energy emitted by the sun, nation of the AM convention

The significance of radiation received on the ground globally is determined by adding to the latter the diffuse radiation, which concerns the radiation whose trajectory between the sun and the observation point is not geometrically straight and which is scattered or reflected by the atmosphere or the ground. By considering this, we obtain a reference of the global spectrum noted AM 1.5 with a power of 1000W/m², figure I.4 corresponding to our latitudes [17].

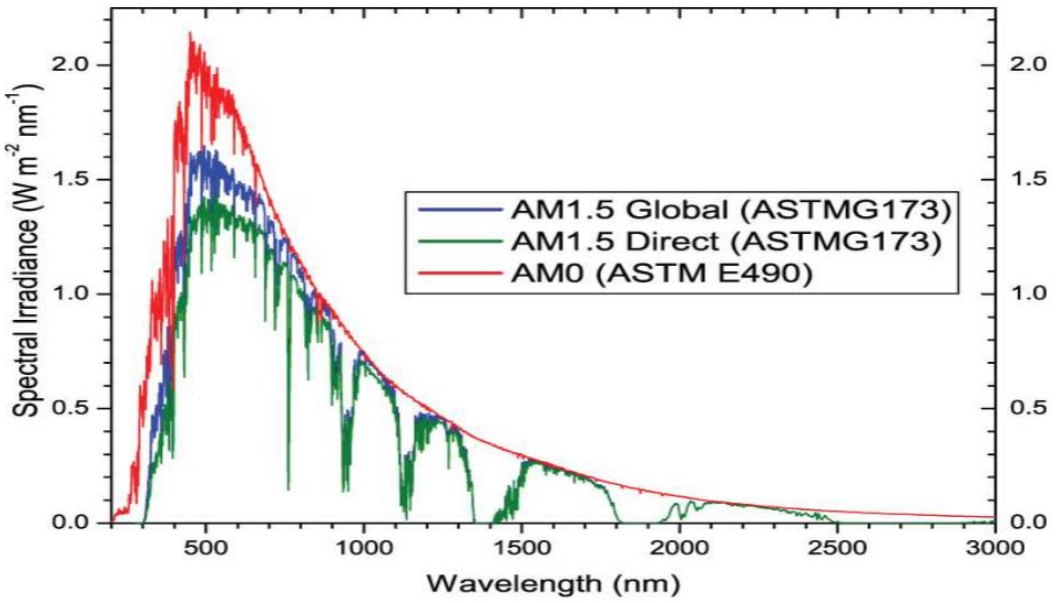


Figure I. 4 Solar spectra recorded under several conditions according to the AM convention (source NREL solar spectrum) [18].

Antoine Becquerel discovered the photovoltaic effect in 1839 in a battery consisting of electrodes of platinum and oxidized copper immersed in an acid electrolytic solution [19]. Additionally we call the photoelectric all the electrical phenomena caused by the action of light on cell that cause an ejection of electrons from the material:

– Photoelectric emission

– Photoconductivity

– The photovoltaic effect.

With the latter also associated, by the judicious choice of a suitable material, the appearance of electromotive forces, which allows a direct conversion of the energy of the radiation into electrical energy [16]. From a historical point of view, these different effects were discovered experimentally during the 19th century. However, it was not until 1905 that Albert Einstein resolved the difficulties posed by the interaction between light and cell[20], by introducing quanta of light to interpret the law of radiation proposed in 1900 by Max Planck [21]. Albert Einstein produced a theory that explained photoelectric phenomena by introducing the concept of photons [20], both particle and wave. In this theory, it demonstrated that the energy of a photon is entirely transferred to the photoelectric current is proportional to the number of photons and an electron of the material, therefore to the luminous flux. From the energy point of view, solar

electromagnetic radiation consists of photons of wavelength λ carrying an energy given by the relationship:

$$E = hv = hc/\lambda \quad \text{I. 1}$$

With:

E (day) energy

h (day.s) Planck's constant (6,62.10-34)

c (m.s-1) light speed (3.108)

λ (m) wavelength (often expressed on micrometer)

v (Hz) frequency

I.6 Photovoltaic generator

I.6.1 Photovoltaic cell:

A photovoltaic cell is a sensor made of a semiconductor material that transforms the absorbed light energy into electric current. The Principle of functioning based on the absorption properties of light radiation by semiconductor materials. The choice of materials used for the construction of PV cells is made depending on the physical properties of the electrons that are likely to release from their atoms when excited by photons from the solar spectrum [22]. Once released, the movement of these electrons in the material forms a direct-type electric current, which gives rise to an electromotive force at the terminals of the cell. This phenomenon physical called photovoltaic effect. Figure I.5 illustrates the composition of a cell silicon photovoltaic.

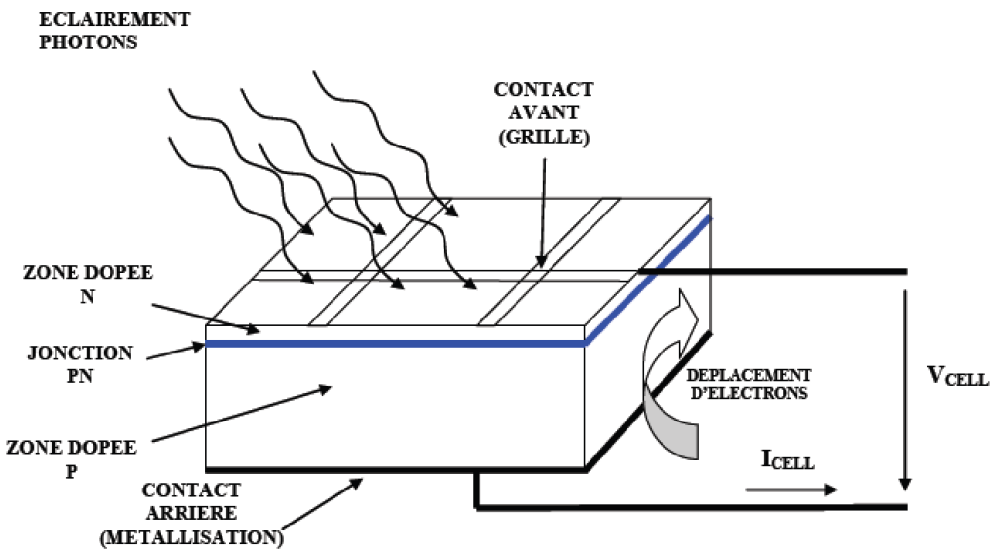


Figure I. 5 Structure of a photovoltaic cell.

As in the case of a conventional diode, a PV cell can be made from two layers of silicon, one positively doped and the other negatively doped. Between the two areas develops a P-N junction with a potential barrier [16].

Different types of photovoltaic cell manufacturing technologies exist on the market. In fact, photovoltaic cells based on crystalline silicon dominate the market with more than 90%. There are two categories of cells manufactured from crystallized silicon, those from mono-crystalline silicon and those from polycrystalline silicon. Mono-crystalline silicon is more expensive than polycrystalline silicon but of higher efficiency. Silicon is also used in the so-called amorphous technology, during its transformation; the silicon produces a gas, which will be projected on a sheet of glass. This type of cell has the advantage of being integrated on flexible or rigid supports; it is generally used for calculators and watches. Table I.1 shows the performance of the different silicon sectors currently on the market.

Table I. 1 Performances of the different silicon sectors

Technology	typical performance	Temperature influence	Degradation rate
Monocristallin	12 to 16 %	-0.442% per °C	-0.38% per year
Poly-crystalline	11 to 14 %	-0.416% per °C	-0.35% per year
Amorphe	6 to 7 %	-0.175% per °C	-1.15% per year

In the following, we cite some types of photovoltaic cells that can encountered, such as:

-The organic photovoltaic cell: Organic photovoltaic cells are cells in which at least the active layer is made up of organic particles. The yield of these cells is still less than 3% but their cost is low because of the low price of the raw material [23].

- The multi-junction photovoltaic cell: These cells consist of several thin layers combining semiconductor materials. For example, a triple junction cell consists of the semiconductors GaAs (gallium arsenide), Ge (germanium) and GaInP2 (indium gallium phosphide). The efficiency of multi-junction cells is very high, sometimes exceeding 40%. These cells have developed primarily for space applications because of their very high manufacturing cost [24].

- The CIGS photovoltaic cell: The technique consists of depositing a semiconductor material based on copper, indium, gallium and selenium on a support. This news high-performance techniques use rare metals such as indium whose global production is low, which makes the manufacturing cost high [25].

When the photons are absorbed by the cell, they transmit their energy to the atoms of the P-N junction so that the electrons of these atoms are freed and create pairs of electron holes. The maximum current occurs when the cell terminals are short-circuited, this current is named current of short-circuit (I_{SC}) highly dependent on the level of radiance (E). This then creates a potential difference (0.6 to 0.8 Volts) between the two layers that can be measured between the positive and negative terminals of the cell, called open circuit voltage (V_{OC}) strongly dependent on temperature. Through a continuous charge, carriers can also be harvested. The maximum cell voltage is about 0.6 V for zero current. Figure I.12 illustrates the nonlinear characteristic I (V) of

a silicon-based PV cell for a given irradiance and temperature, with the presence of a maximum power point (PPM) characterized by its voltage and current optimal (V_{OPT} and I_{OPT}) [26].

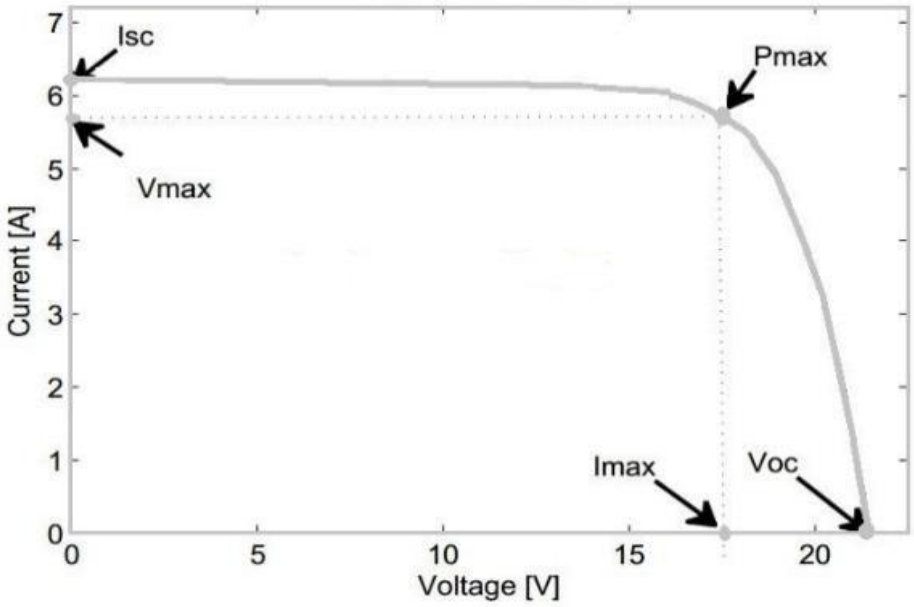


Figure I. 6 I (V) characteristic of a photovoltaic cell

I.6.2 Modeling of a photovoltaic cell

To develop an equivalent model of a PV cell, it is necessary to make a judicious choice of the electrical circuits, which constitute it and to understand the electrical characteristics and the physical configuration of the components of the cell. For that, numerous mathematical models developed to represent the nonlinear behavior of semiconductor junctions. In the following, we present two models of a photovoltaic cell, namely the two-diode model and the one-diode model [27].

I.6.3 The one-diode model

The "standard" model with one diode represents the photovoltaic cell. This model has one less diode compared to the two-diode model as shown the figure I.7.

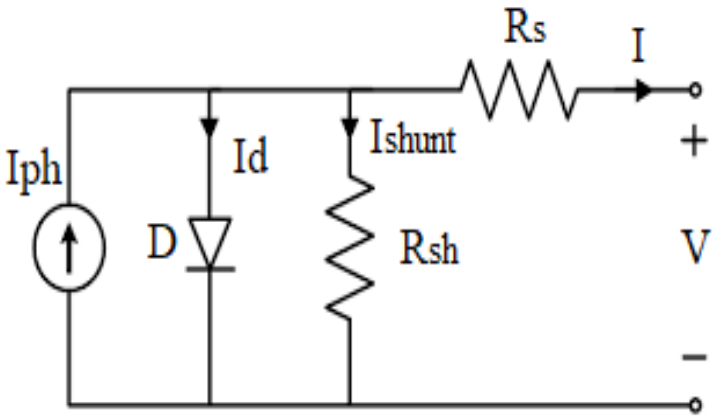


Figure I. 7 Electrical model equivalent to a photovoltaic cell one-diode**.**

The expression of current I given as:

$$I = I_{cc} - I_0 \left[e^{q\left(\frac{V+I*R_S}{nkT}\right)} - 1 \right] - \frac{V+I*R_S}{R_{sh}} \qquad I.\ 2$$

The parallel resistance R_{sh} is very large compared to the series resistance R_s. Thus, its effect is neglected, so this module is widely used, and becomes easier to study. Figure I.8 illustrates this simplified model of cell photovoltaic.

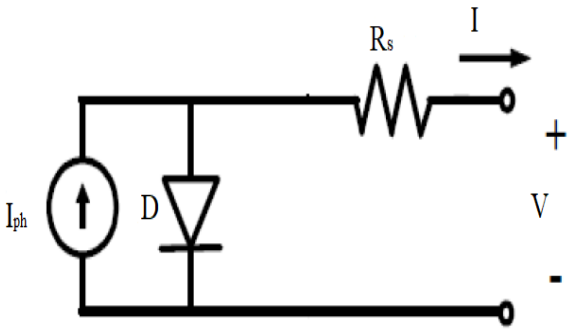


Figure I. 8 Simplified equivalent electrical model of the photovoltaic cell

Equation given as follow:

$$I = I_{cc} - I_0 \left[e^{q\left(\frac{V+I*R_S}{nkT}\right)} - 1 \right] \qquad I.\ 3$$

I.6.4 The two-diode model

Figure I.9 represents the equivalent circuit of a solar cell, realized by the parallel connection of two diodes with saturation currents I_{01} and I_{02} and diode factors n_1 and n_2, a current source producing the short-circuit current of the cell which depends on the solar radiance. The series resistance R_s takes into account the resistivity of the material and the semiconductor-metal contact. Its value can be determined by the inverse of the slope of the characteristic I (V) for the open circuit voltage V_{co}[28]. The parallel resistance R_p translates the leakage current in the junction.

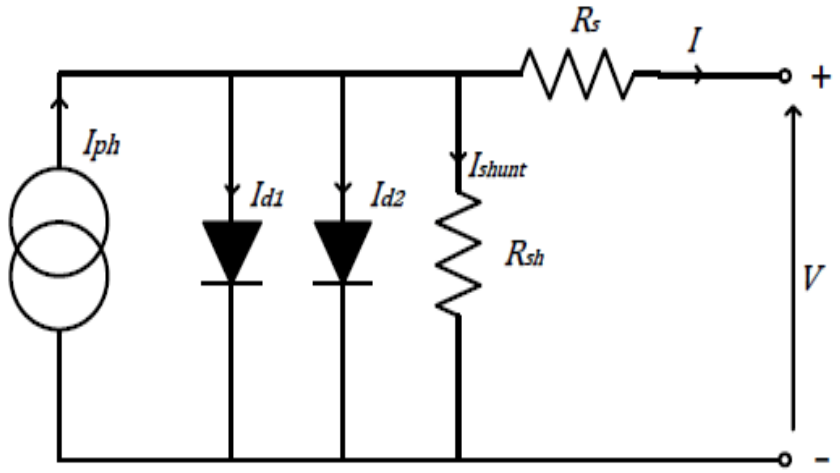


Figure I. 9 Electrical model equivalent to two diodes of the photovoltaic cell

The current I delivered by the cell is given by the following expression [27]:

$$I = I_{cc} - I_{d1}\left[e^{q\left(\frac{V+I*R_S}{n_1 kT}\right)} - 1\right] - I_{d2}\left[e^{q\left(\frac{V+I*R_S}{n_2 kT}\right)} - 1\right] - \frac{V+I*R_S}{R_{sh}} \qquad I.4$$

With:

I_{CC} (A), the short-circuit current of the cell depending on the sunshine and the temperature.

I_{d1} (A) corresponds to the saturation current of diode1.

I_{d2} (A) corresponds to the saturation current of diode2.

K (1.381×10-23 J/K), the Boltzmann constant.

T (K), the effective temperature of the cell.

q (1.602×10-19 C), the charge of the electron.

n_1, the non-ideality factor of the junction of diode 1.

n_2, the non-ideality factor of the junction of diode 2.

I (A), the current supplied by the cell.

V (V), the voltage across the cell.

R_{sh} (Ω), the shunt resistance characterizing the junction leakage currents.

R_S (Ω), the series resistance representing the various resistances of the contacts and connections.

First should be calculating the current of short-circuit I_{sc} with a temperature T of cell:

$$I_{sc} = I_{sc(Tref)} \cdot \left[1 + a\left(T - T_{ref}\right)\right] \qquad I.\ 5$$

Moreover:

$I_{sc\ (Tref)}$ Current of short-circuit in temperature reference T_{ref}, given by manufacturer's data sheet (measured under 1 KW/m^2 sunlight).

T_{ref} reference temperature of the cell on Kelvin unit ($K^{o)}$, generally is 298 K° & 25 C°.

A is the coefficient of temperature in I_{sc} en (%/C^{o}) given by the manufacturer's data sheet.

The short-circuit current I_{sc} is proportional to the intensity of the sunshine, its vale for a given sunshine (E) will therefore be:

$$I_{cc(E)} = \left(\frac{E}{E_0}\right) I_{cc(E_0)} \qquad I.\ 6$$

Where: E_0 is the nominal value of the sunshine, generally 1 KW/m^2.

The reverse saturation current (I_0) of the diode at the reference temperature (T_{ref}) is given by:

$$I_0 = \frac{I_{cc}}{\left(e^{\left(\frac{q.V_{oc}}{nkT-1}\right)}\right)} \qquad I.\ 7$$

The equation of the resistance R_s for the open circuit voltage is:

$$R_s = -\frac{dV}{dI_{(Voc)}} - \frac{\frac{nkT}{q}}{I_0.e^{\frac{qV_{oc}}{nkT}}} \qquad I.\ 8$$

I.7 Constitution of a photovoltaic generator (GPV)

Under standard weather conditions (1000W/m^2, 25°C, AM 1.5), the maximum power delivered by a 150 cm^2 silicon cell is approximately 2.3 W under a voltage of 0.5 V. This low power is insufficient for most domestic or industrial applications. The photovoltaic generator is made up of a series/ parallel connection of numerous photovoltaic modules, grouped together in photovoltaic panels made up of identical modules. When the cells are assembled in series, the voltage increases, whereas if they are connected in parallel, the current will increase. These cells must have the same characteristics [22].

I.7.1 Photovoltaic Cell Connection

In the case of an array of n_p cells in parallel connection, the cells rest to the same voltage but the current is increased. Figure I.10 illustrates the results of characteristic whit [29]:

$$I_{cc}n_p = n_p * I_{cc} \ \ and \ \ V_{co}n_p = V_{co} \qquad I.\ 9$$

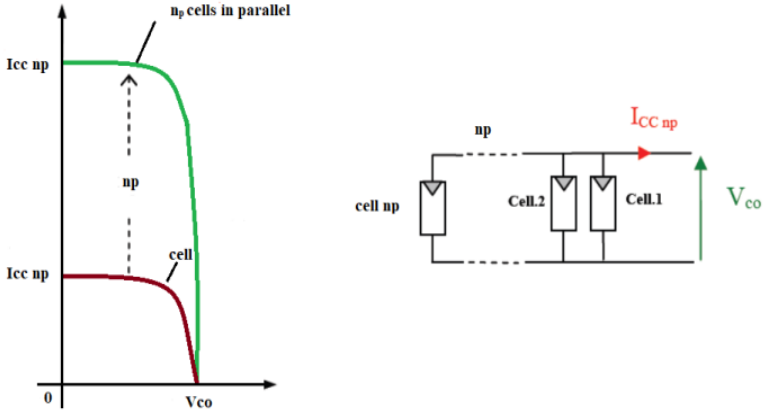


Figure I. 10 Characteristic results of parallel cells group

In a series connection, shown in the figure I.11 below, the same current flows through each cell, while the overall voltage is the sum of the voltages across all the cells.

$$I_{cc}n_s = I_{cc} \quad and \quad V_{co}n_s = n_s * V_{co} \qquad I.\ 10$$

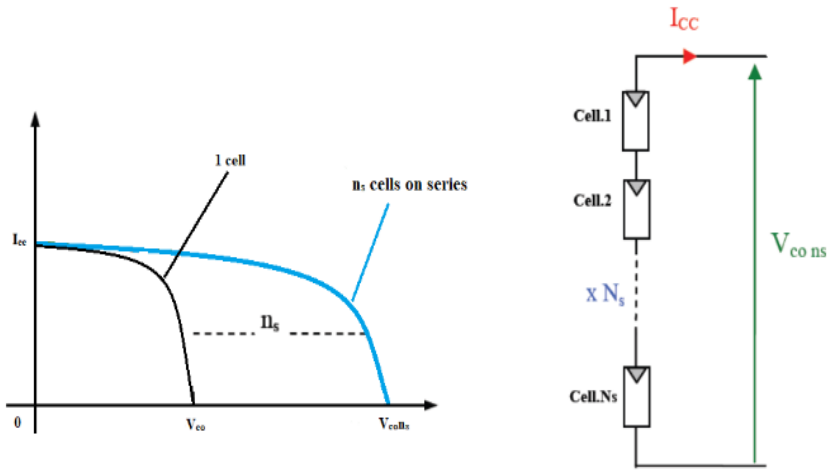


Figure I. 11 Characteristic results of series cells group

I.7.2 Protection of a photovoltaic generator

A photovoltaic installation produced electrical energy during years. Therefore, it is mandatory to add electrical protection to the modules, to avoid damaging and breakdown the links among series and parallel connection of cells. We have two conventionally types of protection used in installation until now:

-The anti-reverse diode-preventing negative current in the GPVs. This phenomenon can appear when several modules connected in parallel, or when a load in direct connection can switch receiver mode to generator mode ‘for instance a battery overnight’ [16].

-The bypass diodes used to isolate a set of cells when the lighting is not homogeneous to avoid the appearance of hot spots and the destruction of the cells.

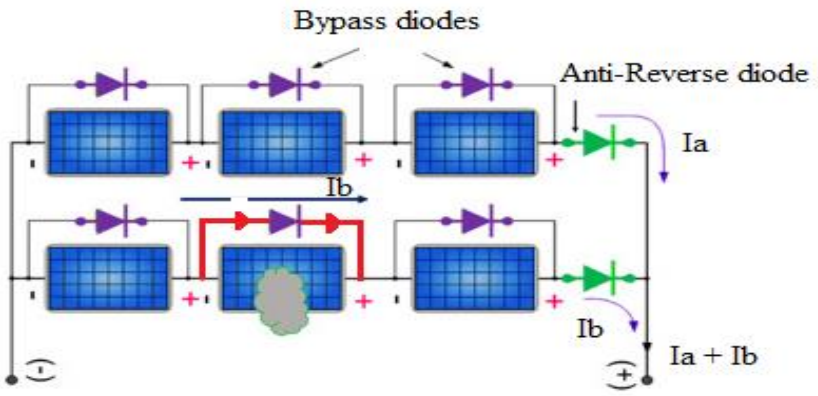


Figure I. 12 Protect the photovoltaic cell by the bypass and anti-reverse diode

I.8 Applications of photovoltaic systems

Marked by a wide variety allowed by the intrinsic characteristics of photovoltaic cell technology, the list of photovoltaic applications can divided into two main categories:

Stand-alone application, it is not connected to the grid.

Connect to grid application, photovoltaic tied to grid or public electricity.

I.8.1 Stand-alone application

Autonomous or "stand-alone", these isolated installations are not connected to the grid, but must ensure load demand coverage at all times. In addition, the autonomy of the system is ensured by a storage system of energy, an inverter and control system [16].

The conversion chain of an autonomous PV installation given by the figure I.13:

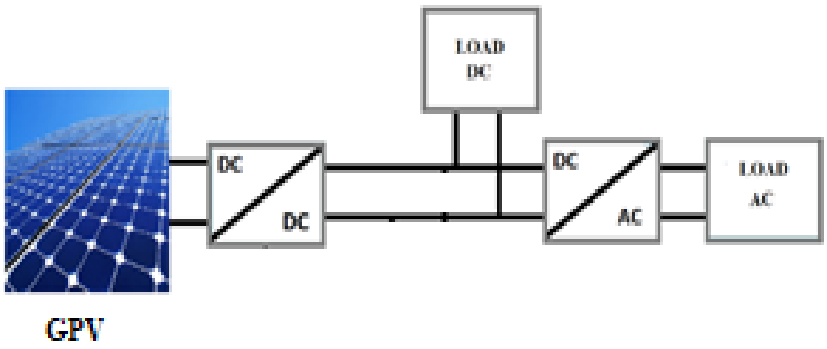


Figure I. 13 Autonomous system of photovoltaic

The production-Consumption in isolation to the grid is dependent on weather conditions. Thus, if there are several successive days unfavorable to the production of electricity, the production-consumption also risks being deprived of electricity when his storage device is completely discharged. On the contrary, if the conditions are favorable for production and all the storage capacity is completely used, he must stop consuming or reduce the load and go to the power saving procedure [30].

I.8.2 Photovoltaic connect to the grid

A grid connected PV system is a PV production connected to utility network. The system consists of solar panel, inverter, control system, and the equipment of grid it show in figure 1.14.Therefore, in economical version, the inverter can only operate in the presence the grid, a possible failure of the inverter renders the production system inoperative. A reversible inverter is necessary if you have a current load unstable. If the local consumption is higher than the production of the plant's PV, the utility grid provides the power. Otherwise, the energy is supplied to the public utility and used to supply neighboring consumers. In addition, at night the consumer is supplied by the utility grid. The main advantage of grid-tied systems is that they allow the energy produced and not consumed on site to resell to the grid provider. On the other hand, these systems can only work in the presence of the network. In case of a cut to the grid, although having its own systems of electricity production the independent producer deprived of electricity [16].

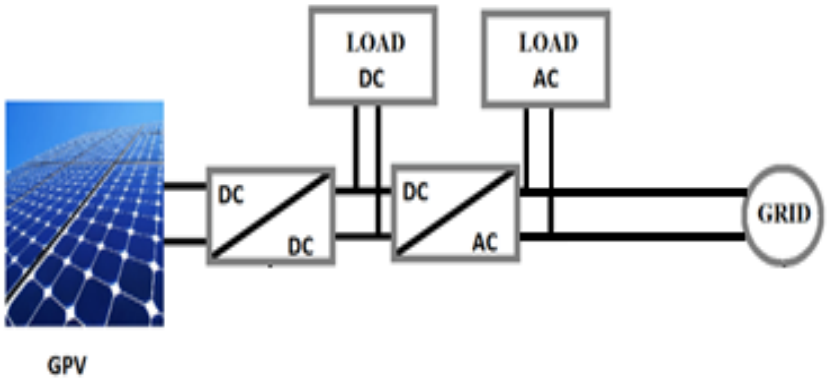


Figure I. 14 Grid connected system of photovoltaic

I.8.3 Hybrid system

This system can consist of the combination of two or more technology supplements to increase energy supply. Energy sources such as the sun and wind do not deliver constant power. The multi-sources combination can make it possible to achieve more continuous electricity production. Hybrid systems operate such as the batteries charged by solar during the day and by the wind generator when there is wind.

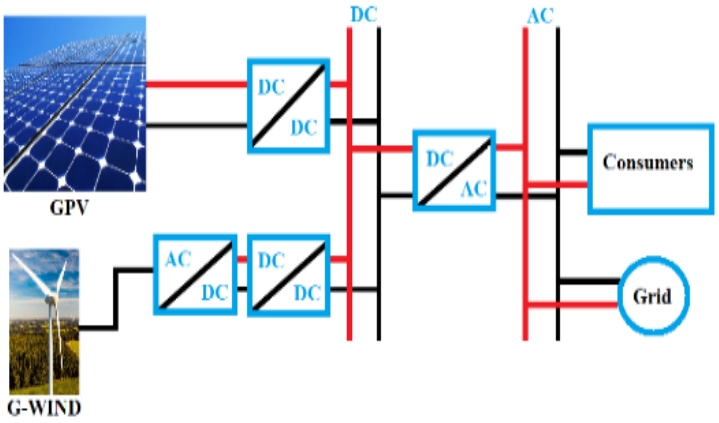


Figure I. 15 Hybrid system of photovoltaic

I.9 Current-Voltage (I-V) characteristic at variable irradiation and temperature

I.9.1 Influence of temperature:

Temperature is an important parameter in the behavior of photovoltaic modules because of their exposure to solar energy conversion. Indeed, the temperature of the cell can sometimes exceed 70°C at noon. This increase in the temperature will cause a decrease in the width of the forbidden band of the P-N junction, which results in slight increase in the current, and a significant decrease in the voltage due to strong increase in the direct current of the diode. Figure I.16 illustrates the curves (I-V) simulated for a variable temperature from 25°C to 45°C with constant irradiation 1000 W/m^2 [31].

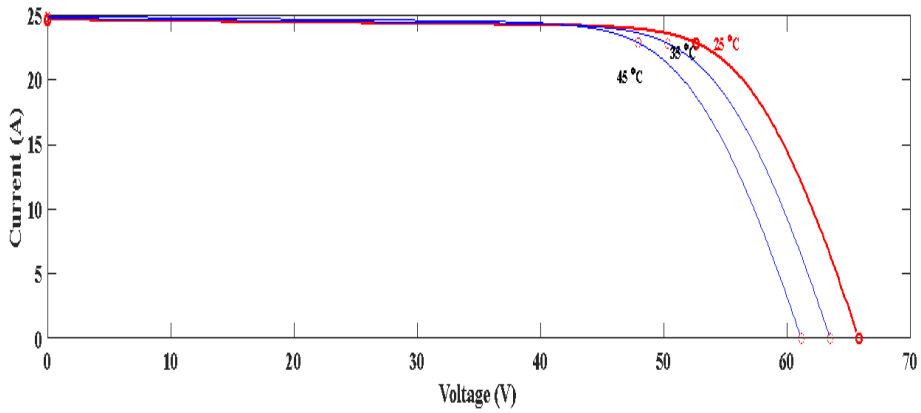


Figure I. 16 The Voltage-Current characteristic with different temperatures

I.9.2 Influence of irradiation

The figure I.17 presents the (I-V) curves simulated for constant temperature of 25°C and variable irradiation between 200 W/m^2 to 1000W/m^2. It shows that the short-circuit current is proportional to the value of the insolation, which explained by the relation (I.2) already demonstrated in the first chapter, while the open circuit voltage changes slightly with sunshine [31].

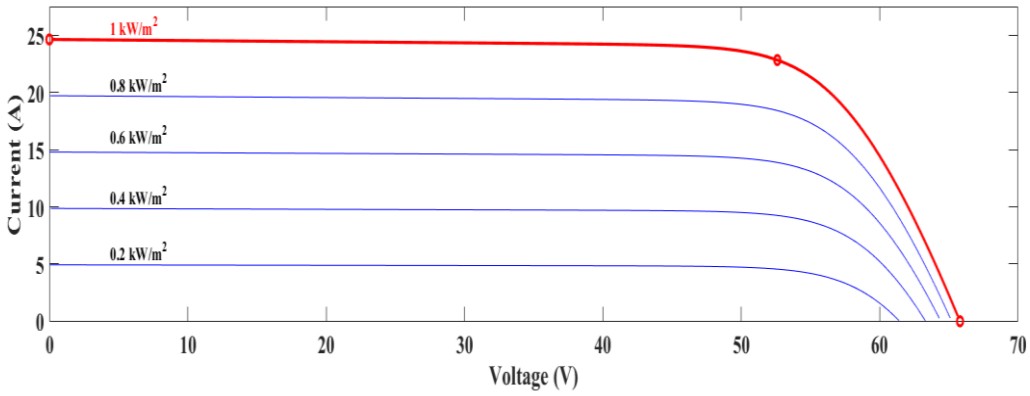


Figure I. 17 The Current-Voltage characteristic with different irradiations

I.10 Power-Voltage (I-V) characteristic at variable irradiation and temperature

Taking into account the characteristic (I-V) presented above, we can deduce the characteristic (P-V). Figure I.18 illustrates the (P-V) curves for constant irradiation 1000 W/m^2 and a variable

temperature ranging from 25 to 45°C, while the figure I.19 shows the curves (P-V) for a constant temperature 25°C and various irradiation from 200 W/m^2 to 1000 W/m^2 [31].

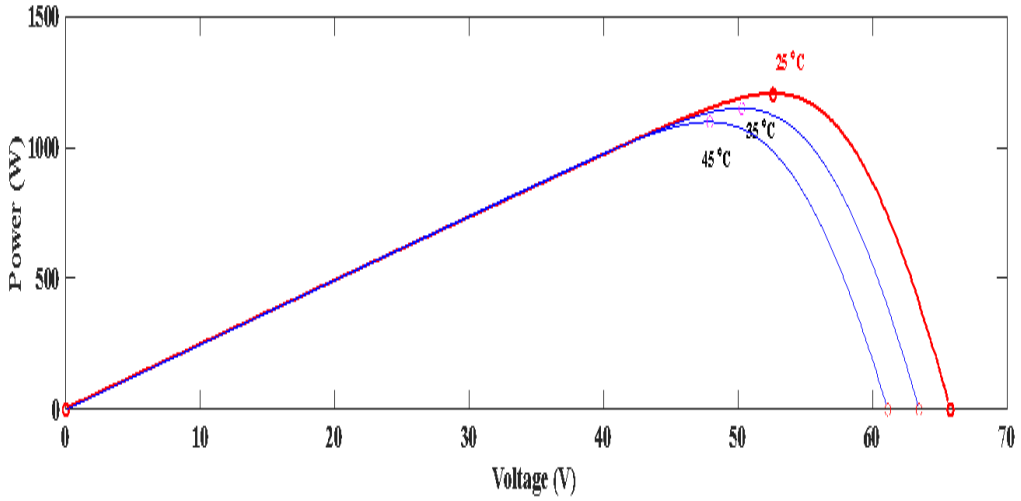


Figure I. 18 The Voltage-Power characteristic with different temperatures

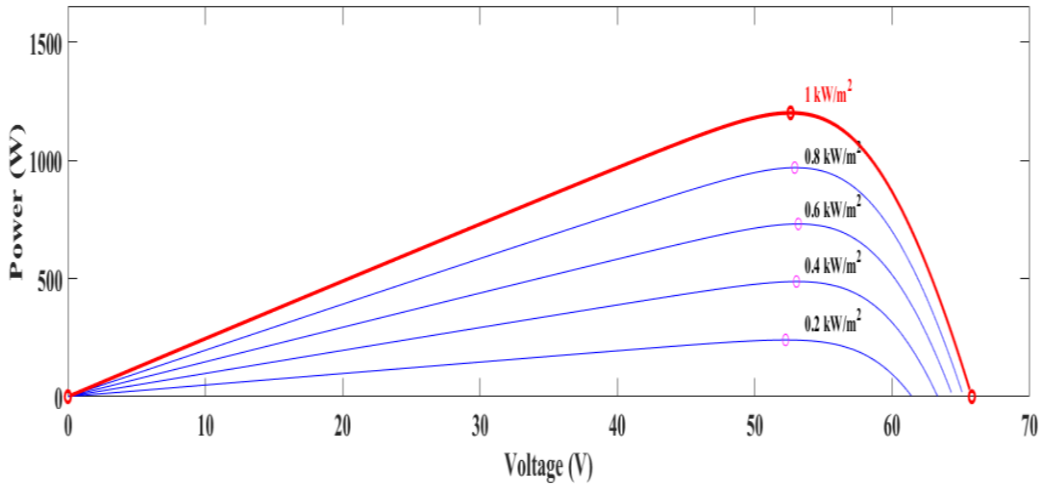


Figure I. 19 The Voltage-Power characteristic with different irradiation

I.11 Advantages of photovoltaic energy

- In general the photovoltaic installation has a high reliability, little failure, and requires little maintenance.

- Photovoltaic energy is a clean and non-polluting energy that emits any greenhouse gases and does not generate waste.

- The operating cost is very low and does not require fuel, transportation or highly specialized personnel.

I.12 Disadvantages of photovoltaic energy

- The manufacture of photovoltaic solar panels is high technology requiring a lot of research and development and therefore costly investments. This reflected in the price of the installation, which today, remains expensive.

- The lifespan of a photovoltaic installation is not eternal but of the order of 20 to 30 years. In addition, the efficiency of photovoltaic cells decreases with the passage of time.

- The level of electricity production is not stable and not predictable but depends on the level of sunlight.

I.13 Conclusion

In this chapter, we started by giving an overview on the production of electricity in general and that of renewables in the world. For the case of Algeria, we have shown that since 2019 the situation has become in deficit because the demand for electricity begins to exceed production. Then we presented the energy trends in the world, for this, the forecasts of renewable energy needs until 2030. Show that from the year 2020 the production of energy in the world becomes unable to meet the needs.

We then presented the constitution of a GPV through the principle of photovoltaic conversion and the modeling of solar cells. Then, a modeling of the photovoltaic panel made under the environment. The model is easy to use and it has a simple protection, especially when adding other stages to the photovoltaic system such as the converter, the load, the MPPT control, etc. We then presented the electrical behavior of the photovoltaic generator. Indeed, the simulations of the main characteristics of this generator, namely the current-voltage and power-voltage characteristics have clearly shown the influence of temperature and irradiation on its performance of electrical behavior. In what follows, we will study in chapter 2, the problems of direct connection between a GPV and the load and need to introduce an adaptation stage. Then, we present the problems of energy storage to guarantee the supply of energy whatever the weather-conditions.

II Electrical Conversion of Photovoltaic System

II.1 Introduction

PV generators have non-linear characteristics with a maximum power point (MPP) that depends on temperature (T) and irradiation (I). The short-circuit current of the PV panel mainly depends on the level of irradiation (the intensity of light). When the irradiation increases, the output current of the PV panel increases, therefore, the maximum power increases, as shown in Figures I.17 and I.19. Moreover, the open circuit voltage of the PV panel mainly depends on the temperature; as the temperature decreases, the power of the PV array increases, as shown in Figures I.16 and I.18.

A photovoltaic installation requires the connection of a chain for the conversion of light energy into electrical energy based on the photovoltaic effect. Whatever the architecture of this conversion chain, it can be divided into several subsystems defined according to their functionalities. In addition, we will seek to optimize the PV system in order to have a better adaptation performance and a good quality of stand-alone and in the system when we connect it to the electrical utility. In the following, we will present the architectures of the different PV systems, focusing mainly on the basic functions of conversion and regulation. There is a wide variety of topologies; we will show the modeling and control of a DC-DC converter and a DC-AC coupling inverter. Furthermore, we introduce nonlinear tuning strategies (MPPT controls, inverter control system, synchronization, and so on).

II.2 Architecture of different photovoltaic conversion chains

Many strategies and topologies have been developed and exist to connect the GPV to the load or grid. A simple diode is the simplest way to make a direct connection. By using the static convertor topologies, it is more sophisticated and can integrate very complex systems. The choice will depend on the use, cost, and efficiency.

II.2.1 Generator photovoltaic-load connection

II.2.1.1 Direct connection

The simplest system that can be designed consists of a photovoltaic generator (GPV) and a load that directly uses the energy produced by the GPV. This system is strongly dependent on the irradiation, the nature of the load, and the temperature. So, the direct connection is mainly used

because of its simplicity of implementation, its minimal cost is due fundamentally to the absence of electronics devices, also regardless of the lower cost.

For this type of connection, a diode is inserted between the GPV and the load, see figure II.1. This diode prevents the GPV from becoming a receiver when it is no longer lit and being destroyed if it reaches its operating limits as a receiver (load). However, this configuration does not offer any type of limitation or adjustment of the voltage load. Moreover, in the case where the load is a battery, it is the voltage of the latter that fixes the operating point of the system, which therefore risks no being located or stability on PPM of the GPV and therefore not using all of its available power. By chance, the load was found on the MPP of the module, it would only last a few moments, with the slightest variation in sunshine, cell temperature, or battery charge level varying the PPM [32].

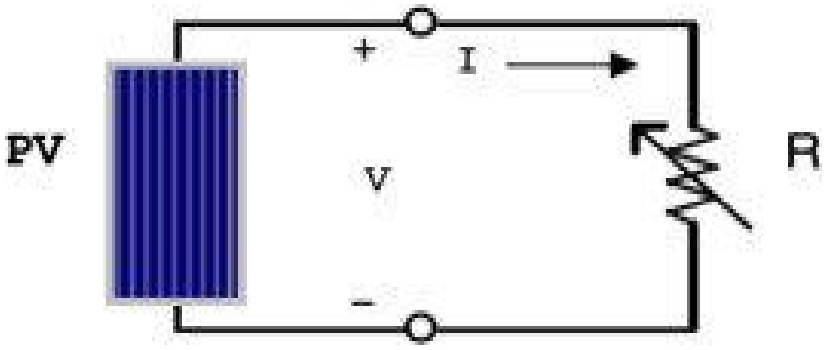


Figure II. 1 PV systems direct connect to the load

II.2.1.2 Indirect connection via adoption stage

II.2.1.2.1 Connection via DC-DC convertor

As previously illustrated, the PV generator exhibits nonlinear I (V) characteristics with PPM. The changes to environmental parameters strongly affect this characteristic. The MPP is therefore constantly modified. Inserting a DC-DC adaptation stage between is necessary to extract at any time the maximum power available at the terminals and transfer it to the load is to in accordance with figure II.2. The adapter commonly used in PV is a static convertor equipped with a controller, which ensures the tracking of the MPP in real time. The convertor controlled by the MPP algorithm, the using of the current and voltage parameters of GPV allow the maximum transfer of energy.

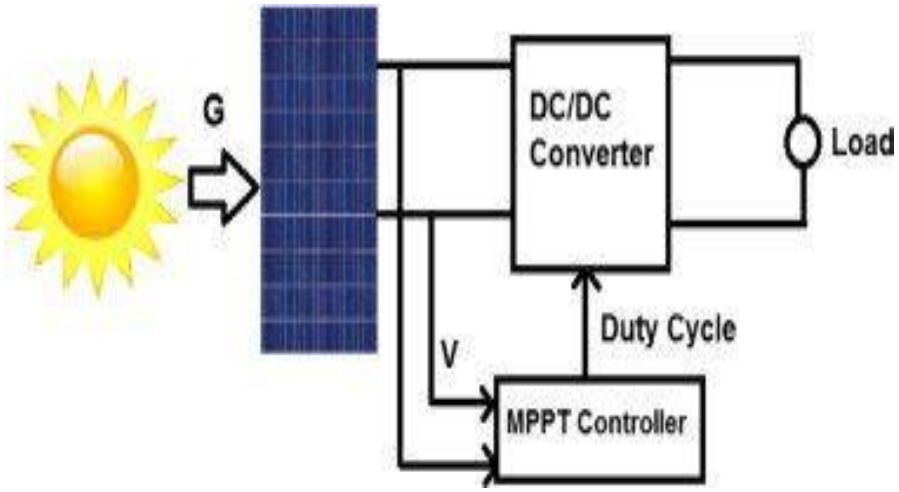


Figure II. 2 Structure of PV system connect to the load DC through DC-DC convertor with an algorithm of control

II.2.1.2.2 Connection via DC-AC inverter

Political decisions in favor of PV have encouraged individuals to use photovoltaic connection to the load as AC autonomously, see figure II.3.

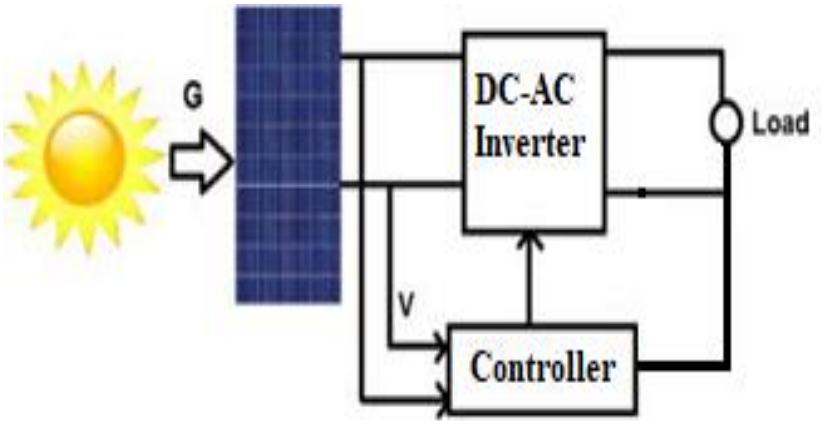


Figure II. 3 Structure of PV system connect to the load AC through DC-AC inverter with a controller

II.2.2 Generator photovoltaic-Grid connection

II.2.2.1 Connection via DC-AC inverter

Thanks to the power electronic components, specialized companies have produced inverters designed to be connected directly to the AC medium voltage grid operation. In this context,

decentralized or distributed topologies are becoming more and more attractive. A great diversity of PV field topologies exists; we will present only the most used and the most interesting figure II.4.

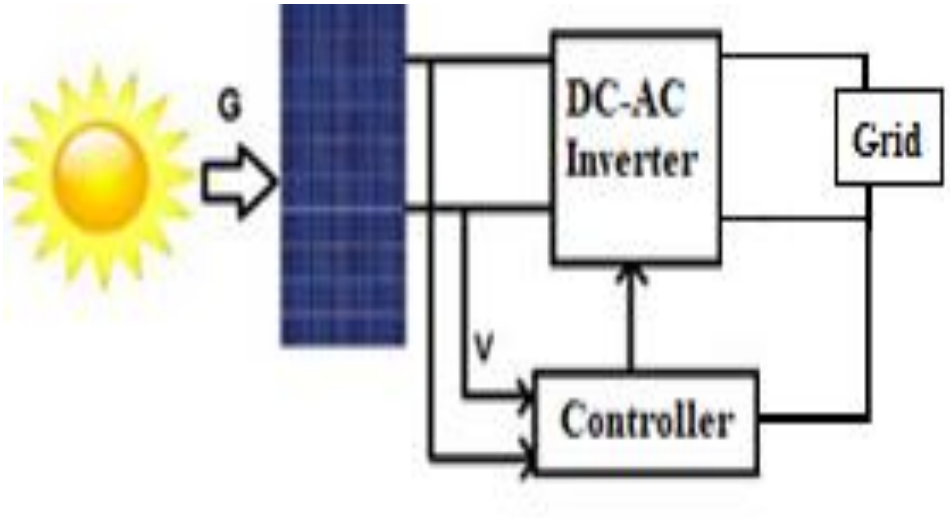


Figure II. 4 Structure of PV system connect to the grid

II.2.2.2 Connection via two stages

Figure II.5 presents the structure of a complex PV system. The main function of this system is to make the conversion more stable and reduce chatter, but on the other hand, it has an effect on the cost. The DC-DC converter and DC/AC inverter that are connected to the grid are fed by the PV array [33].

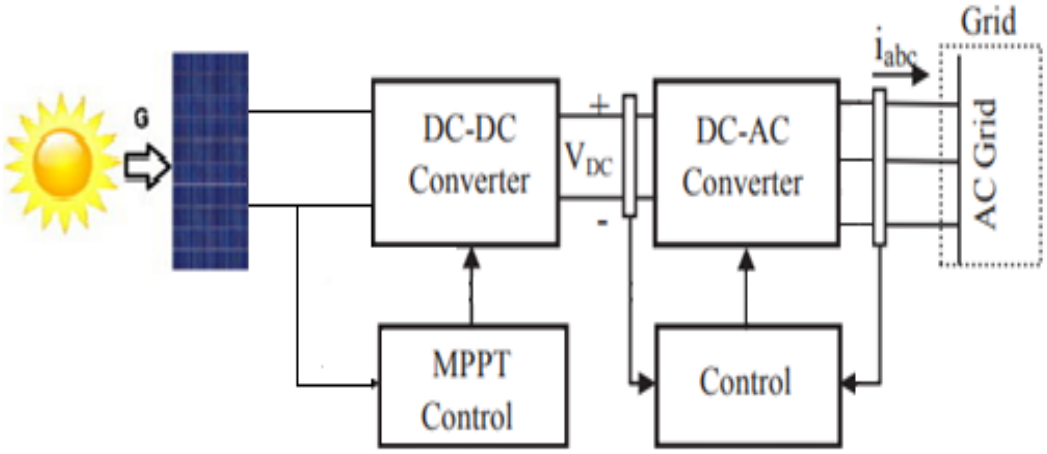


Figure II. 5 Structure of PV system connect to the grid by two stage

II.2.3 Generator photovoltaic connected to multi-sources

PV-connect to multi-sources typically consists of power conditioning devices, locally connected loads, multiple power sources that dispatch power to meet demand, and an energy control system. Four different subsystems can be identified when designing a PV-multi-source. Many proposed topologies has been done [34],this structure divided into following: The subsystem for power conditioning devices, subsystem for energy storage, and the management component power electronic convertors and energy storage technologies are suitable components that are chosen for the aforementioned PV system based on power dispatching strategies and utility grid constraints.

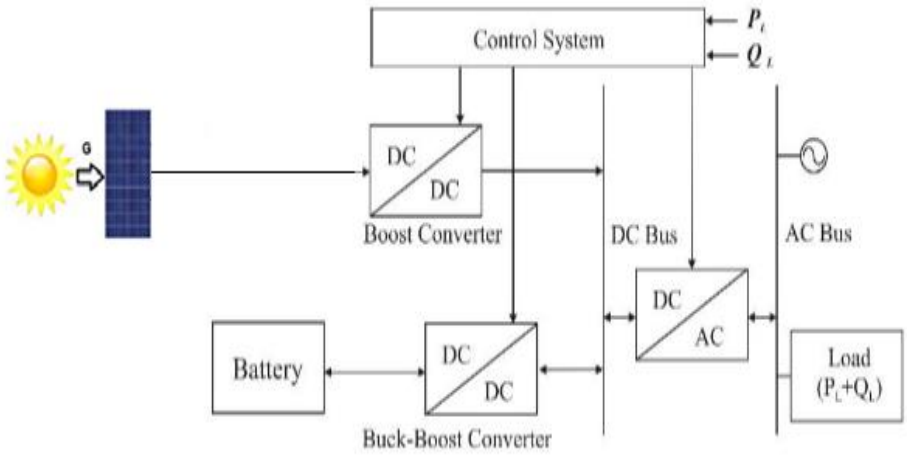


Figure II. 6 Structure of PV system connected to multi-sources

II.3 DC-DC convertor

The DC-DC convertors are used to convert an unregulated DC voltage at the input into a regulated DC voltage at a required voltage level at the output. The output voltage regulation is achieved by varying the duty cycle of the switch. For this reason, all the conversion of exchanged power must be carried out around the energy storage components (inductors, capacitors, and resistance) and switches [31].

The power switches used depend on the level of power to the converted or controlled. MOSFETS (Metal Oxide Field Effect Transistors) are usually used at relatively low power and IGBTS (Insulated Gate Bipolar Transistors switches) at higher powers. Thermistors have been generally used also at higher power levels. Unlike other convertors, choppers have the particularity of working practically lossless and with high efficiency since they use electronic components operating in periodic switching.

The convertors are used today in wide ranges of voltage, current, and power. Their applications range from switching power supplies for electronic assembly to supplying trams and locomotives from DC links. One of the interesting applications of converters is their use as a matching stage in photovoltaic systems.

II.3.1 Boost converter

Is known by the name “Voltage Booster”. The structure in figure II.7 represents the electrical circuit of the booster. It is often used in systems powered by storage batteries and requiring a high supply voltage, a converter of this type is useful in this case in order to reduce the number of elements necessary to reach the level of the desired voltage.

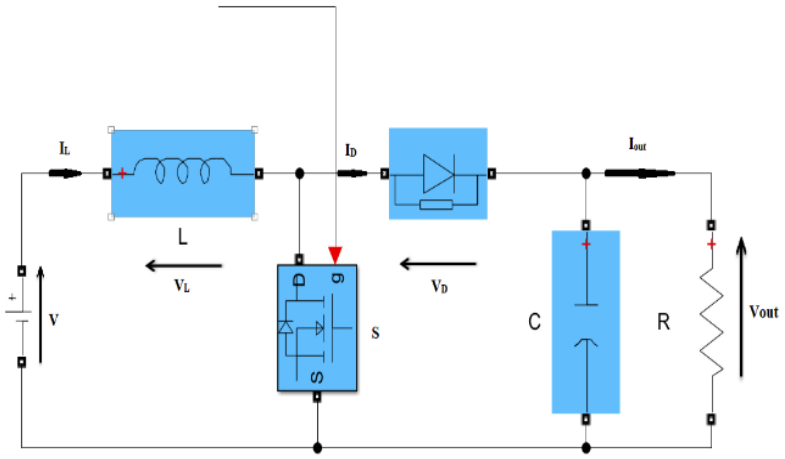


Figure II. 7 Basic schematic of DC-DC BOOST Converter

The circuit is powered by a voltage source V, the output is loaded by a resistance R through current I_{out} and V_{out}. The operation of a boost convertor can be divided into two different phases depending on the state of switch S.

-Phase 1 ($0 < t < \alpha T$)

When the switch is closed (on state), this causes the current to increase in the inductor and therefore the storage of a quantity of energy in the form of magnetic. Diode “D” is then blocked, and the load is then disconnected from the power supply. The figure II.8 gives the equivalent schema of the boost when the switch is closed.

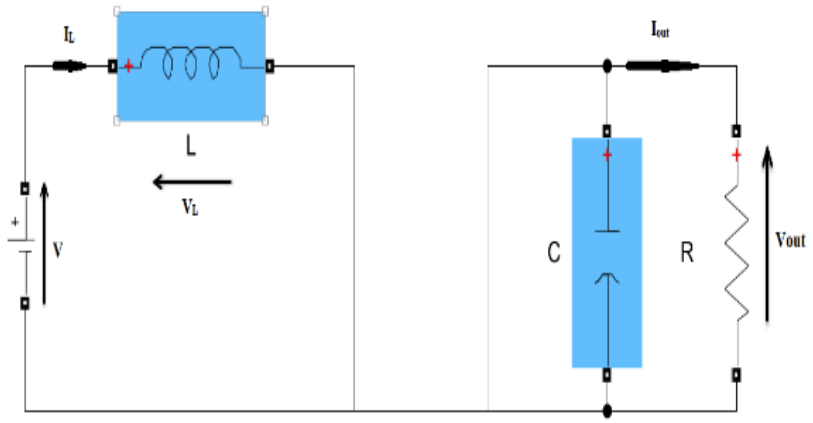


Figure II. 8 Schematic of DC-DC BOOST Converter (S closed)

We have:

$$V_L = L\,\frac{dI_L}{dt} \qquad \textit{II. 1}$$

Where:

$$i(t) = I_{min} + \frac{V}{L}.t \qquad \text{II. 2}$$

At time t = αT, the current in the inductor reaches the peak value:

$$I_{max} = I_{min} + \frac{V}{L}.\alpha T \qquad \text{II. 3}$$

-Phase 1 (αT < t < T)

A t = αT the switch S is opened. The inductor is then series with the generator and its f.e.m is added to that of the generator (boost effect). Diode becomes conductive, the current flowing through the inductor then flows through the inductor then flows through the diode, the capacitor C and the load R. this results in a transfer of the energy accumulated in the inductor towards the capacitor. The figure II.9 gives the equivalent schema of the boost when switch S is open.

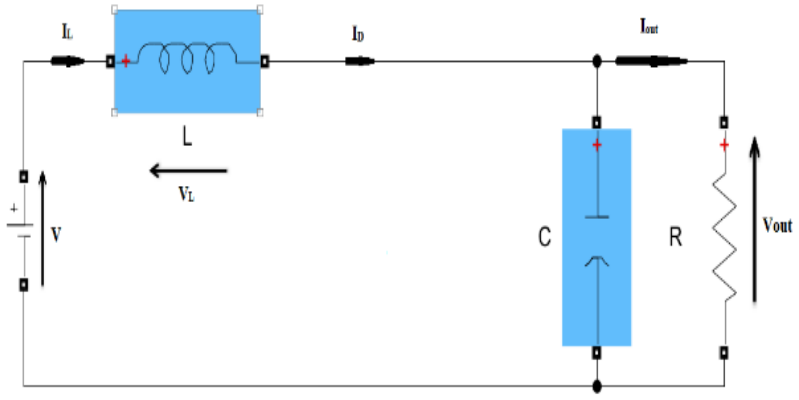


Figure II. 9 Schematic of DC-DC BOOST Converter (S open)

We have:

$$V - V_{out} = L \frac{dI_L}{dt} \qquad \text{II. 4}$$

Current of inductor can write as following:

$$i(t) = I_{max} - \frac{V_{out}-V}{L}.(t - \alpha T) \qquad \text{II. 5}$$

At the t = T the current in the inductance reaches its minimum value:

$$I_{min} = I_{max} - \frac{V_{out}-V}{L}.(1 - \alpha).T \qquad \textit{II. 6}$$

Waveforms of currents and voltages when the boost converter works in continuous mode, the current I_L flows the inductance are never lost. Figure 2.8 shows the current and voltage waveforms in a boost converter. In one state, the current I_L has increased.

$$\Delta I_{LON} = \int_0^{\alpha.T} dI_L = \int_0^{\alpha.T} \frac{V}{L}.dt = \frac{V.\alpha T}{L} \qquad \textit{II. 7}$$

In the blocked state, the current I_L in the inductor is given by:

$$\Delta I_{LOFF} = \int_0^{(1-\alpha).T} dI_L = \int_0^{(1-\alpha).T} \frac{(V-V_{out})}{L}.dt = \frac{(V-V_{out})(1-\alpha)}{L}.T \qquad \textit{II. 8}$$

In steady state, the current through the inductor is the same at the open and close of each switching cycle:

$$\Delta I_{LON} + \Delta L_{OFF} = 0 \qquad II.\ 9$$

By replacing equations II.7 and II.8 in II.9, we find:

$$\frac{V.\alpha T}{L} + \frac{(V - V_{out})(1-\alpha)}{L}.T = 0 \qquad \text{II. 10}$$

The equation of the output voltage given by:

$$\frac{V_{out}}{V} = \frac{1}{1-\alpha} \qquad \text{II. 11}$$

It can be seen that the output voltage of the converter depends only on the input voltage and on the duty cycle α. As this is always between 0 and 1, it boosts the voltage.

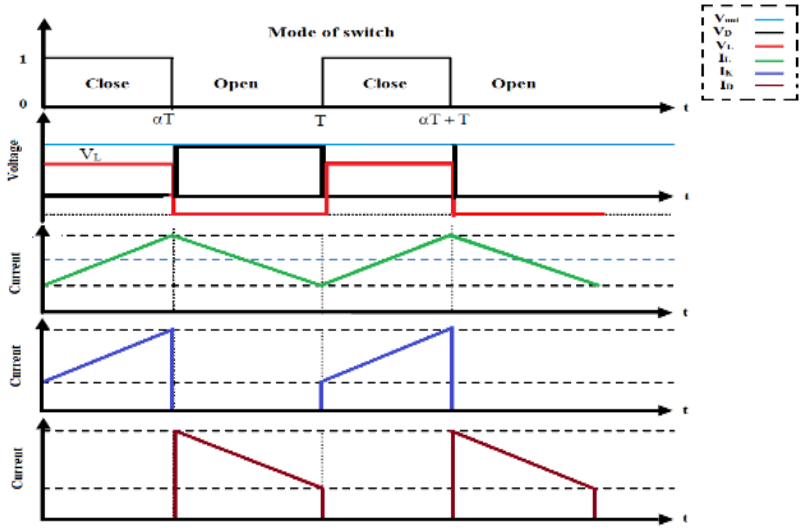


Figure II. 10 The format of the current and voltage during the switching in boost converter

II.3.2 Buck convertor

A buck converter, or lower converter, is a switched-mode power supply that converts a DC voltage into another DC voltage of a lower value. It is well designed, has a high efficiency (up to 95%), and regulating the output voltage can be done through this method instead of using a voltage divider, which dissipates the excess voltage in the form heat and has a low efficiency, that is prohibitive for power electronics applications. This type of converter, whose basic diagram is represented by figure II.11.

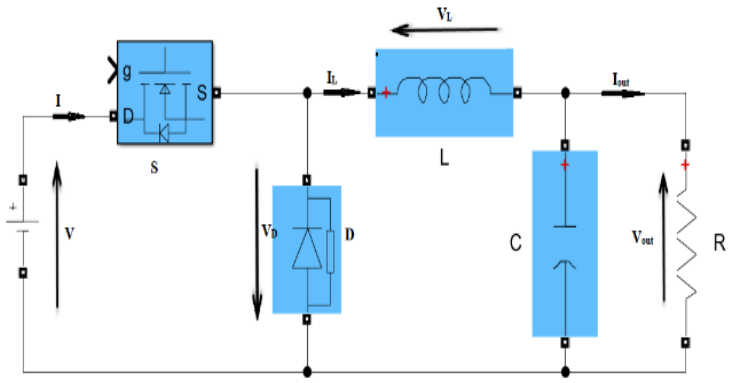


Figure II. 11 Basic schematic of DC-DC Buck Converter

Principles of operation for the buck converter uses controlled switches S figure II.12 with no isolation between the input source and the output (load). The operation of such a converter can be divided into two configurations depending on the state of switch S.

-Phase Closing

In the on state, switch S is closed figure II.12, the voltage across the terminals of inductance is:

$$V_L = V - V_{out} \qquad \text{II. 12}$$

The current I_L does not increase immediately, but rather linearly with a rate of increase imposed by the inductance L.

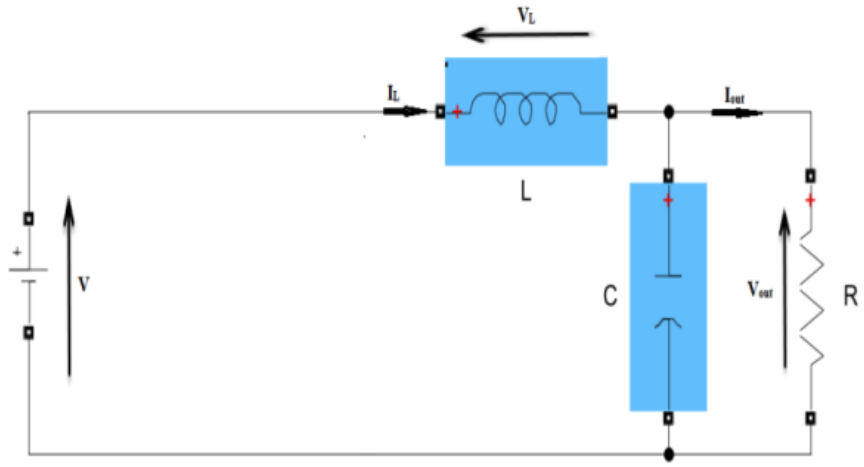


Figure II. 12 Schematic of DC-DC Buck Converter (S closed)

In the open state, when switch S is opening figure II.13, to ensure the continuity of passing the current in the inductance we need to use the diode in order to conductively. The output voltage is written by:

$$V_{out} = -V_L \qquad \text{II. 13}$$

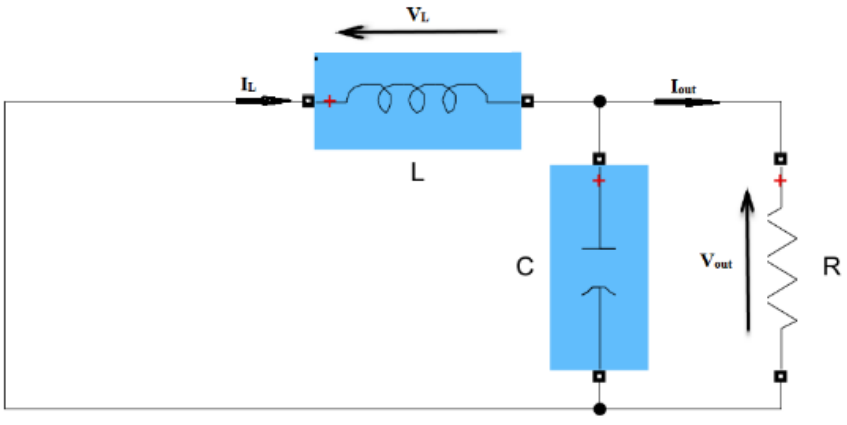


Figure II. 13 Schematic of DC-DC Buck Converter (S open)

II.3.3 Buck-Boost convertor

The basic scheme is shown in figure II.14 is a switching power supply that converts a DC input voltage into another DC voltage of lower or higher value but of opposite polarity.

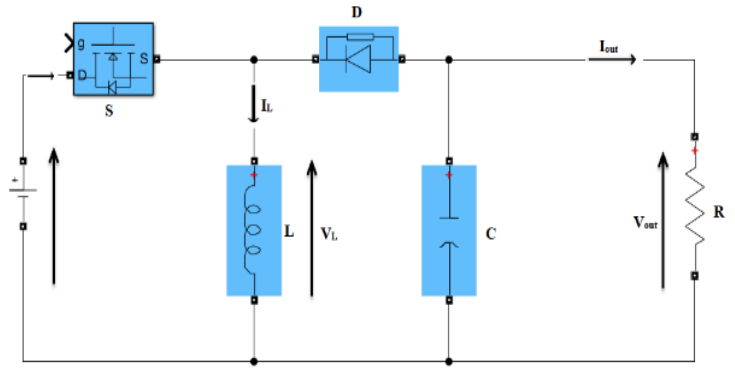


Figure II. 14 Basic schematic of DC-DC Buck-BOOST Converter

We were only interested in the continuous operation mode, as with the previous Boost study and buck converter. The switching states are controlled with a constant period and a variable duty cycle, and over a period of time T, the operation of the circuit passes through two phases:

-Phase 1 ($0 < t < \alpha T$)

While the switch is closed (in the on state), this leads to an increase in the current in the inductor L and the voltage. Figure II.15 gives the equivalent boost diagram when the switch is closed.

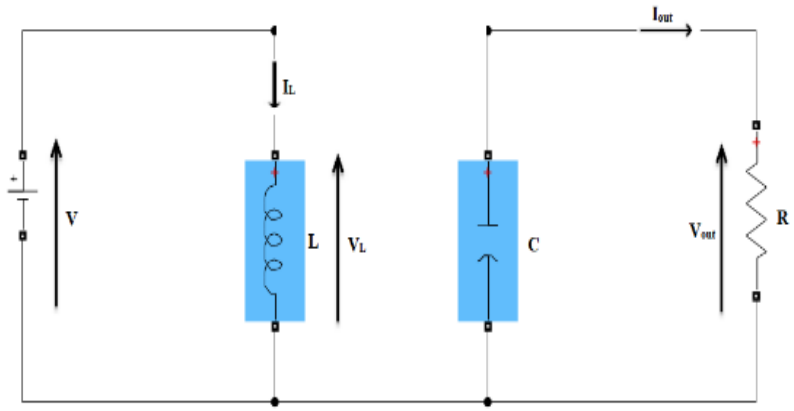


Figure II. 15 Schematic of DC-DC Buck-Boost Converter (S close)

During a period, equal to **αT:**

$$V = V_L = L.\frac{dI_L}{dt} \qquad \text{II. 14}$$

-Phase 2 (αT < t < T)

When switch S is turned on, current flows through the inductor to the load. If we consider a zero voltage drop across the terminals of the diode and capacitor large enough to keep their voltage constant, the voltage across L becomes:

$$V_{out} = V_L = L.\frac{dI_L}{dt} \qquad \textit{II. 15}$$

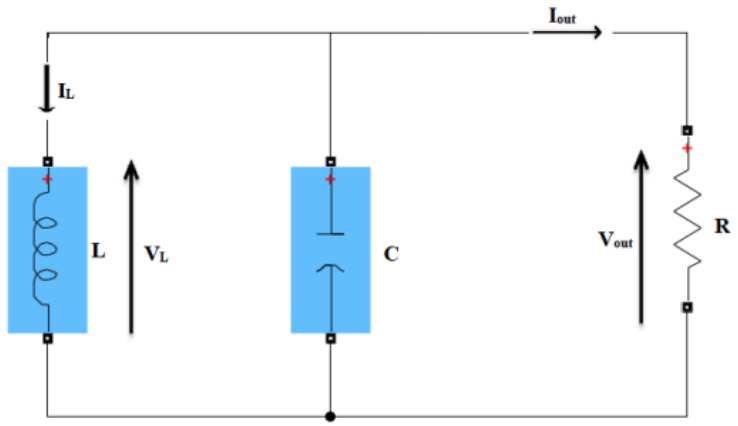


Figure II. 16 Schematic of DC-DC Buck-Boost Converter (S open)

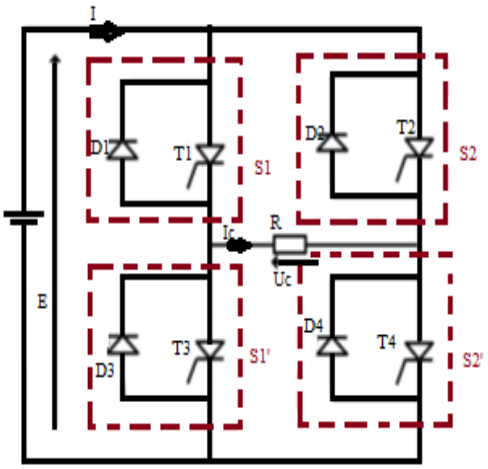
II.4 DC–AC Inverter

Political decisions in favor of PV have encouraged individuals to use photovoltaic systems connected to the distribution and power supply networks. Thanks to the evolution of power electronics components, specialized companies have produced inverters designed to be connected directly to the medium-voltage grid of the various local or national operators. In this context, inverter off-grid or inverter on grid connection topologies are becoming more and more attractive, a great diversity of PV array topologies exists. We present only the most used and the most interesting.

-Firstly, I will explain of different type of inverters on two category of voltage:

II.4.1 DC-AC Single Phase

A voltage inverter is a DC-AC converter that is powered by a source of continuous voltage. We present in figure II.17 the principal of the voltage inverter. If the output is single-phase (the four-switch bridge assembly) S1-S2, S1'-S2', (S1-S2, S1'-S2') must be complementary so that the voltage source does not is never short-circuited, and so that the current circuit is never open [35]. Figure II.17 represents the power circuit of such an inverter (bridge), and figure II.18 shown the control signals and voltage waveforms:



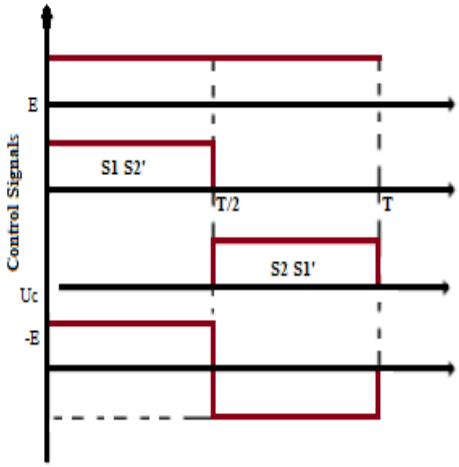


Figure II. 17 *DC-AC Single Phase* Inverter

Figure II. 18 Control Signals of Inverter

The states of the controlled switches allow us to give the expression of the voltage across the load $U_{c\,(t)}$ as follows:

If the input voltage of the inverter is constant and equal to E, whatever I we have:

For 0<t<T/2: the switches, S1 and S2' are closed, and S2 and S1' are open;

$$Uc = +E \qquad \textit{II. 16}$$

For T/2 <t<T: the switches, S1 and S2' are open, and S2 and S1' are closed;

$$Uc = -E \qquad \textit{II. 17}$$

The output current is therefore the same as the current I at the input, it depends on the load placed on the side alternative.

Note that the switches Si of the inverter figure II.17 is formed by setting parallel Ti semiconductors controlled by opening and closing and Di diodes. The latter ensures the continuity of current and thus allows the conduction of current negative if the current is out of the phase with output voltage.

II.4.2 DC-AC Three-Phase

Figure II.19 gives the block diagram of the three-phase voltage inverter; it is placed between sources of DC voltage, therefore of constant voltage, and load balanced three-phase currents through which i_a, i_b, i_c from a three-phase system balanced sine wave. The three-phase inverter is an assembly of three single-phase half-bridges each consisting of two switches in series (S1-S1', S2-S2', and S3-S3'). Switches of the same half-bridge must be complementary so that the voltage source is not never short-circuited, and so that the circuits of the currents i_a, i_b, i_c are never open. Therefore, the six switches can impose the output voltages, regardless of whether the currents a, b and c through these switches must be bidirectional. Each of them is made up of a semiconductor with controlled opening and closing plus a diode in parallel [36].

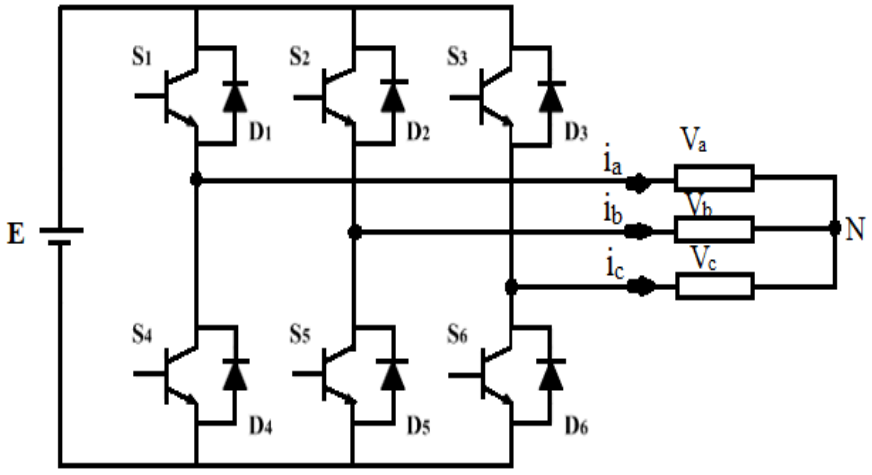


Figure II. 19 DC-AC Three-Phase inverter

Equations (2.18) and (2.19) describe the DC-AC inverter conversion model. For two stages:

$$[V_a\ V_b\ V_c\ ] = E.[2/3\ -1/3\ -1/3\ -1/3\ 2/3\ -1/3\ -1/3\ -1/3\ 2/3\ ].[c_1\ c_2\ c_3\ ] \quad II.\ 18$$

$$I_{DC} = c_1 i_a + c_2 i_b + c_3 i_c = [c_{123}]^T . [i_{abc}] \quad \textit{II. 19}$$

E: is the input voltage, I_{DC}: the current of DC input, V_a, V_b, V_c: the voltage of three-phases of inverter, and C_1, C_2, C_3: the signals generated from PWM strategy of control.

-As a result, we can use the two above categories according to the (on or off) grid. In the following context, I will explain when and where to use this inverter.

II.4.3 Inverter off-grid

A major issue arises when an inverter is connected to an off-grid or island system because the supply and demand power balance is significantly changed.

The supply and demand and power balance issues are pertinent for all grids, despite the fact that the working principle and problems are the same for all off-grid or island systems. Off-grid type inverters should be used to design and connect the PV system in an off-grid system so that power production and consumption are proportionally matched. Off-grid inverters can then adjust their output in response to the power demand of the off-grid system. Although such a design is inefficient (because extra power is wasted), it functions harmoniously with the other system parts. As an illustration, figure II.20 depicts an off-grid system with PV connected to the system using an off-grid type inverter with storage batteries. When excess power is detected, as shown in figure II.20, an off-grid type inverter limits its power production then exploits it to charge the battery or switch-off some panel for adjust the balance between consumption and production even though the irradiation (as well as the potential to produce power) [37].

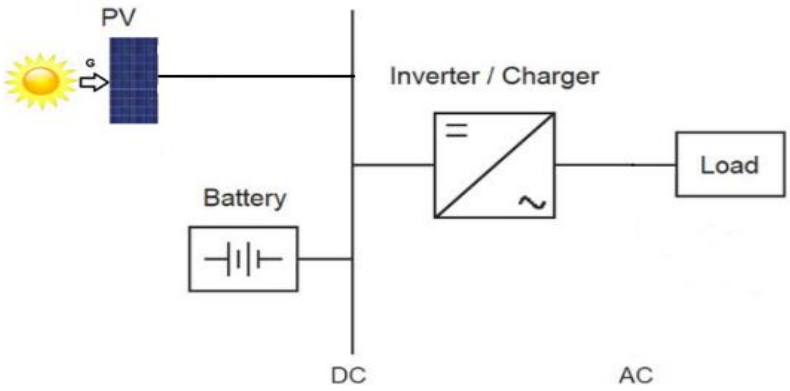


Figure II. 20 Schematic of the topology off-grid inverter

The type inverter off-grid system operates by setting the reference voltage, current, and power. Because the change in atmospheric conditions from morning to evening has a direct effect on power production, it is critical to use batteries to compensate for the loss in PV production in the morning and evening and to capitalize on the extended production in the afternoon.

II.4.4 Inverter on-grid

Transforming the DC power produced by the PV array into utility AC power is called a grid-connected PV system. The control unit design seeks to deliver the maximum power from the PV arrays at the output with the desired power factor and low harmonic distortion (THD),

The designed controller must be able to reject disturbances and follow the reference. It is essential to create a strong dynamic model inverter in order to effectively implement a ZSI behavior control strategy [38]. To examine the performance of the entire system, a number of small-signal analyses and mathematical models have been presented in the literature [39].

Figure II.21 shows the system using an inverter on-grid. The features of it, its support for feeding all power products from the PV array during the day, So that it does not need the storage batteries and also relies directly on the situation of the grid; that is, when the grid is on, the inverter is working and conversantly, the power, and if the grid is off, the inverter is also off.

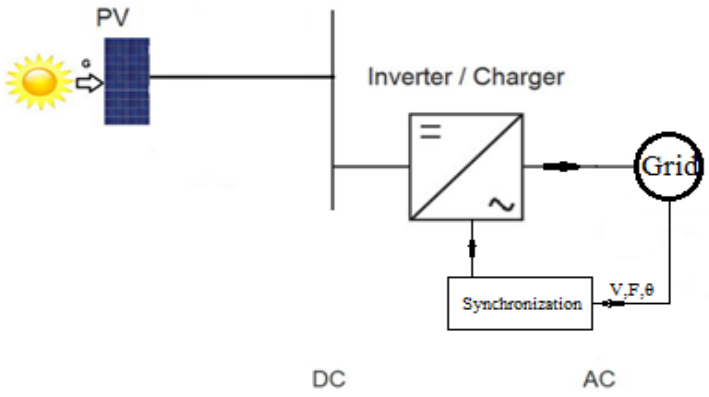


Figure II. 21 Schematic of the topology on-grid inverter

Therefore, the main issue for inverters on-grid is that they cannot operate in island mode due to grid parameters, and they must protect against load consumption.

All possible direct current (DC) power is converted to alternating current (AC) power by the grid-tied inverter control algorithm.

II.5 Control of the electrical conversion chain of a PV system

II.5.1 Control the DC/DC converter

There are specific control laws named in literature “external control” for physical devices that must operate at the maximum points of their characteristics even if, a priori, these points are not known. In advance, these can even change at any time for various reasons. In the case of energy sources, as a result, one to several maximum power points (PPM) is present. When this kind of control is used to concurrently search for the MPP and ensure perfect adaptation between the generator and its load in order to transfer the maximum power produced to the load it is sometimes referred to in the literature as "Search for the Maximum Power Point Tracking MPPT". Figure II.3 represents a typical elementary chain of photovoltaic conversion associated with a command.

An MPPT control is a control that tracks the maximum power point of a photovoltaic module by operating the PV module at its optimum operating point, regardless of atmospheric conditions (temperature, irradiation) and the value of the load. It is generally based on adjusting the duty

cycle of the static converter until it reaches the PPM. During the operation of the GPV, several disturbances can modify the PPM figure II.22 represents three cases of disturbances [40].

MPPT provides electrical power to a DC load. As indicated in this chain, the MPPT command is necessarily associated with a quadruple (static converter) having one to several degrees of freedom depending on its structure, this allows for the adjustment of the GPV impedance to the charge. In the case that solar energy is converted into electricity, the quadruple can be achieved using a simple DC-DC static converter at one degree of freedom denoted and corresponding to the duty cycle 10, so that the power supplied by the GPV at its input corresponds to the maximum power (P_{MAX}) that it can generate at any time. Moreover, this power must be able to be transferred. Simultaneously and completely directly.

In this section, much thought has been given to power maximization commands, known as MPPT (Maximum Power Point Tracking) techniques along with their improvements as documented in the literature over the period 1954–2018 [41]. Therefore, many researchers have tried to develop algorithms to extract the maximum energy converted by the panel and then allow optimal operation of the photovoltaic system. In addition, many methods have been done in the literature to achieve the objective of the algorithm (MPPT). These techniques can be classified into three categories shown in figure II.23 [42], as follows:

-Indirect methods which are based on prior knowledge on the measurement of a fraction open circuit voltage FOCV or a fraction open short-circuit FOSC, the measurement of temperature (T), and on voltage or current feedback.

-The direct methods or conventional MPPTs which include the Perturbation and Observation P&O method, Incremental Conductance INC and hill clamping HC[43].

-Algorithms based on artificial intelligence (AI), including those based on fuzzy logic [44]. Each of these methods has a distinct approach to achieving the MPP [45].

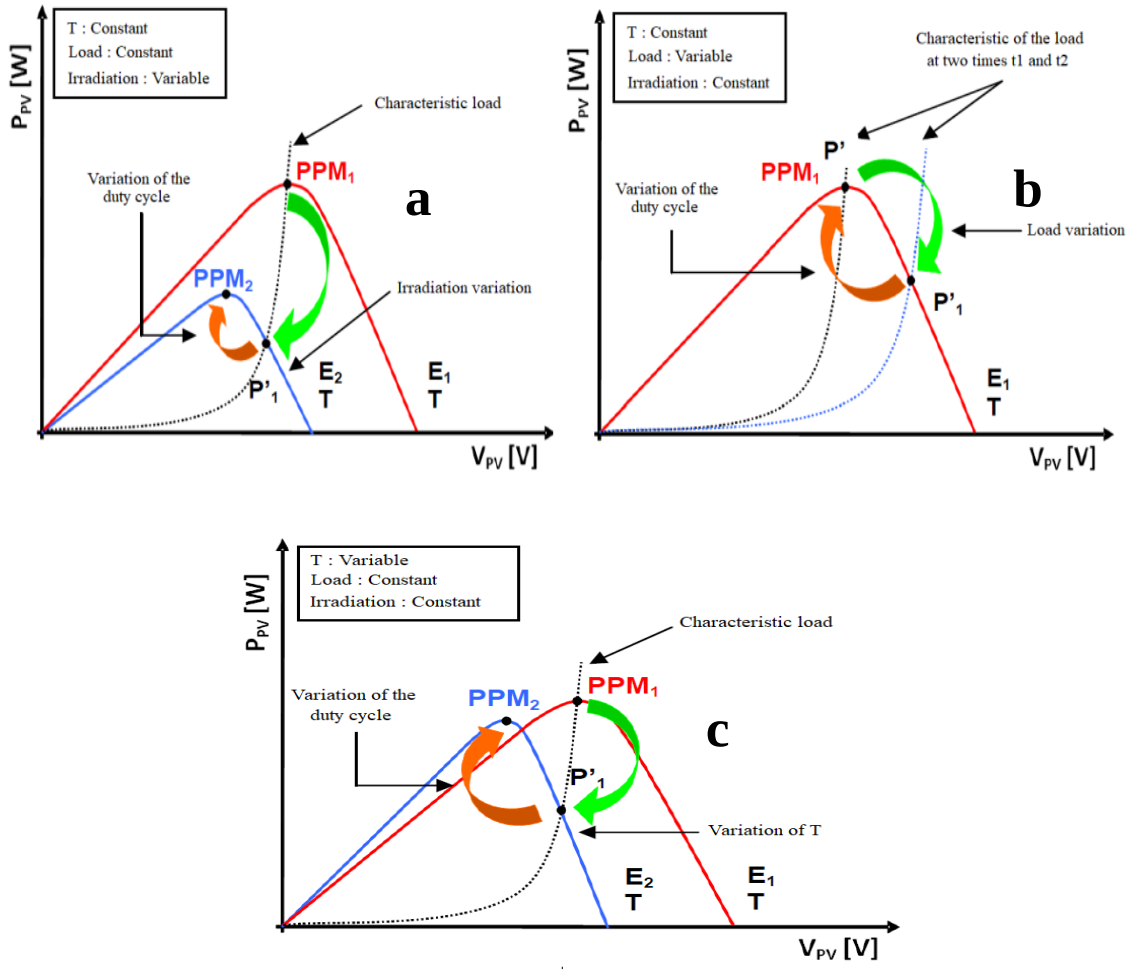


Figure II. 22 Finding and recovering the Maximum Power Point, a) Variation in irradiation at the level of the GPV, b) Variation in consumption loads, and c) Temperature variation at the level of the GPV.

II.6 Conclusion

In this chapter, we have highlighted the problems caused by the direct connection between GPV and load. In this sense, with the aim of optimizing the power provided by the GPV, an adaptation stage, or two, must be introduced between the source and the charge. This adaptation stage must be associated with a search control for the point of maximum power. We also presented the constitution of the photovoltaic system, in the case of a DC-DC adaptation stage, and in the case of a DC-AC adaptation stage.

Different topologies of non-isolated DC-DC converters have been studied. The structure of boost type was adopted for its simplicity and relatively higher voltage gain. Some methods of maximum power tracking cited in the literature are presented. In particular, we studied the

perturb and observe technique and some basic MPPT techniques. In order to study the behavior of the photovoltaic system and know more about the approach to control.

In the next chapter, in order to gain a deeper understanding of MPPT techniques, we will initially simulate the system for different values of temperature and/or irradiation by using a classical method. We will show the INC algorithm compared to sliding mode control SMC.

III Techniques MPPT for DC/DC Stand-Alone photovoltaic system

III.1 Introduction

In the previous chapter, we exposed that for a photovoltaic (PV) generator to operate under optimal conditions, it must be equipped with a matching quadruple. This quadruple can be a DC-DC converter. When the system is supplying a DC load and the external constraints change (irradiation and temperature), the adaptation of the PV generator to the load can be done through the converter by adjusting the duty cycle of the signal controlling the switch of the converter. The problem that arises is to design an adaptation approach (MPPT control) which makes it possible to automatically adjust this duty cycle to its optimal value at any time. However, due to these sudden load instabilities or variations.

The goal of the algorithms (SMC, FL, INC, and PSO) application is to provide the MPPT system with the necessary control support for stability robustness against parameter uncertainties and fast dynamic responses under rapidity changing environmental conditions. Conventional MPPT controllers, whether digital or analog cannot meet these requirements without continuous controller parameter adjustment and complex controller architecture,

In this thesis, a cascaded boost converter under the control techniques has been applied for finding and tracking the maximum power point for a PV system. It will be used as a solution to adapt the electrical energy coming from PV panels, in order to be able to supply the loads. The objective of this chapter is to simulate in the MATLAB SIMULINK environment an autonomous PV system (PV generator, DC-DC Converter and DC load), whose operation is regulated by an MPPT control under different mode in this system to ensure the reliability of them, the converter is cascaded BOOST choppers. Moreover, we analyze and evaluate the dynamic response of the PV system exposed to different conditions that occur using the simulation results of the PV system as designed. The various electrical parameters (Current, Voltage, and Power), the system's behavior in response to climatic changes, and its stability in the face of load disturbances are the main topics of these simulations.

III.2 The research principal of MPPT

Is based on two approaches [46].

-By applying an initial value of the cyclic ratio and measuring the corresponding power, another (only) value of the cyclic ratio is applied and we observe how evolve (increase or decrease) the electrical power of the GPV, to choose the new value of the cyclic ration allowing the increase of the electrical power.

-We apply successively several values of the duty cycle and we collect the different values of corresponding electrical powers of the GPV, and then maintain the D values with maximum power to be added to a new D cycle value vector. The latter will be applied to collect the new corresponding electrical power values of the GPV and maintain the D value or offering the maximum power. The process continue until the maximum power point is reached figure III.1

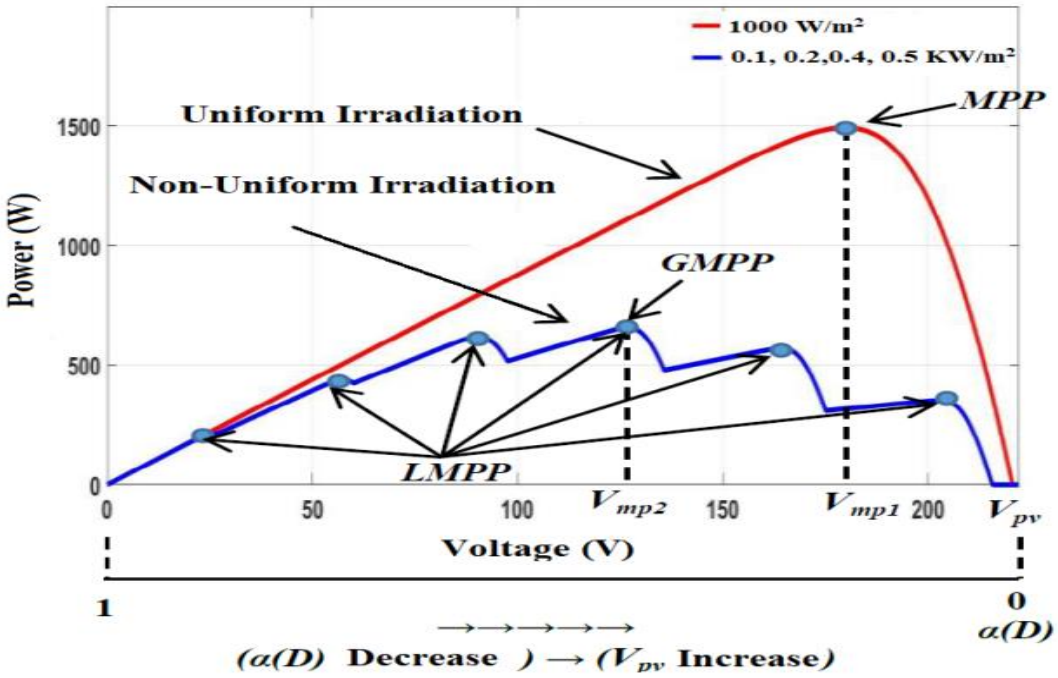


Figure III. 1 Appearing the different MPP types

III.2.1 Local MPP (LMPP)

Numerous maximum power point methods have been developed to allow the system to extract the maximum power from GPV. LMPPT controls can generally be classified according to the search approach adopted into three types of MPPT [46][47][48][49] and [50].

III.2.2 Global MPP (GMPP)

When the GPV receives uniform radiation, the PV characteristic curve displays a single point of maximum MPP power. Nevertheless, if the GPV receives a differently distributed amount of radiation partial shading (PS), several peaks, one of which is GMPP, will characterize the PV curve and remaining peaks are LMPP. Conventional MPPTs are very likely to operate in LMPP, which reduces the output power and thus greatly reduces the efficiency of PV systems. Unlike GMPPT techniques, it is able to track the global peak because it has a mechanism to distinguish between local and global extremes. In the literature, several GMPPT techniques have been proposed and implemented. They can be reduced to two large groups; soft computing techniques and hybrid methods are mentioned in the previous section.

III.3 Challenges facing MPPT techniques

Techniques and their advancements, as reported in the literature among 1954 and 2018, are included by choosing the method for MPPT, all researchers focused on it from 1954 to1988 on choosing the module and/or load so that the intersection of the current-voltage characteristic curves for the module and load is close to the MPP. During this time, some researchers tried to determine the proper battery parameters to connect to the PV system in order to improve the matching between the characteristics of the module and the load because this matching is not always satisfied under varying irradiation levels and ambient temperature

Hooke et al. conducted a design study on a resistive load in 1961 to confirm that the MPP is the point at which the I-V curves of the module and resistive load intersect. Biran et al. conducted a design study on a dynamic load in 1976 to confirm that MPP is the point at which the I-V curves of the module and the dynamic load meet. Braunstein conducted a design study on a battery load in 1977 to ensure that the MPP is the point at which the I-V curves of the module and the battery load intersect [41].

Appelbaum concentrated on resistive load and storage in his design study in 1977 battery fed by a solar power system. In their design study from 1985, Anis et al. focused on a volumetric pump powered by a PV system. In their design study from 1988, Saied et al. Concentrated on the DC motor supplied by a PV system. In their design study from 1989, Khouzam et al. focused also on

pumps powered by PV systems. Below the figure III.2 appear the problems that are still faced to the PV system.

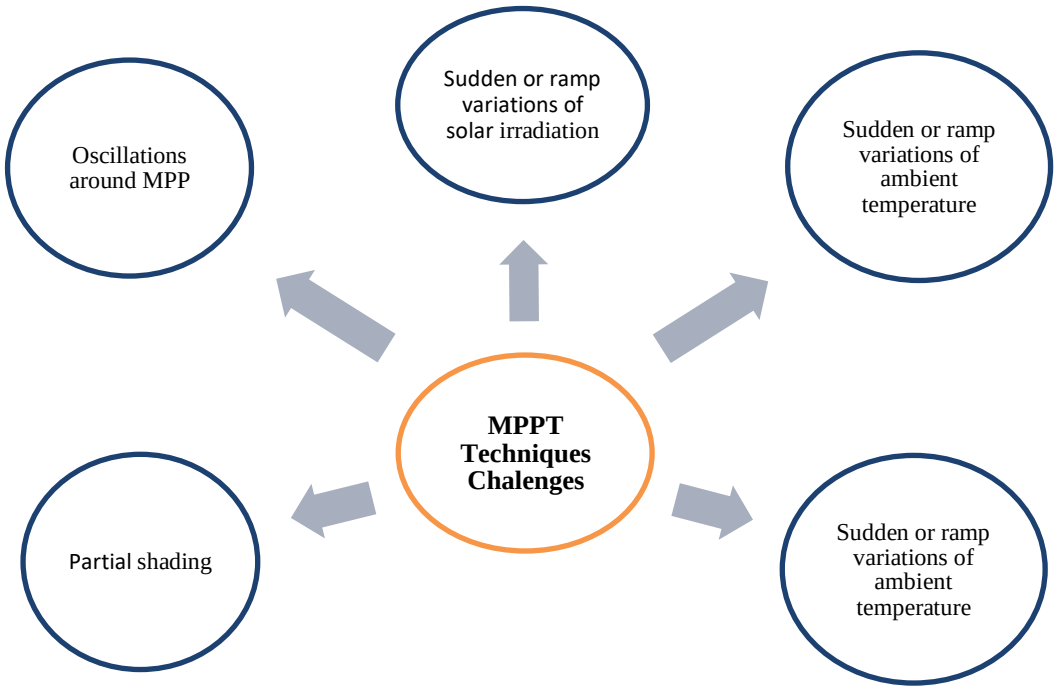


Figure III. 2 Challenges facing MPPT techniques

This partial shading can occur in different configurations as shown in figure III.3 Some of the panels can be hidden by shadows or snow, also we take into account the orientation of the panels on the same string is not identical for the construction strategy of panels. A suboptimal layout of the panels therefore implies that a string can receive inhomogeneous irradiation that can disrupt the search for PPM. The solution in terms of energy savings is to move towards a more individual management of the panels by integrating for example an adaptation stage of GPV.



Figure III. 3 Partial shading for PV modules.

III.4 MPPT techniques

PV systems that operate in environments with non-uniform temperatures and irradiance experience partial shading. Only one GMPP with numerous LMPPs is allowed under PSC. In order to get the most power and high efficiency out of a PV system, maximum power point tracking control is necessary. The tracking and settling time needed tracked power, and efficacy of MPPT techniques. Under these categorizations, various MPPT techniques are studied in this below part.

The classification of all these MPPT techniques is presented in figure III.4.

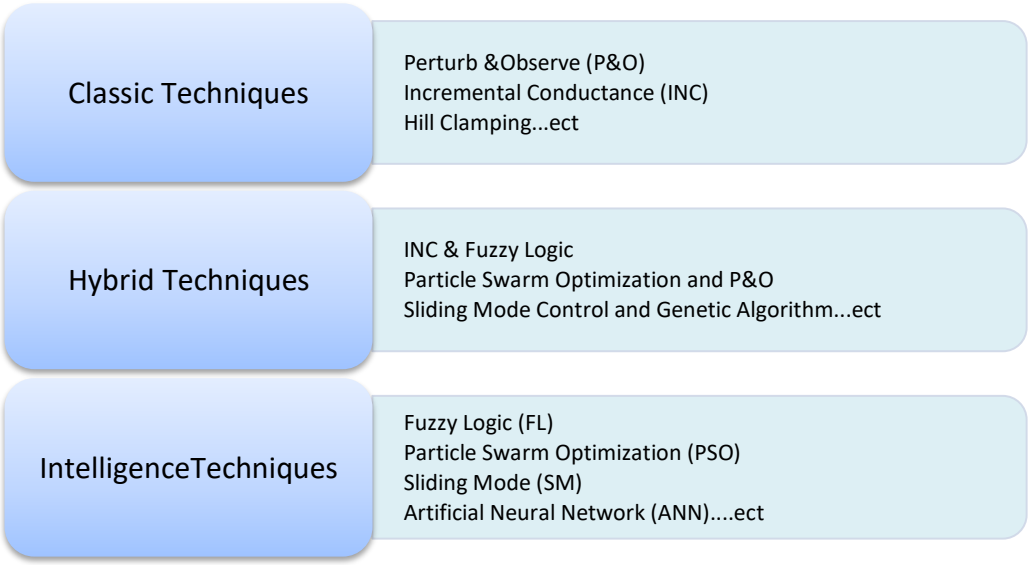


Figure III. 4 MPPT Techniques [41]

III.4.1 Classic Methods

The common techniques explained in subsections as following:

III.4.1.1 Perturbation and Observation (P&O)

The algorithm involves a disturbance on the system by increasing or decreasing the operating voltage ΔV_{pv} and observing the effect on the output power ΔP_{pv}. In this technique, the sign of the last disturbance and the sign of the last power increment are used to decide the next disturbance, as shown in figure III.5.

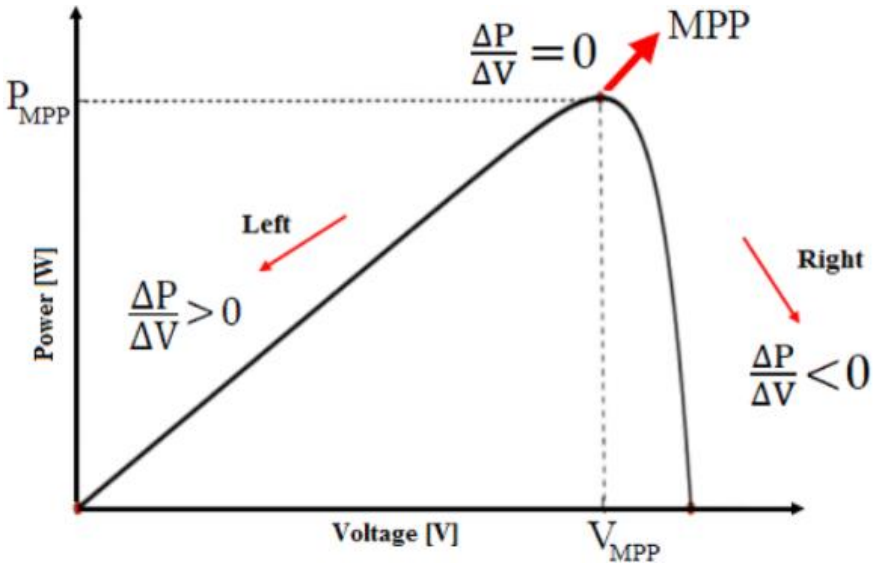


Figure III. 5 *P-V curve of the P&O algorithm* [51]

The follower's work method is shown in figure III.6 by the flowchart, if the power increases, the disturbance causes the operating point to move towards the MPP. The voltage will be perturbed in the same direction by the P&O algorithm. On the other hand, when the power drops decreases Ppv disturbance go beyond the MPP's operating point. The direction of the next will reverse to other disturbance [52][53].

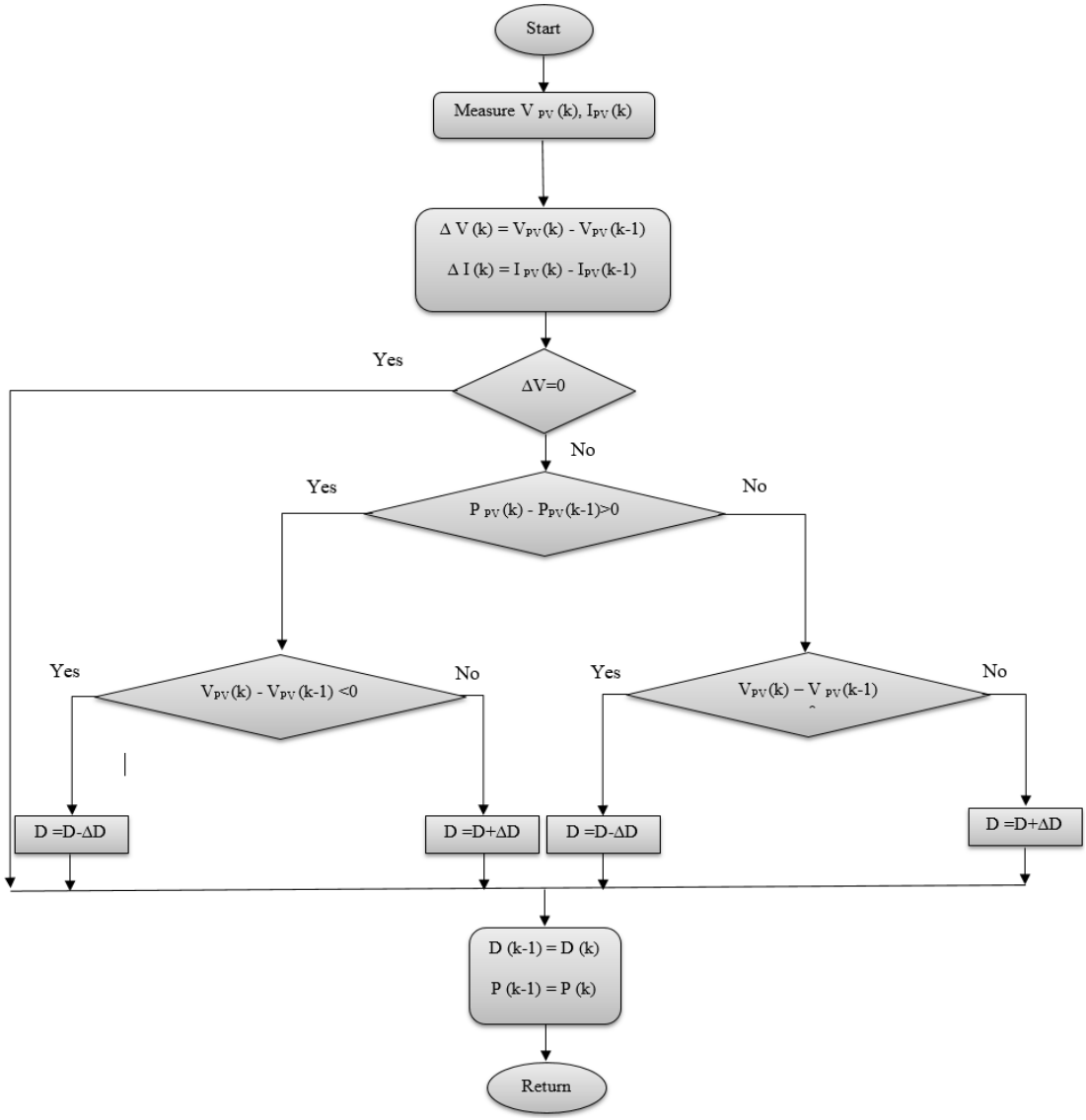


Figure III. 6 Flowchart of the Perturbation and Observation (P&O) method

III.4.1.2 Incremental conductance (INC) method

This technique was produced to overcome the P&O MPPT technique's control [39]. When the MPPT is reached, the INC can beat the perturbation in the operating point.

The instantaneous and Incremental conductance of PV arrays utilized to track the MPP at which the maximum power can be tied below as an equation;

$$\frac{I}{V} = \frac{dI}{dV} \qquad \text{III. 1}$$

Where dI/dV and I/V is the incremental conductance and the instantaneous conductance respectively.

According to the derivative rule in order to get the full control point, the voltage level ratio and the power shift must be zero.

$$\frac{dP}{dV} = \frac{d(V.I)}{dV} = V\frac{dI}{dV} + I \qquad \text{III. 2}$$

As given in Eq III.2 the instantaneous and incremental conductance becomes opposite and equal to achieve MPP, the details as follows:

- If PV voltage is equal to the power "dP/dV=0" that means the duty cycle will be decreased.
- If PV power is less than the voltage "dP/dV < 0" the duty cycle must be decreased.
- If dP/dV > 0 this means the PV power is higher than the PV voltage, which produces an augment to the duty cycle [54].

INC and P & O. determine the actual peak power from the PV arrays. The INC technique is more accurate than P&O technique. In addition, the INC Method shows the exact value of atmospheric change [39].

Figure III.7 clarify the flowchart work method of the follower INC:

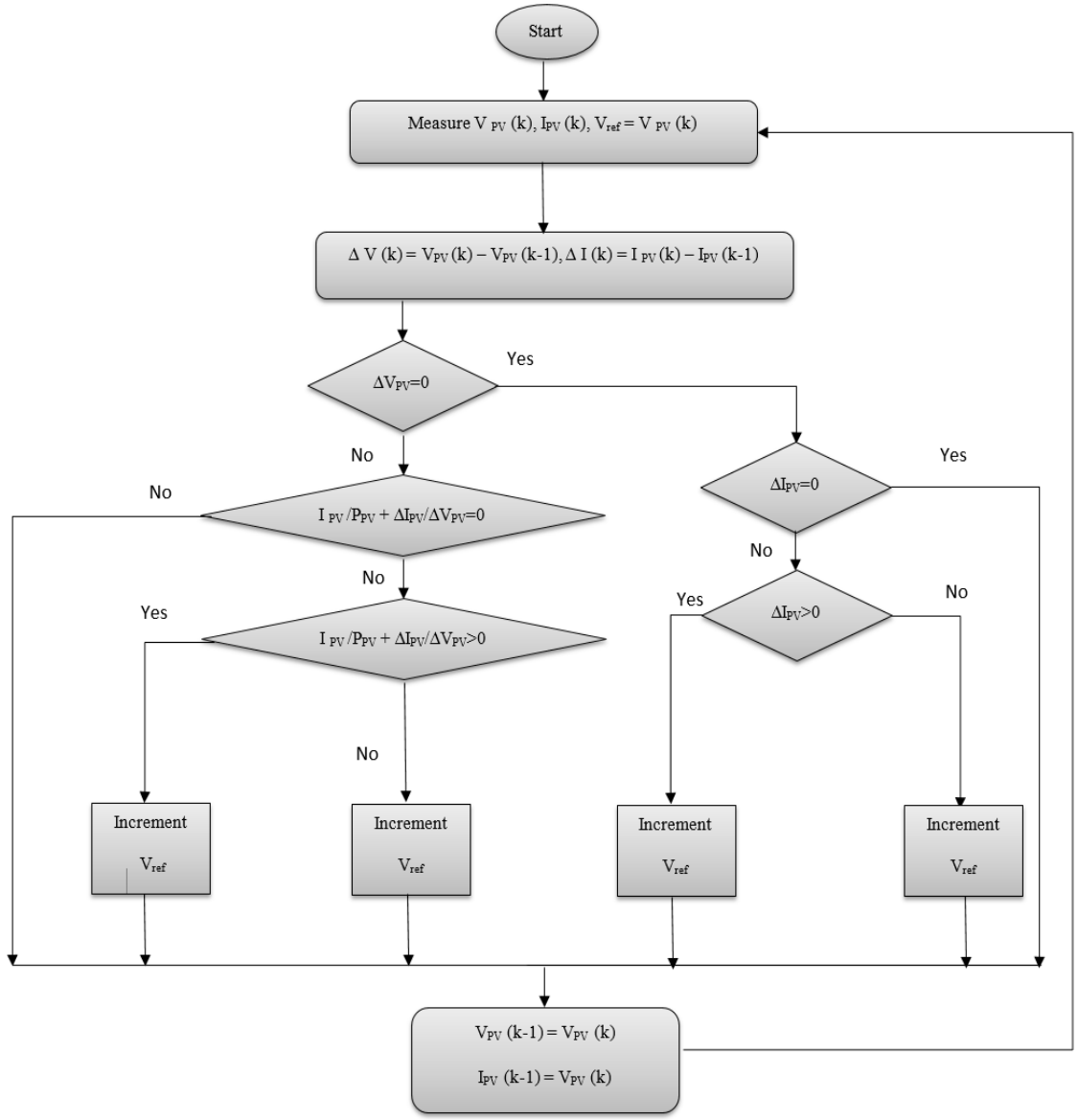


Figure III. 7 Flowchart of the Incremental conductance

III.4.1.3 Adaptive Reference Voltage ARV:

The ARV methodology takes into account climatic conditions, unlike constant voltage MPPT. In order to estimate the levels of temperature T and irradiation, utilize two more sensors than in the conventional CV and one more sensor than in the P&O approach, this system is a little more expensive. However, this cost element was offset by the enhanced efficiency. The extension method to the constant voltage technology is the AVR-based MPPT system because of it adaptability to changing weather condition. The MPPT uses deliberate radiation and temperature condition to modify the RV (Reference Voltage). Figure III.8 displays the schematic block

model for the AVR-based MPPT technique. There are multiple divisions within the radiation working range at a particular temperature, and the comparison RV is stored offline in a truth table. through the simulation comparison of this method with the CV methodology, the inaccuracy between the reference PV voltage is evaluated and compensated using the appropriate proportional integral PI controller to provide an acceptable D proportional to fitting converter. Under constant radiation conditions of 1000W/m2 the efficiency increases for both approaches are almost identical, at 99.7 % [55].

However, the efficiency of CV drops to 98.3% when the irradiation drops to 400 W/m^2 while this ARV technique has the same effectiveness in all conditions variable radiation.

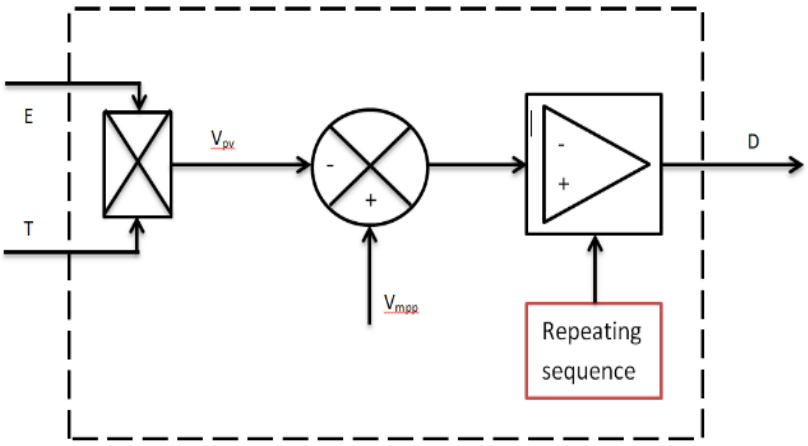


Figure III. 8 Function scheme of ARV-MPPT technique

III.4.1.4 Open Circuit Voltage OCV MPPT

This MPPT OVC also another offline technique, measures an off-line parameter, the open circuit voltage V_{oc}, which will be closer to V_{mpp} and V_{oc} is given by Eq III.3

$$V_{mpp} = k_V \times V_{oc} \qquad \text{III. 3}$$

The practically determined k_v value is in the range of 0.7 and 0.8 and can be known using the data sheet provided by the manufacturer. Figure III.9 is illustrated in the implementation of this technique [56].

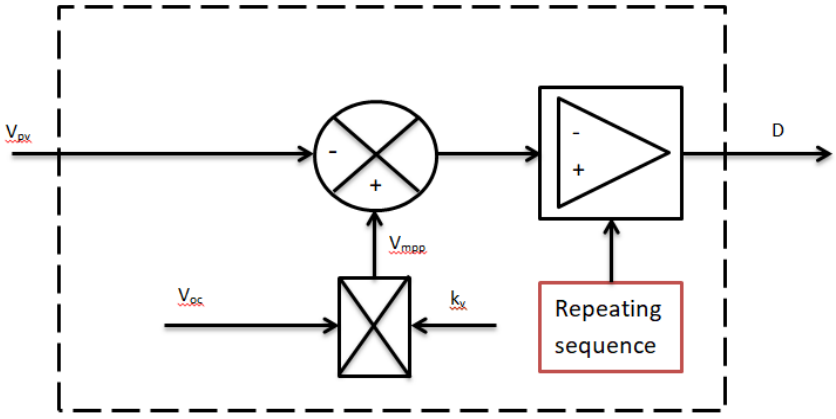


Figure III. 9 Function scheme OVC Method

Due to it primarily relies on the rule of approximation; it is better suited for low-voltage and high-current applications. Inconsistent VOC measurement leads to wasteful power use. To obtain the desired voltage, a closed-loop controller is employed after V_{MPP}'s approximate value has been obtained. As the connection is only an estimate, the PV panel in fact, doesn't ever work at MPP [57], they create the timer intelligent VOC technique, an enhanced method that tracks the MPP in CSPs. We can estimate the hold circuit and sample frequency with this smart timer. This technique is implemented on hardware, and its efficacy is evaluated in comparison to traditional VOC. There are many applications for this technique because it works well in low-power applications. For sampling and tracking values, it makes use of the DG412 estimator, the NSL - 19M51 smart timer, and the LTC1440 estimator.

III.4.1.5 Short Circuit Current SCC-MPPT

This technique determines the ideal operating current for maximizing the power output by measuring the current flowing through the PV module. It appeared that this MPPT approach off line was straightforward to apply algorithmically. Under some arbitrary environmental circumstances, the current at MPP IMPP typically seems near to the short-circuit current ISC. Equation III.4 can be used to calculate the current at the MPP.

$$I_{mpp} = k_I \times I_{sc} \qquad \text{III. 4}$$

Where the k_I factor varies between 0.75 and 0.9 as validated in [58]. The above condition reveals this strategy is only an approximation, and therefore it does not work at defined MPP. The

implementation of this technique is illustrated in figure III.10. This technique is suitable for low current and high voltage applications. In addition, the operation full day requires erratic Isc ratings, resulting in loss of power. A new hybrid method of Fcs with the method P&O that we will see later, is explained in reference [59]. This combination improves overall tracking efficiency...etc. It gives 93.4% and 91.93% under normal weather condition and dynamics, respectively.

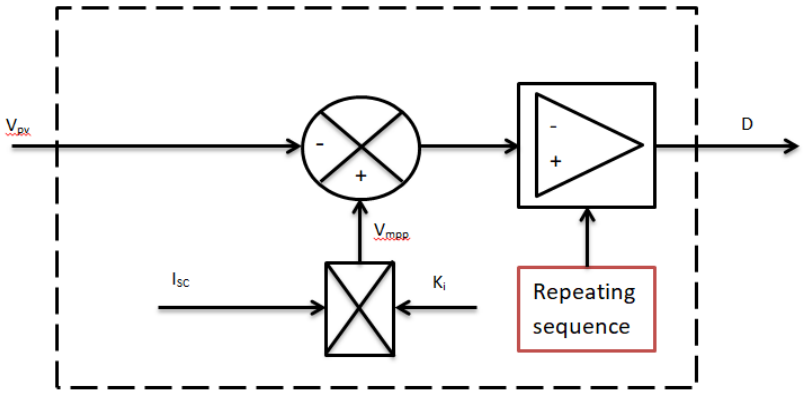


Figure III. 10 Function scheme of SCC method

III.4.1.6 Hill Climbing Methods HC

This very simple technique is widely used in photovoltaic systems because it doesn't require any prior information or a model of the source's attributes. By increasing the characteristic generator's operational point to a maximum of figure III.11, two alternative slopes can be achieved using this technique. In theory, when the maximum power point is achieved. The search ends, this technique is predicated on the correlation between the panel's power and the the duty cycle value applied to the DC/DC converter. The maximum power point will be reached When the converter switch forces dPPV/dD to zero [41]. Figure II.11 displays this method's algorithm. Depending on which direction we need to provide the search to raise the panel's output power, the value of the variable S can take on the values of 1 or -1. The PPV power (k) is periodically compared to the previously calculated value, PPV (k-1), and the sign of the S value either changes or stays the same because of comparison. The duty cycle changes as a result of this. The system oscillates around the latter endlessly after it reaches the MPP. The value of the

selected step determines the oscillation's amplitude. Therefore, when meteorological condition abruptly changes, research on loss occasionally occurs for high amplitude oscillations [60].

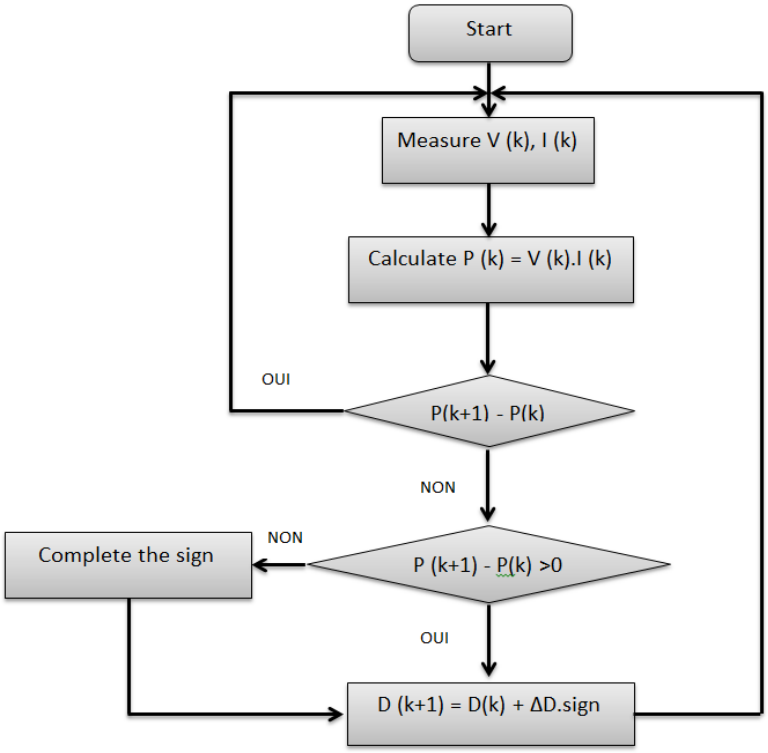


Figure III. 11 Organogram of HC methods

III.4.2 Modern Methods "Artificial Intelligence"

In this previous part, the classical methods and maximum power tracking mechanisms most encountered in the literature were presented. On the other hand, it describes intelligent techniques newly introduced in the field of MPPT commands. The term "artificial intelligence", created by Johan McCarthy in 1956 [61], is often abbreviated by the acronym AI. Therefore, it has been defined by the search for means capable of endowing computer systems with intellectual capacities comparable to those of human beings. Therefore, the artificial side is defined by the use of computers or elaborates electronic processes, and the intelligence side associated with its goal of imitating human behavior. There are mainly artificial fuzzy logic, neural networks, and genetic algorithms, which are currently appearing in electrical control. Furthermore, AI consists of several branches, namely, expert systems, problem solving and

planning, knowledge representation, logic programming, pattern recognition, hybrid intelligent systems, epistemology, ontology, ect.

Two wide AI techniques are used in MPPT control such as:

- **Soft computing techniques** [41]**:**
  Particle Swarm Optimization PSO
  Gray Wolf Optimization GWO
  Ant Colony Optimization ACO
  Algorithm Genetic AG…etc.

- **Hybrid techniques** [41]**:**
  ANN + INC
  ACO + P&O
  FLC + INC
  PSO + INC

In this part we present some common technique mixed between the soft computing and hybrid techniques as follows:

III.4.2.1 Artificial Neural Network (ANN)

As soon as introduced in 1943: Warren McCulloch and Walter Pitts introduced models of neurological networks, calculating nearly any logic or arithmetic function (electronic brains) [62]. ANN is electronic models based on the neural structure of the brain, which are often used for the optimization of MPPT algorithms. Indeed, neural networks can be used to find the position of the maximum power point with a reduced number of iterations to reach the MPP and a reduction to minimum of oscillations around it. Figure III.12 presents the general diagram of an artificial neural network.

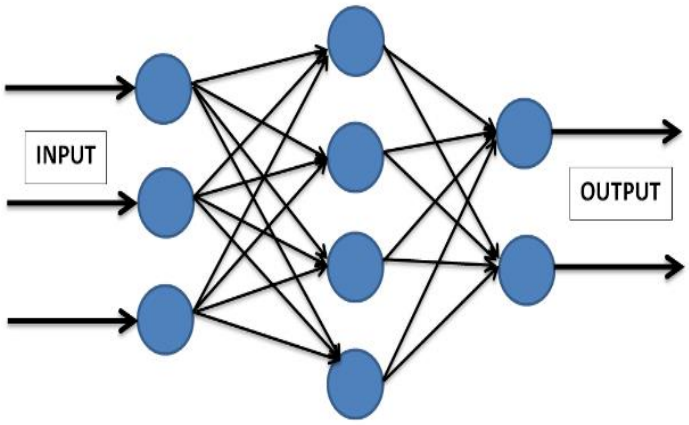


Figure III. 12 Three layer feed-forward neural network

III.4.2.2 Genetic Algorithm

It was introduced by Johan Holland [63] during the 1960s and 1970s, and popularized by one his students, David Goldberg [64]. Since then many versions of evolutionary programming have been tried with varying degrees of success.

Genetic algorithms are stochastic optimization methods based on the mechanisms of natural selection and genetics, inspired by Darwin's survival theory. Due to the remarkable performance of GAs, they have invaded several research fields in which they have brought appreciable satisfactions because of their advantages, namely the speed and the possibility of solving nonlinear equations with several variables. The simplified organization chart of an AG shown in figure III.13 [65].

It's one of the smart approaches used to track the maximum power point PPM of photovoltaic cells so that they can take maximum advantage of solar energy and quickly track.

Many works have been done that GAs give very interesting results in which convergence is assured, with computation times and simple operations. Nevertheless, FA have a drawback which lies in the use of probability relations, thus making the result sometimes unpredictable and the performance less controlled [66].

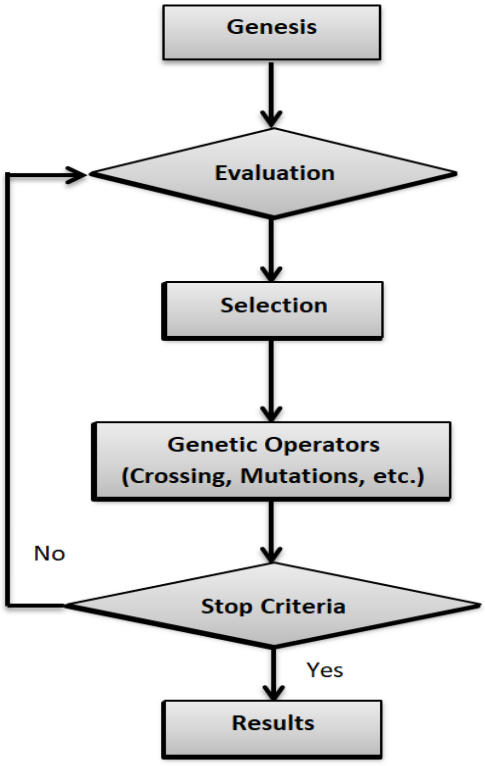


Figure III. 13 General principles of genetic algorithms

III.4.2.3 PSO & ANN-based Hybrid MPPT Method

PSO is a stochastic search technique that tracks a global peak over an extended period of time. As a result, some adjustments were needed; an Artificial Neural Network (ANN) provides the initial particle position of the Particle Swarm Optimization (PSO) method in the new ANN and PSO-based hybrid method. This global MPP is close to this initial particle position (INC). Therefore, the range of the PSO algorithm is reduced. The PSO algorithm uses this starting value to determine the PV array's output current at global MPP. detects the output current of the PV array at global MPP. Additionally, the PSO algorithm is now capable of finding the global MPP quickly [61].

Furthermore, artificial neural networks ANN are able to identify sudden changes in solar irradiation and provide the PSO algorithm with a new initial particle position (INC). figure III.14 shows the flow chart for this procedure.

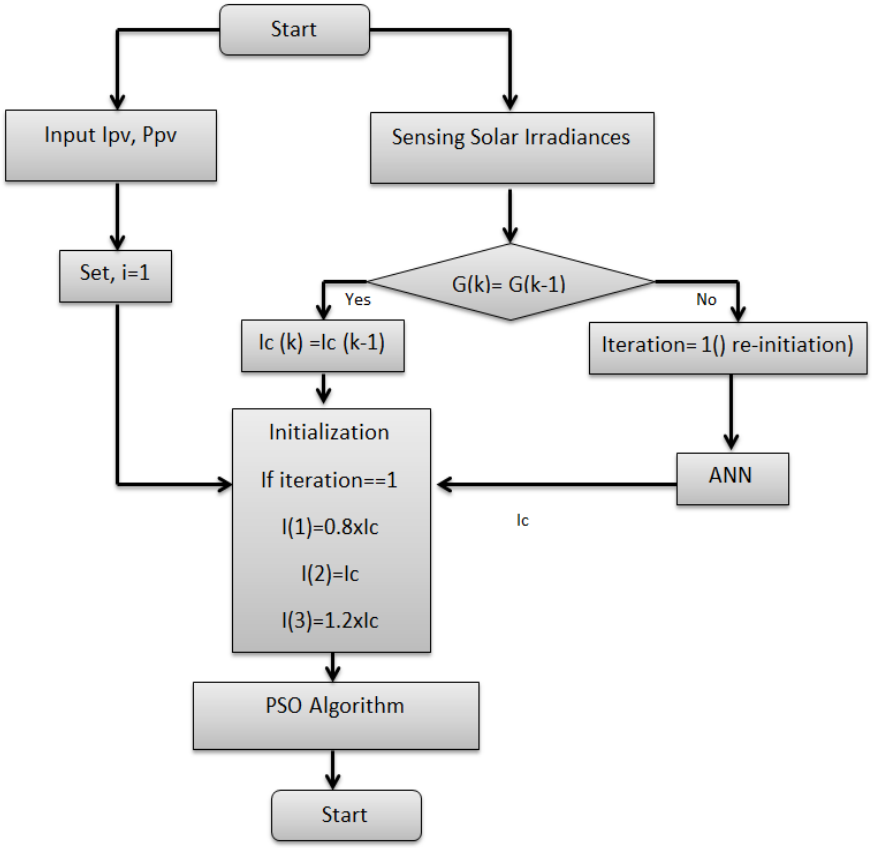


Figure III. 14 Flow Chart of the Hybrid Method

III.5 MPPT based on Sliding Mode Control (SMC) for Stand-Alone System (SAS) "proposed method"

PV systems are not connected to the grid summarized in the term "stand-alone PV system". A PV panel, DC/DC boost converter, load, and a control circuit MPPT are used to operate the system [33], [67]. The figure III.15 shows the description of PV system parts, the modules are connected to PV arrays (2 series and 3 parallel). The specifications of the PV module are as detailed below on table:

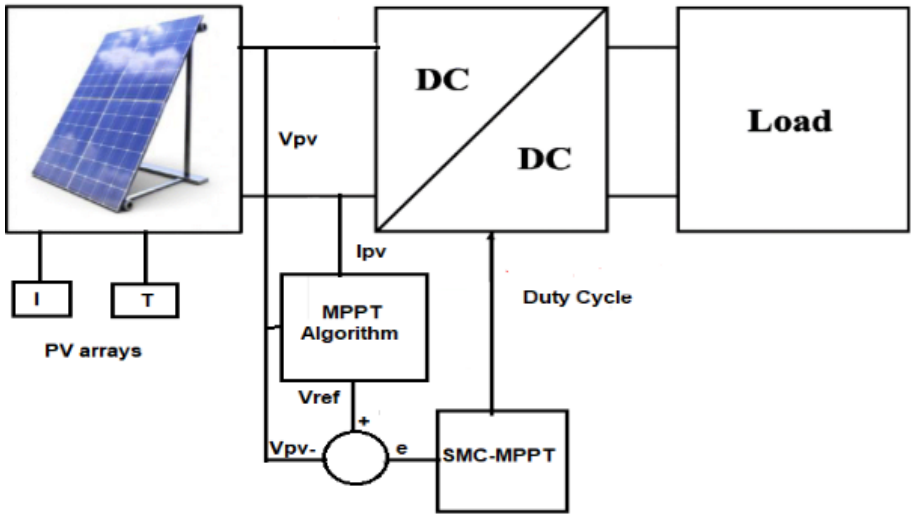


Figure III. 15 The basic structure photovoltaic system

Table III. 1 KC200GT Data Sheet under STC Conditions and internal parameters

Number of cells in series of each panel (Ns)	54
Power maximal (Pmax)	200.143 W
Current of short-circuit (Isc)	8.21 A
Voltage of circuit open (Vco)	32.9 V
Current of MPP (Impp)	7.61 A
Voltage of MPP (Vmpp)	26.3 V
Resistance series (Rs)	0.0036 Ω
Factor ideal (n)	1.4099
Courant inverse de saturation (Io)	4.0992 e-7 A
Photo current (Iph)	8.2100 A

Installed between PV arrays and load a DC-DC boost converter. The latter's parameters as follows:
Can express the duty cycle as follows:

$$D = \frac{V_{out} - V_{pv}}{V_{out}} \qquad III.\ 5$$

The following interval serves of the duty cycle:

$$D_{max} = \frac{V_{out_max} - V_{pv_min}}{V_{out_max}} \qquad III.\ 6$$

And,

$$D_{min} = \frac{V_{out_min} - V_{pv_max}}{V_{out_min}} \qquad III.\ 7$$

The inductor's maximum current can be expressed as follows:

$$I_{L\,max} = \frac{P_{max}}{V_{pv_min}} \qquad III.\ 8$$

We consider a 10% ripple in the inductor's maximum current (ΔI_L), and 5% fluctuation in the capacitor's voltage (ΔV_{out}).

Given the inductor value as follows:

$$L_{max} = \frac{D_{max} V_{pv\,max}}{f \Delta I_L} \qquad III.\ 9$$

$$\Delta V_{out} = 0.05 V_{out\,max} \qquad III.\ 10$$

We express the maximum current as following:

$$I_{pv\,max} = \frac{P_{out\,max}}{V_{out\,min}} \qquad III.\ 11$$

We defined the capacitor value by:

$$C_{max} = \frac{D_{max} I_{out\,max}}{f \Delta V_{out}} \qquad III.\ 12$$

The input capacitor C_{input} established to the equation below:

$$C_{input} = \frac{D_{max}}{8.L_{max}.f^2.0{,}02.V_{pv}} \qquad III.\ 13$$

Significantly increase tracking accuracy and decrease the size of ripples on both sides of the boost converter. Undoubtedly, the proposed scheme can offer a faster time response to close and track the expected MPP, which is a time faster than that of INC.

III.5.1 SMC MPPT technique

This control, which first appeared in the Soviet Union in the 1950s, provides good dynamic and stability in results even with significant variations in power or load [68], [69]. The theory of structure-system variables (SSV) makes it possible to complete the task. In equation III.18 shown the derivative of power is equal to zero [70].

We take based on the equation III.10 of the sliding surface in the present document:

$$S = dP \qquad III.\ 14$$

The relation expressed the control signal as follows:

$$D = D_{eq} + D_n \qquad III.\ 15$$

Where U_n is the switching control and U_{eq} is the equivalent control. U_{eq} found from the steady condition and given as below:

If $U=U_{eq} \leftrightarrow S=0$ & $\dot{S}=0$ the derivative of the sliding surface is:

$$\dot{S} = \frac{d}{dt}[dP] = \frac{d}{dt}[d(V.I)] \qquad III.\ 16$$

$$\dot{S} = dV.\frac{dI}{dt} + dI.\frac{dV}{dt} = k_1.\frac{dI}{dt} + k_2.\frac{dV}{dt} \qquad III.\ 17$$

$$k_1 = dV \ \ \& k_2 = dI \qquad III.\ 18$$

The laws of voltage and current in the circuit in two cases (switch off & on) of figure III.16, by applying Kirchhoff's function:

$$\frac{dI}{dt} = \frac{V_{pv}}{L} - \frac{V_{out}}{L}(1-D) \qquad III.\ 19$$

$$\frac{dV_{out}}{dt} = \frac{I_L}{C}(1-D) \qquad III.\ 20$$

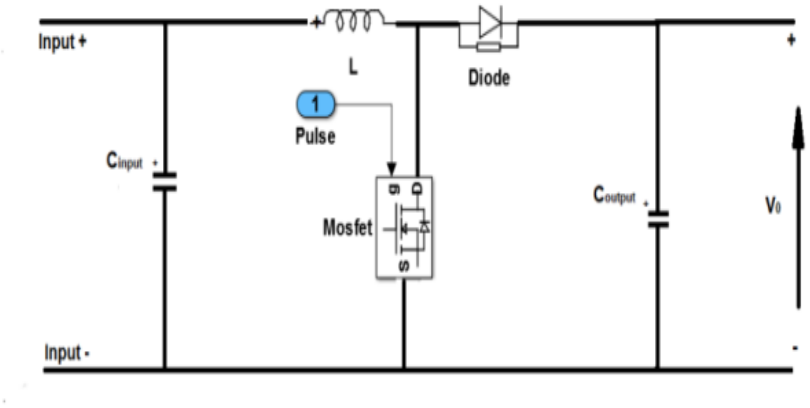


Figure III. 16 The electrical diagram of the boost converter

Substituting Eq (III.20) & (III.18) into Eq (III.21) results as:

$$\dot{S} = k_1\left[\frac{V_{pv}}{L} - \frac{V_{out}}{L}(1-D)\right] + k_2\left[\frac{I_L}{C}(1-D)\right] \qquad III.\ 21$$

By imposing, this is conditions $S=0$ & $\dot{S}=0$ we get:

$$\dot{S} = 0 \rightarrow k_1\left[\frac{V_{pv}}{L} - \frac{V_{out}}{L}(1-D)\right] + k_2\left[\frac{I_L}{C}(1-D)\right] = 0 \qquad III.\ 22$$

According to Eq (II.11), the control input is taken as:

$$D_{eq(t)} = 1 - \frac{V_{pv}}{V_{out}} \qquad III.\ 23$$

The trajectory of the sliding surface is so essential, that the U_n is selected for the stability criterion ($\dot{S}.S < 0$).

$$D_{n(t)} = \frac{V_{pv}}{V_{out}} - B \qquad III.\ 24$$

Where B is calculated according to Lyapunov's stability criteria and considered as a control signal.

Substituting Eq. (III.24) and Eq. (III.25) into Eq. (III.26) as follows:

$$D_t = 1 - B \qquad III.\ 25$$

The Lyapunov function was adopted to explain the stability.

$$P = \frac{1}{2}S^2 \quad then \ \dot{P} = S.\dot{S} \qquad III.\ 26$$

Replace Eq. (III.22) and Eq. (III.27) with Eq. (III.28), which shows the following result:

$$\dot{P} = \left(k_1\left[\frac{V_{pv}}{L} - \frac{V_{out}}{L}(1-D)\right] + k_2\left[\frac{I_L}{C}(1-D)\right]\right).S \qquad III.\ 27$$

$$\dot{P} = \left(B\left[\frac{V_{out}}{L}.k_1 - \frac{I_L}{C}.k_2\right] + \frac{V_{pv}}{L}.k_1\right).S \qquad III.\ 28$$

The convergence result is given below:

$$\{if\ S < 0 \Rightarrow B < \frac{V_{pv}.k_1.C}{V_{out}.k_1.C - I_L.k_2.L}\ if\ S > 0\ \Rightarrow B > \frac{V_{pv}.k_1.C}{V_{out}.k_1.C - I_L.k_2.L}\ if\ S = 0\ \Rightarrow B = \frac{V_{pv}.k_1.C}{V_{out}.k_1.C - I_L.k_2.L}$$

III.5.2 Simulation Results and Discussion

Three PV modules KC200GT connected in series and two parallel connections, which are under the supervisor of INC and SMC controllers. Are used to carry out the simulation. The stand-alone system, which has been built and simulated in Matlab / Sim Power, it is being monitored by the controllers.

The irradiation and the temperature used are variable as shown in figures (III.17& III.18) and the load is considered constant R = 350Ω.

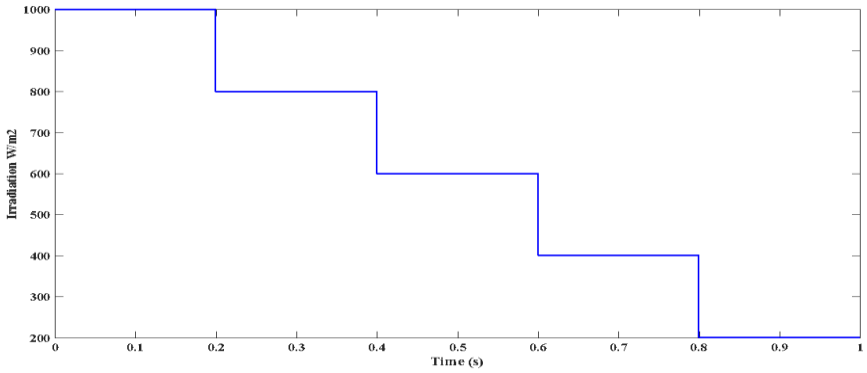


Figure III. 17 The variation of irradiation

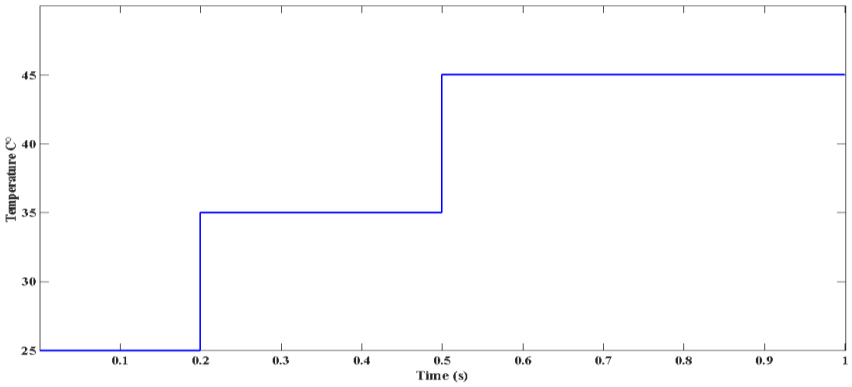


Figure III. 18 The variation of temperature

The irradiations were varies as chosen in figure III.17 and the temperature was set at T =25°, where the curves show the results in Figures (III.19 & III.20):

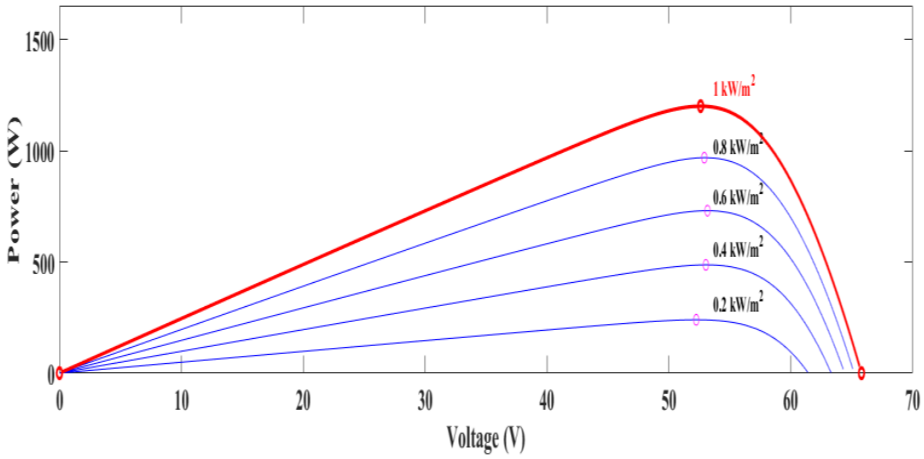


Figure III. 19 The Voltage-Power characteristic with different irradiation

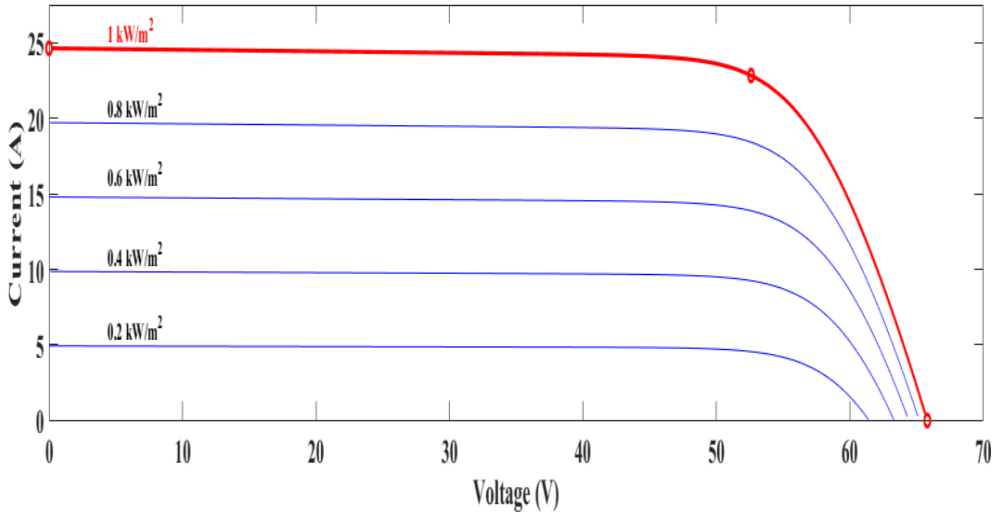


Figure III. 20 The Current-Voltage characteristic with different irradiations

The temperatures varied as chosen in figure III.18 and the irradiation was set at 1000 W/m2, where the curves show the results in Figures (III.21 & III.22):

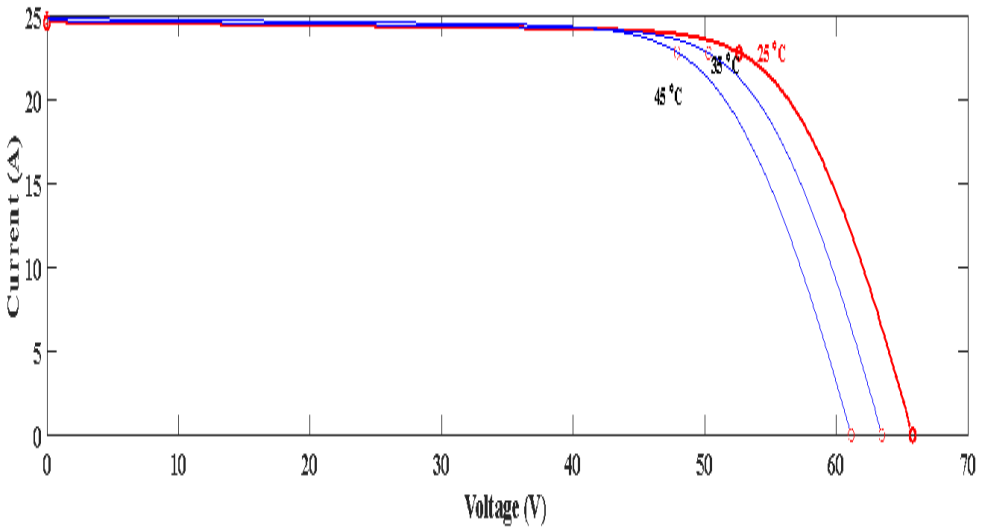


Figure III. 21 The Voltage-Current characteristic with different temperatures

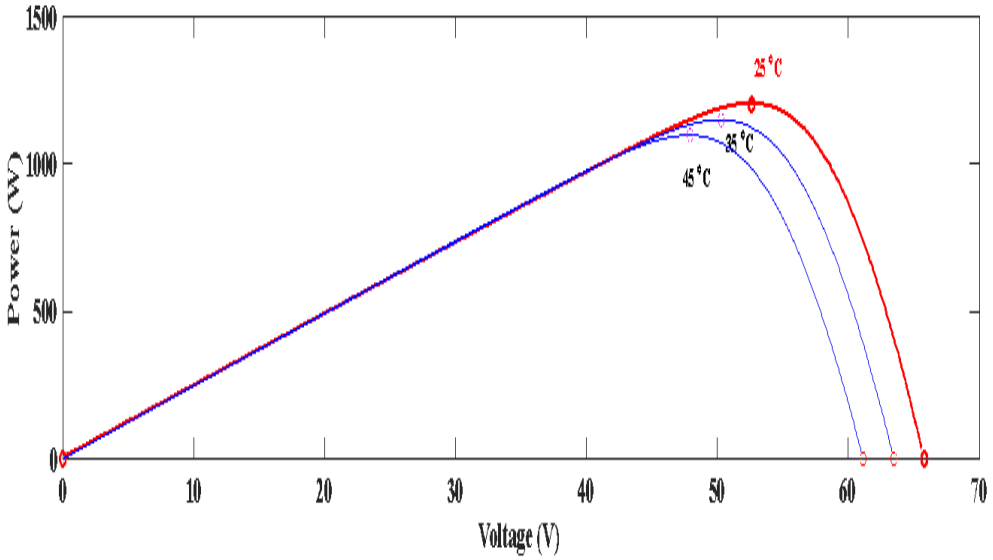


Figure III. 22 The Voltage-Power characteristic with different temperatures

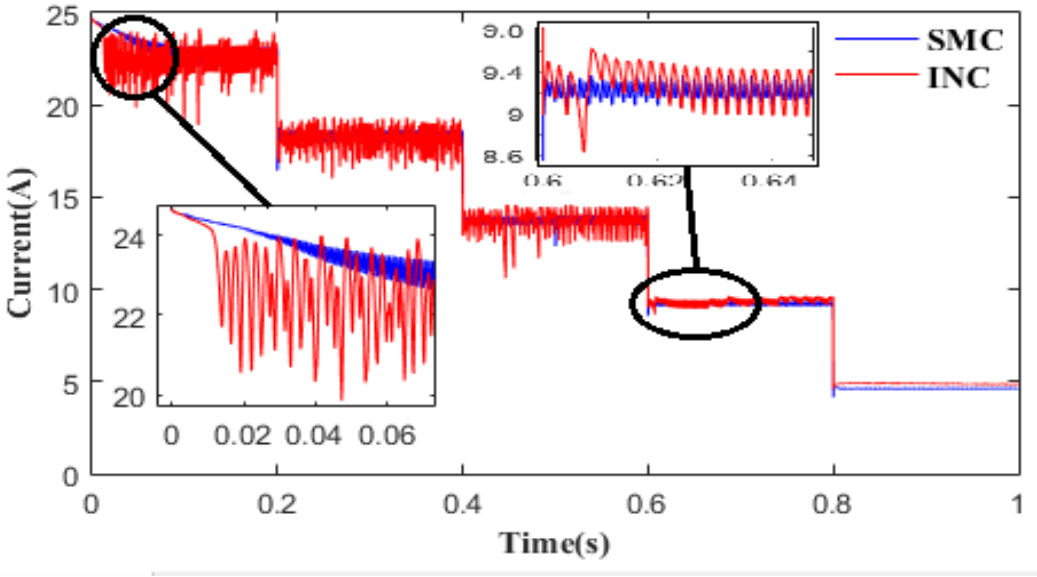


Figure III. 23 Output Current of PV KC200GT arrays

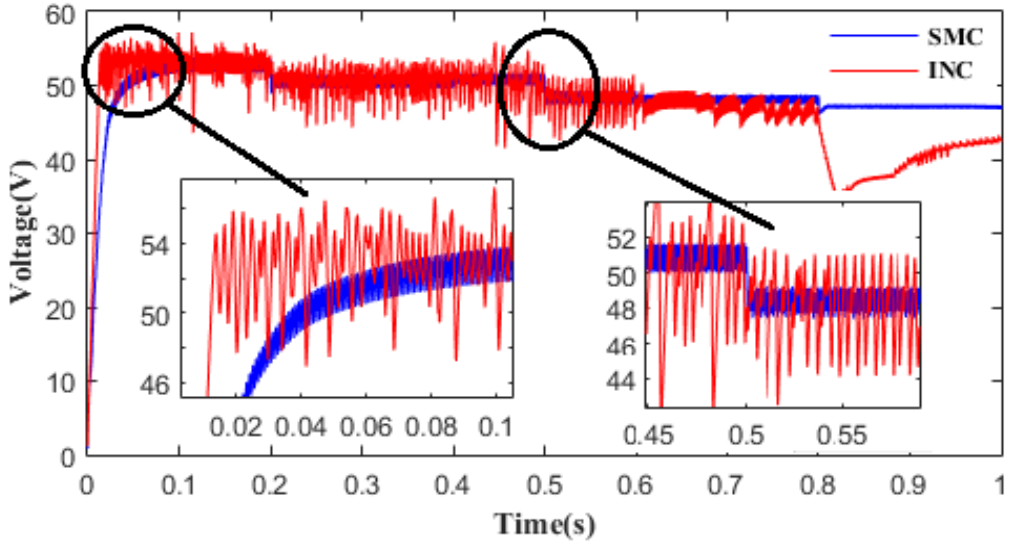


Figure III. 24 The output voltage of PV KC200GT arrays

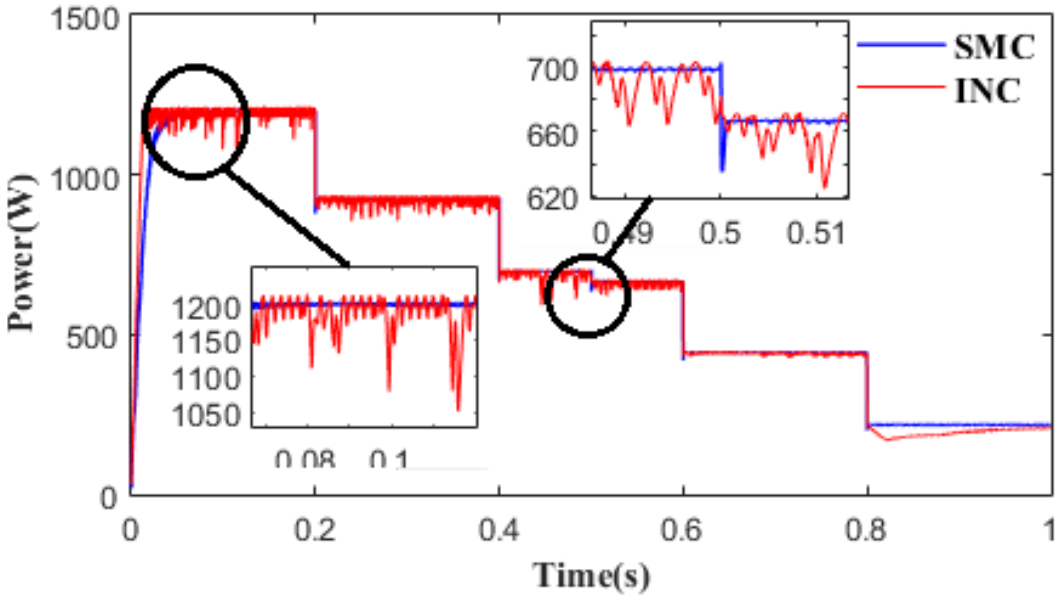


Figure III. 25 Power of PV KC200GT arrays

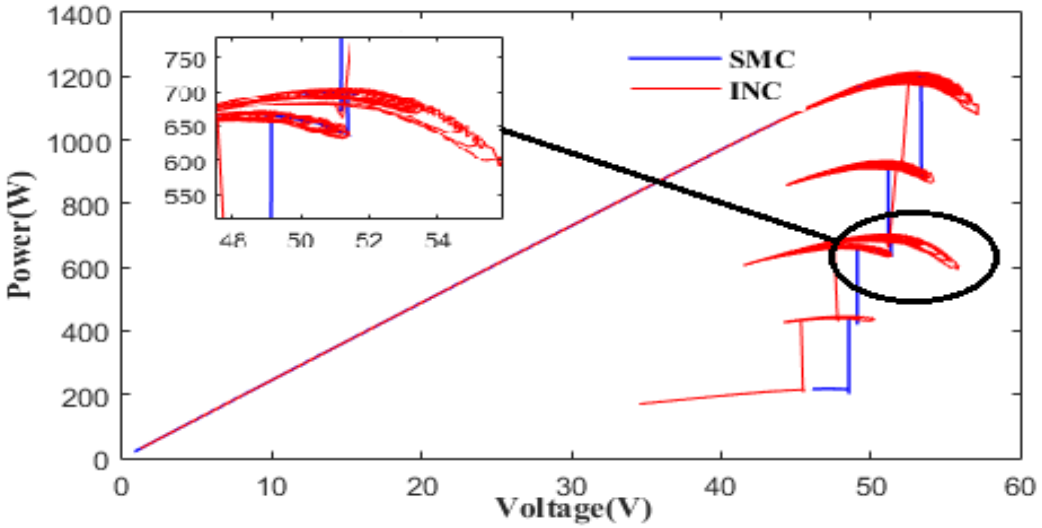


Figure III. 26 Dynamic MPPT of PV KC200GT arrays

The simulation results on the MPP for the sliding mode control and INC were achieved while the metrological conditions changed quickly. In Figure III.24, the sliding mode control (SMC) responds well and demonstrated its capacity to steady the voltage next to the necessary value. The INC is chattering as it approaches the necessary voltage, and after 0.8 seconds, the voltage falls short of what is needed.

The output current is displayed in Figure III.23 when the temperature rises and the irradiance falls on its own. Two controllers experience a current drop. Comparing the SMC controller to the INC controller, the SMC responds better and with fewer disturbances.

This research aims to maximize power output from photovoltaic arrays. When the weather changes, the SMC controller in Figure III.25 operates with accuracy in tracking and stability. On the other hand, INC controllers are highly perturbed around MPP and during climate changes. Additionally, in situations with high temperatures or low levels of radiation, INC controllers are unable to maintain the required load.

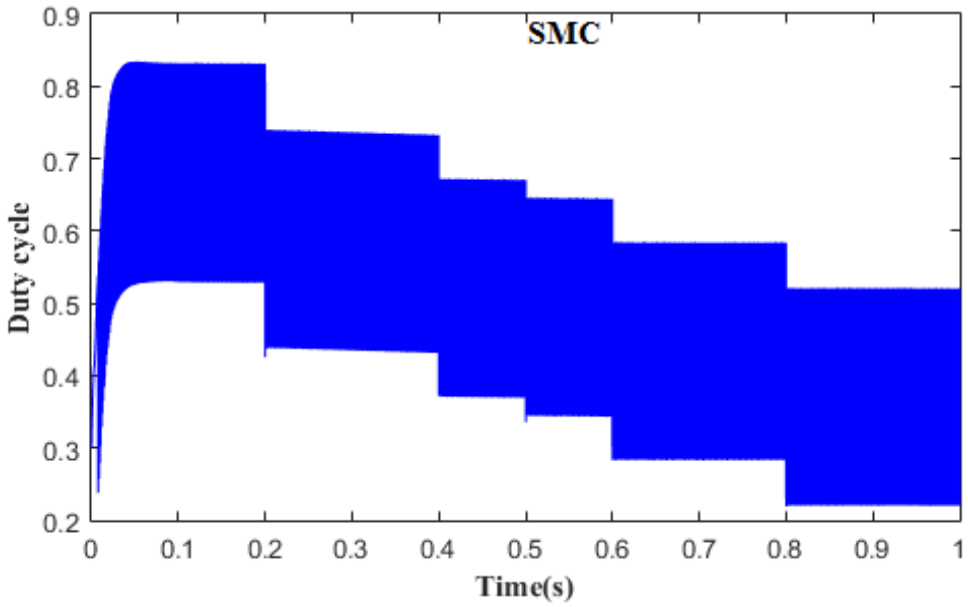


Figure III. 27 The duty cycle of PV arrays by sliding mode control

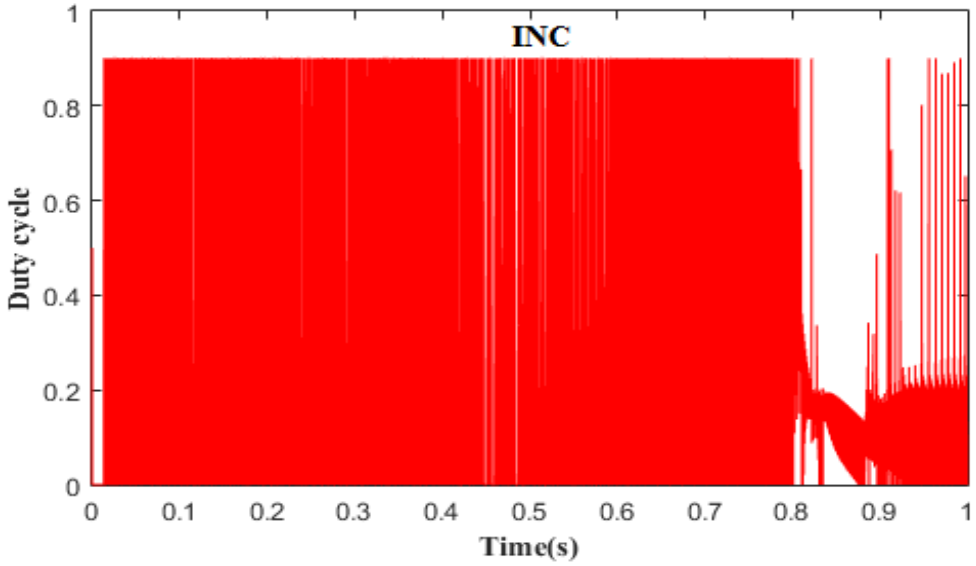


Figure III. 28 The duty cycle of PV by incremental conductance

The difference is so clear in figures (III.27 & III.28), the optimum duty cycle of SMC shows the same reaction on each step, and the trucking graph proposed in figure III.6, a robust and fast response.

The duty cycle of INC has a perturbation that is not stable, not reliable and loses control after 0.8s.

III.6 CONCLUSION

In this section, I explained the challenges that PV systems face and how they forced our research to employ MPPT techniques. On this road, I have been presented with several techniques that have been used and techniques that are still under study. Furthermore, we divided the techniques into three categories: “classic, modern, and hybrid,” and we listed the advantages and disadvantages of each.

Ultimately, the simulation results indicate that a stand-alone PV array system would be best designed with sliding mode control. Furthermore, in terms of overshoot, ripple, speed, and accuracy, it outperforms traditional INC-MPPT by a considerable margin in high environmental variation. Furthermore, the dynamic responsiveness is greatly improved by the SMC-MPPT. The simulation further demonstrates the accurate tracking of the suggested method. Next, we'll demonstrate how INC has been optimized using two different approaches.

IV Optimization of Incremental Conductance for MPPT of a Photovoltaic

IV.1 INTRODUCTION

In recent times, the utilization of renewable energy sources has allowed individuals to meet their energy needs while also preserving the environment [22]. Solar energy, in particular, has witnessed significant growth due to factors such as cost reduction, technological advancements, supportive governmental regulations, job creation, environmental concerns, and its low carbon footprint [71]. This has led consumers worldwide to embrace alternative energy sources like solar and wind. Among these renewable sources, solar energy stands out as a noiseless, clean, and abundant resource that continues to witness industry growth, especially in photovoltaic (PV) systems since the invention of solar cells in the 1970s. Solar cells have experienced notable improvements in efficiency over the years. However, the nonlinearity of solar cell parameters and the influence of operating temperature and irradiance on power generation pose challenges to optimizing the performance of PV cells.

Addressing these challenges, the use of Maximum Power Point Tracking (MPPT) controllers has been recommended to enhance the utilization of solar energy effectively [72]. Various MPPT algorithms have been developed, including perturb and observe (P&O), hill climbing (HC), and incremental conductance (INC) [73]. Advanced artificial intelligence techniques such as fuzzy logic control (FLC) [44], [43] and neural networks (ANN) [74] have also been applied. Hybrid techniques combining different methodologies, like FLC-ANN [75], GA-INC [76], FLC optimized by particle swarm optimization (PSO) [44], and PSO-ANN [61], have gained interest and present further research opportunities.

IV.2 PV optimization Technique

Since the 1600's, expected values for the optimization method by Blaise Pascal have been promising. Figure IV.1 provides an overview of techniques for enhancing the energy output of solar panels and their direct and indirect impacts on partial shadowing and dust buildup on the PV panel surface. Ultimately, the framework seeks to achieve an optimum solar panel arrangement that allows increased energy production under partial shade or in a dusty averment.

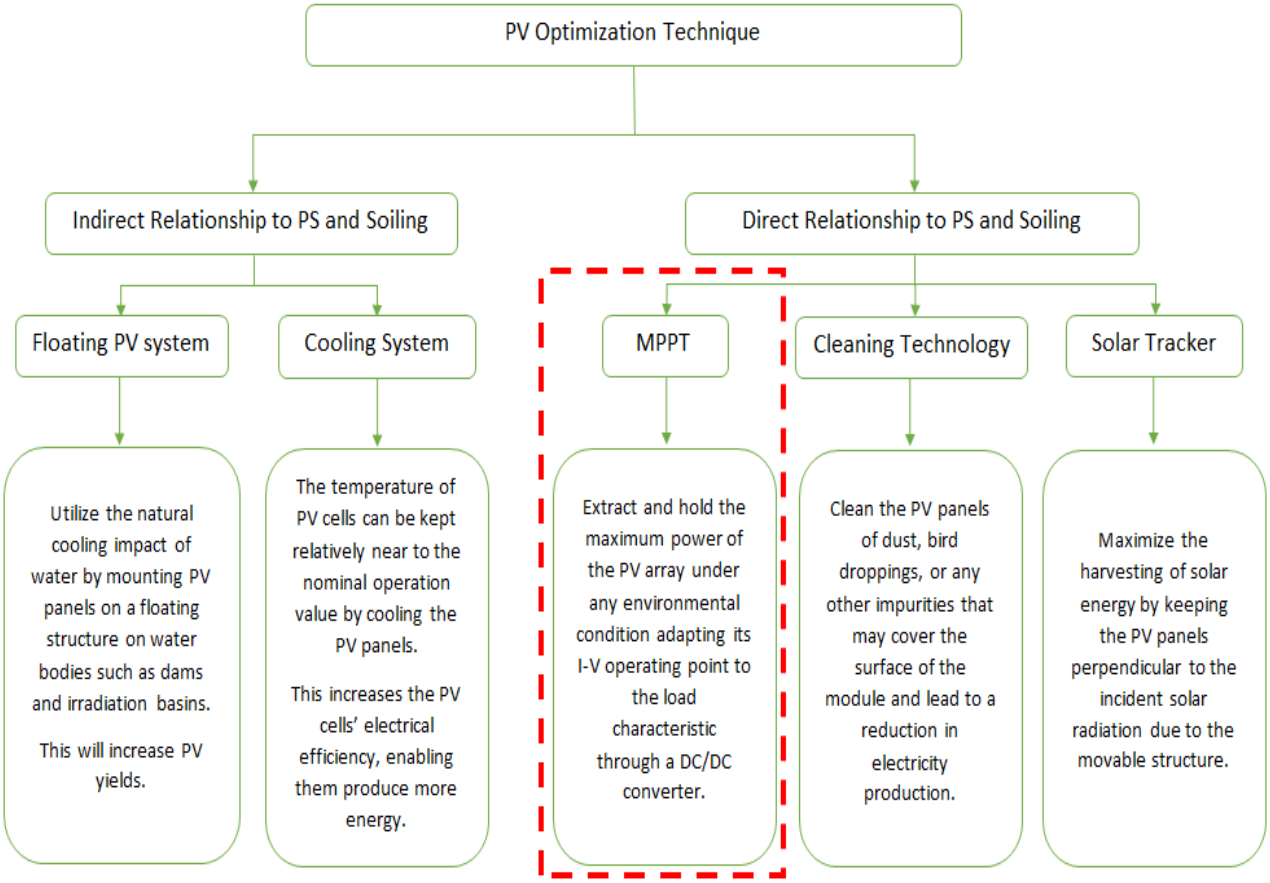


Figure IV. 1 Optimization techniques are commonly used for the output PV system.

In this thesis, we concentrate the work on optimization techniques of MPPT as per Sliding Mode Control (SMC), Incremental Conductance (INC), and Fuzzy Logic Control (FLC).

Increasing the performance and tracking effectiveness of solar photovoltaic systems is the goal of this research. In order to accomplish this goal, the photovoltaic array must be operated at its maximum power while the output ripple issue of DC-DC converters, which affects and stresses sensible electronic loads, is minimized. An advanced maximum power point tracking (MPPT) scheme is used, which can ensure that accessible MPP is tracked without oscillation and that the output side of the DC-DC boost converter has ripple of a smaller magnitude. Using the MATLAB/Simulink environment, various simulations are run under five solar irradiation variation scenarios of standard test condition (STC), and temperature scenarios in order to evaluate and compare the new MPPT scheme's tracking resiliency to the traditional INC MPPT scheme.

IV.3 Optimization of Incremental Conductance Using Particle Swarm Optimization-Tuned PID Controller for MPPT of a Photovoltaic Stand-Alone System

IV.3.1 Particle Swarm Optimization (PSO) algorithm

A search technique used in computing to find near-optimal solutions to optimization problems, proposed in 1995 by [77], [78]. PSO is a swarm intelligence inspired by the social behavior and dynamic movements of insects, birds, and fish. Uses a large number of particles to form a swarm that moves the search space in search of the best solution [79]. Moreover, each particle in search space adjusts its flight according to its own flying experience as well as the flying experiences of other particles, where the global best particle (Gbest) and the best particle (Pbest) are with the utilization of Eq (IV.1), a velocity factor is used to perturb each particle's updated position (Xi).

$$X_{i(t+1)} = X_{i(t)} + V_{i(t+1)} \qquad IV.\ 1$$

Where the perturbation factor, obtained using Eq (IV.2), is represented by the Vi (t+1);

$$V_{i(t+1)} = V_{i(t)} + C_1 r_1 \left[P_{besti} - X_{i(t)}\right] + C_2 r_2 \left[G_{best} - X_{i(t)}\right] \qquad IV.\ 2$$

Where, r1 and r2 are the random numbers in the range [0 – 1]. While c1 and c2 are the cognitive and social constants, respectively.

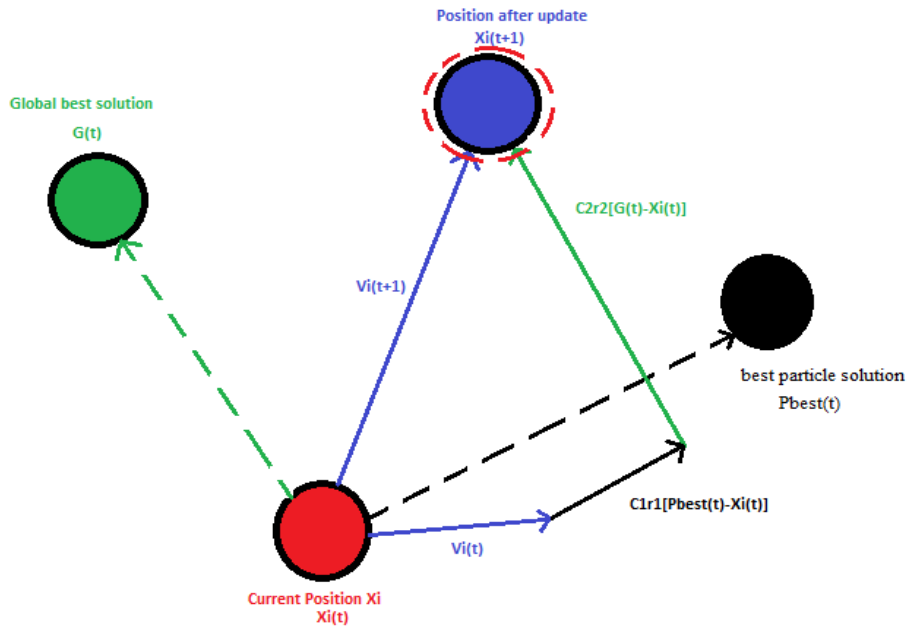


Figure IV. 2 The random movement of PSO model

IV.3.2 PSO-Based Tuning of PI Controller

Conventional PI controllers typically use secondary frequency controls in common power systems, which are typically tuned using a set of predetermined operating points. When the power system's operating conditions change [80]. However, they are unable to deliver the desired performance that was assigned to them. The PI controller will function at its peak if it can continuously monitor the alterations occurring in the power system. FL can therefore be used as a suitable intelligent approach for online PI controller parameter tuning [81].

This work presents a novel modified step size technique of conventional INC. PSO is utilized to improve the gain of the PI controller as shown in the figure IV.3.

$$u(t) = k_p e(t) + k_i \int_0^t e(t).d\tau \qquad \text{IV. 3}$$

Where Kp stands for proportional gain, and Ki for integral gain. Equation's e(t) is optimized to be as small as possible.

$$e(t) = SP - PV(t) \qquad \textit{IV. 4}$$

Where PV stands for process value, SP for set point, e(t) for reference error, t for instantaneous time, and for the integration variable τ that takes values from [0 , t] at the moment of operation.

The four indices ISE, IAE, ITAE, and ITSE frequently used to describe the efficiency of a PI-controlled system [82]. We chose ITSE in this paper, which is the fitness function: Integral of Time weighted Absolute Error (ITAE), which is frequently used, regarded as the fitness function for the best outcome.

$$ITAE \int_{t=0}^{t=final} |\Delta f| \times t \times dt \qquad \textit{IV. 5}$$

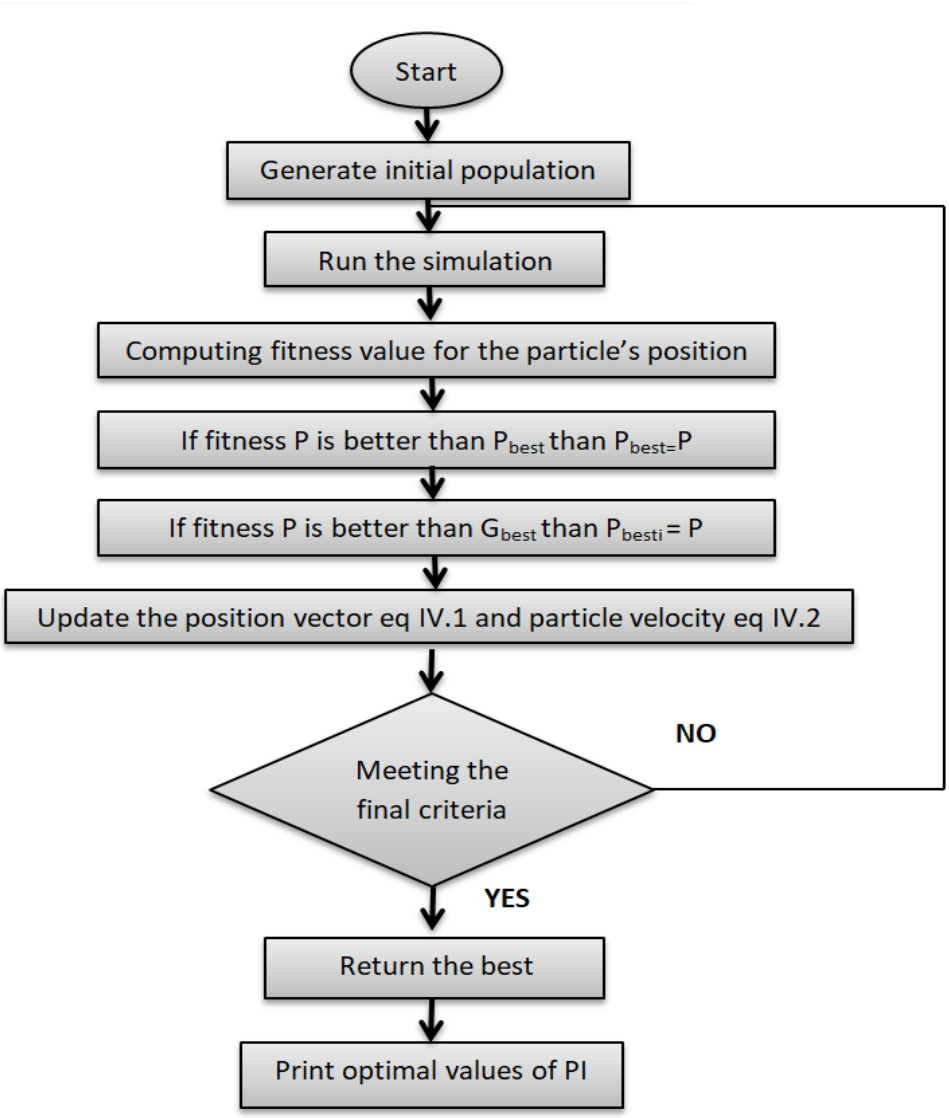


Figure IV. 3 The process to implementing the PSO algorithm for tuning the PI

This makes it possible for the system to respond quickly and dynamically and greatly reduces its complexity. The proposed system shown in Figure IV.4. In order to verify the effectiveness of the tracking algorithm and its response time, was simulated in Matlab, and the response time for the proposed optimization algorithm PSO-INC was looked at following that, the PSO-PID algorithm, which uses particle swarm optimization to tune the PID algorithm, was contrasted with conventional INC techniques. With a fixed step-size of one, INC updates the duty cycle D on a regular basis. The converter's switching frequency was set to 50 kHz [82][28].

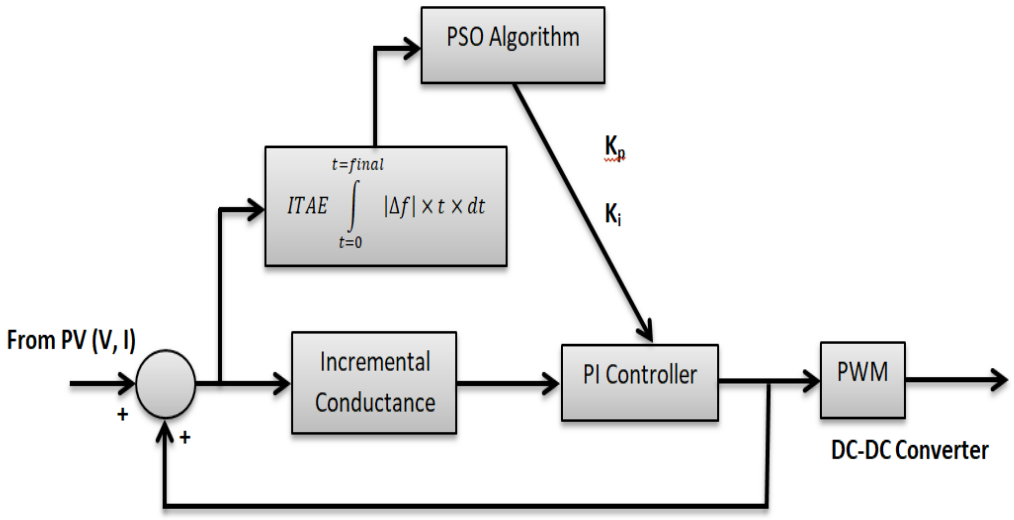


Figure IV. 4 PSO-Based Tuning of PI Controller

The PSO's implementation parameters are listed in Table IV.2 The PID controller's optimized sets are shown in Table IV. 1. Iterations are used because increasing the population size improves efficiency but hinders computation. The likelihood of a crossover depends on the transmission of behaviors to the following generation. New traits are introduced by the particles. In each iteration, it removes stagnation and diversifies the solution. The proposed MPPT control action's detailed flow is presented in Figure IV.3 & IV.4.

Table IV. 1 PSO parameters

PID Optimized Sets			Kp (10^3)	Ki (10^3)
N	MaxIter	noP		
a	10	10	0.90444484381990	0.861139671067111
b	25	25	1.213249730268556	0.890071348863087
c	75	50	1.021601660696307	0.995756944304465
d	100	100	1.075012629815895	1.050644185172168

Table IV. 2 Optimized sets of PI

Description	Value
U_b	[2000 1500]
l_b	[1000 1000]
wMax	1
wMin	0.1
c1 , c2	2

Following the implementing of PSO tuning for the PI parameters, the curves of the iteration on function of weight illustrate the optimization's performance in figures IV.5, providing validated values when the iteration is increased.

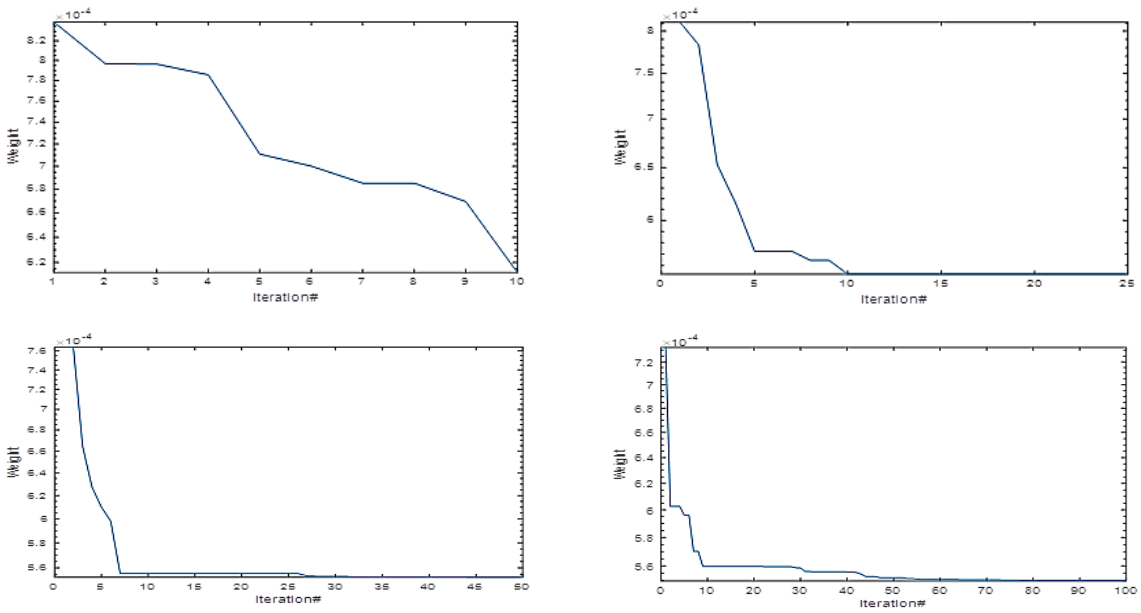


Figure IV. 5 Result of optimized sets of PI using different iterations

IV.3.3 Results and Discussion

The system under consideration is composed of a photovoltaic (PV) module and a BOOST converter, serving as the power interface. To enhance its performance, the system underwent optimization using the Particle Swarm Optimization (PSO) algorithm within the MATLAB/SIMPOWER environment. This optimization focused on implementing Maximum Power Point Tracking (MPPT) by utilizing the PV module's output voltage and current as inputs to the MPPT algorithm, thereby controlling the operation of the BOOST converter's switch.

Figure III.6 and III.7 illustrate the suggested variation in temperature and irradiation conditions.

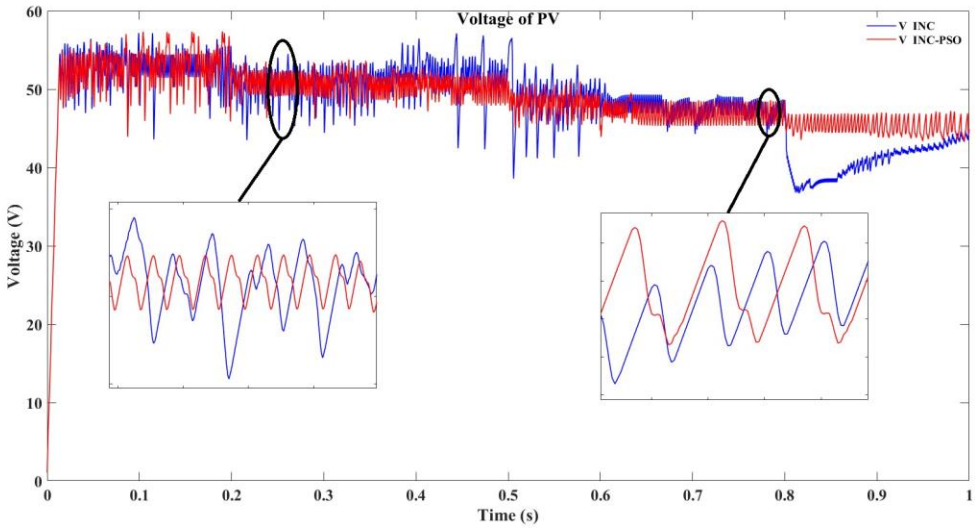


Figure IV. 6 Voltage of PV arrays by using the INC and PSO-INC

Due to the rapid variations in atmospheric conditions, the simulation outcomes of the PSO-INC control and INC exhibit distinct characteristics. The PSO-INC optimization, as illustrated in Figure IV.6, effectively responds and demonstrates the capability to maintain the voltage at a level close to the desired value. On the other hand, the INC approach achieves the desired voltage but with noticeable fluctuations, resulting in an unstable performance. Furthermore, the voltage drops below the desired threshold after 0.8 seconds.

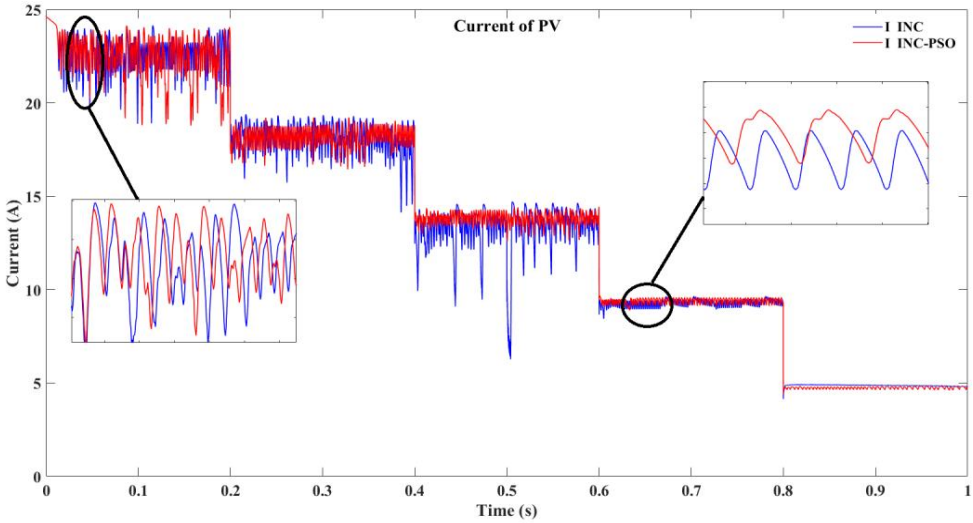


Figure IV. 7 Output current of PV

When the temperature increases and the irradiance decreases. In Figure IV.7 and IV.8, the current outputs of the PV array and the DC-DC converter are depicted. Both controllers

experience a decrease in current. However, the PSO-INC controller demonstrates a superior response with minimal disturbance compared to the INC controller

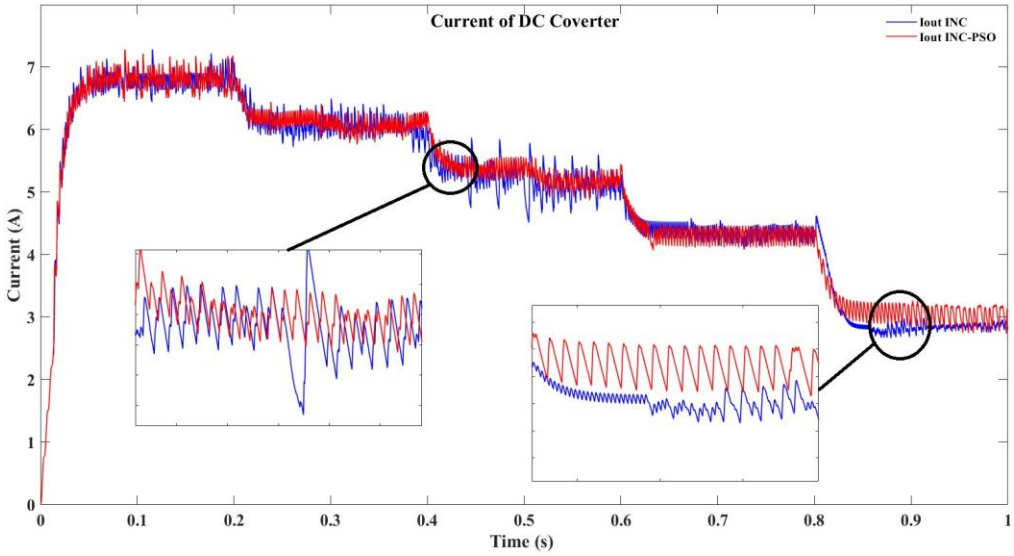


Figure IV. 8 The output current of the DC-DC converter

In order to achieve maximum power output from PV arrays and enhance the efficiency of energy transfer, this paper conducts simulation studies on PSO-INC and INC controllers. Figures IV.9 and IV.10 demonstrate that the PSO-INC controller exhibits precise tracking and stability even in the presence of changing climatic conditions. On the other hand, the INC controllers exhibit significant perturbations during climatic variations and around the maximum power point (MPP). Moreover, the INC controller struggles to meet the load requirements under low irradiation or high temperature conditions.

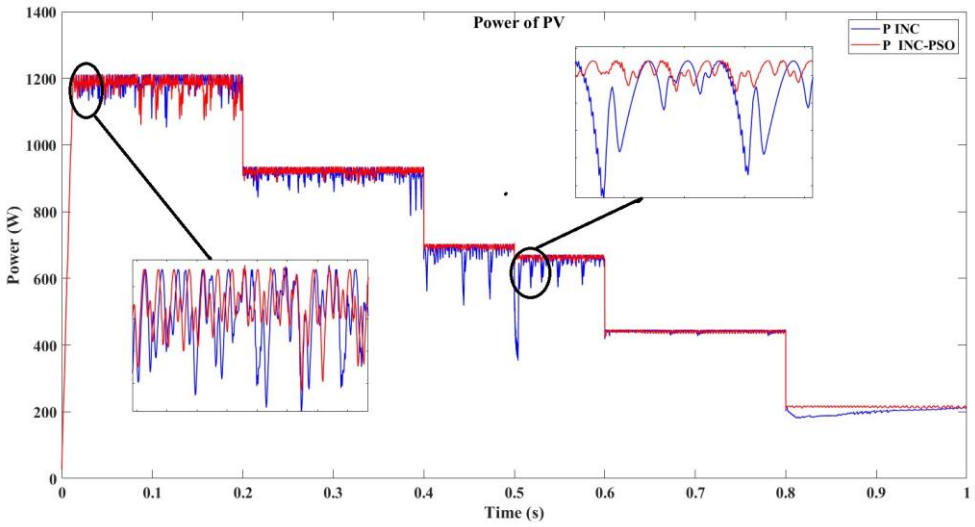


Figure IV. 9 Power of PV arrays by using the INC and PSO-INC

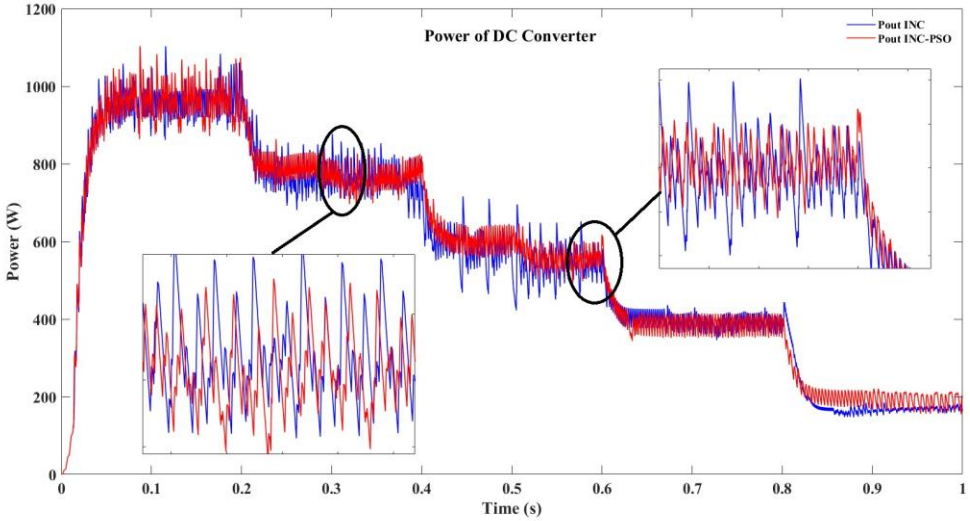


Figure IV. 10 Power of DC convertor by using the INC and PSO-INC

In this part, an enhanced MPPT approach is proposed for standalone PV systems, utilizing PSO to optimize the PI controller and incorporate variable step sizes from the INC method. The simulations and results validate the reliability, practicality, and validity of the proposed model. The presented study effectively addresses the comparisons between the INC and INC PSO methods under rapidly changing irradiance and temperature conditions. The performance of the proposed INC PSO MPPT controller demonstrates significant improvements. Based on the findings, it can be concluded that the suggested MPPT controller outperforms the conventional

INC method in terms of power tracking efficiency, faster response time, and reduced ripple effects.

IV.4 Optimization of Incremental Conductance by combination to Fuzzy Logic Control for MPPT of a Photovoltaic Stand-Alone System

Is an important area of research on which many scientists have focused, because it uses the methodology of human reasoning to solve problems without the need for mathematical modeling. In 1965 professor L.Zadeh [57] founded the theatrical bases of fuzzy logic.

The application of this theory to regulation did not take place until the 1970s [57]. In the field of electrical engineering, FLC has been a topic of several works, in the control of static converters and in the control of electrical machines, in the navigation of mobile robots, etc.

All these applications have demonstrated that a FLC is more robust than a conventional controller [58]. A fuzzy system has the following three blocks: Fuzzification, Rules of Interface, and Defuzzification. This system component, which is represented in figure IV.11 by way of illustration, is the structure of a fuzzy regulator with two inputs and one output, where E1 and E2 represent the input variables, and e that the output or the control.

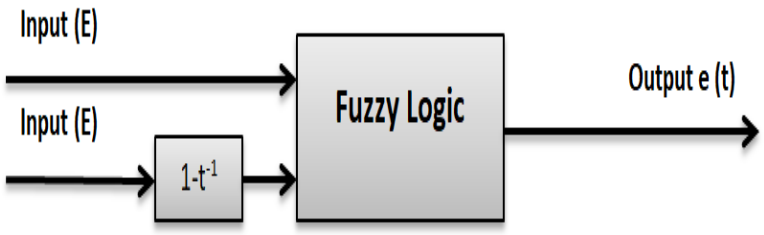


Figure IV. 11 Structure of Fuzzy Logic Control

IV.4.1 Fuzzification

By calculating the associated membership to all linguistic terms of fuzzy sets, the process of constructing crisp values fuzzy based on knowledge is carried out; the fuzzy ranks of these

linguistic concepts are ZE (Zero), NM (negative medium), and PS (positive small). The hazy collection of input and output variables is depicted in figures IV.12.

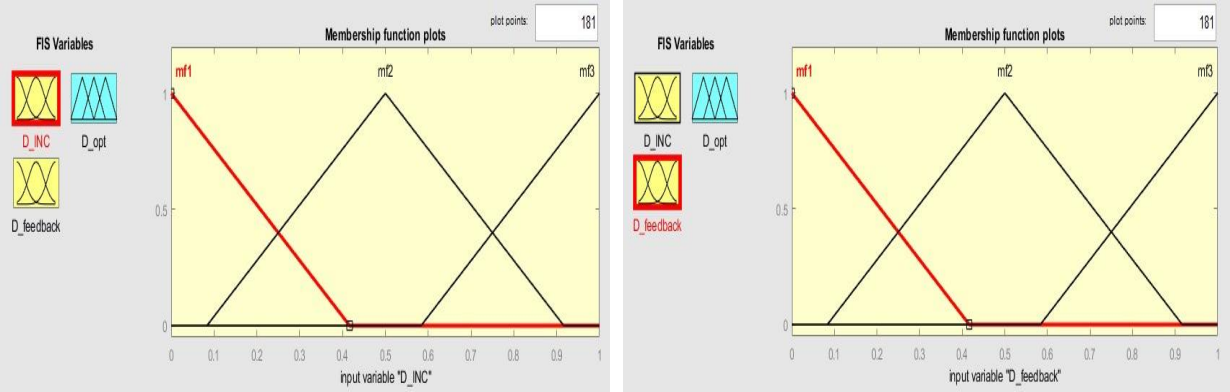


Figure IV. 12 MEs for input variables

IV.4.2 Rule base

If-then rules, which link the fuzzy output to the fuzzy input based on the operation's intelligence, serve as the rule base and assistance to the controller function satisfactorily. Table IV.3 shows the fuzzy subset of 16 rules using different MFs. By computing the firing strength of each rule according to the degree of match of the specified fuzzy sets through the "max, min" interface method, the fuzzy interface may be represented as mapping an input space to an output space [22].

Table IV. 3 FLC rule based

D_INC D_feedback	MF1	MF2	MF3
MF1	MF2	MF1	MF3
MF2	MF2	MF3	MF2
MF3	MF3	MF3	MF1

NB: MF1 is ZE, MF2 is PM, and MF3 is PS

IV.4.3 Defuzzification

Here, we must perform the inverse operation of fuzzification from a fuzzy definition; we must also calculate a numerical number that is understandable by the outside world [78].

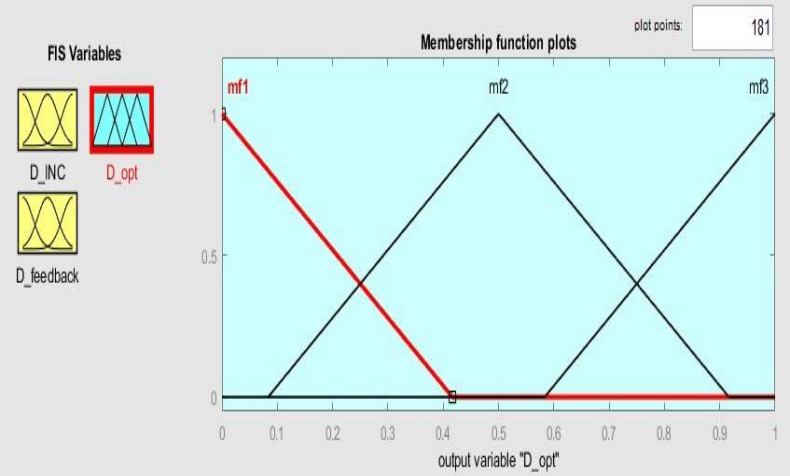


Figure IV. 13 MEs for output variable

IV.4.4 INC-FLC Controller

In the proposed optimization, the FLC is combined into INC, taking the FLC to treat the duty signal of output INC in the first input and taking the feedback of output FLC in the second input, as shown in figure IV.14.

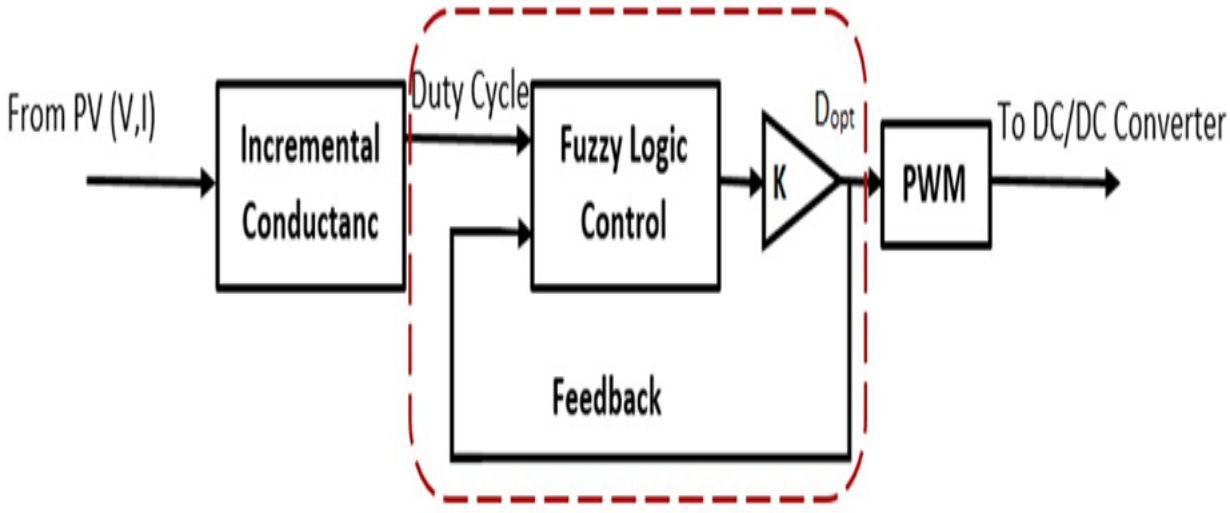


Figure IV. 14 The proposed optimization of INC-FLC

The input to FLC can be expressed as follows, including the error and feedback of duty cycle signal:

$$E(K) = |D_INC(K) - D_INC(K-1)| \qquad IV.\ 6$$

$$\Delta E(K) = D_{feedback}(K) - D_{feedback}(K-1) \qquad IV.7$$

E(K) is the error of the result of INC output, and the ΔE is the error of feedback treated and returned from FLC output to FLC input, as appears in figure IV.15.

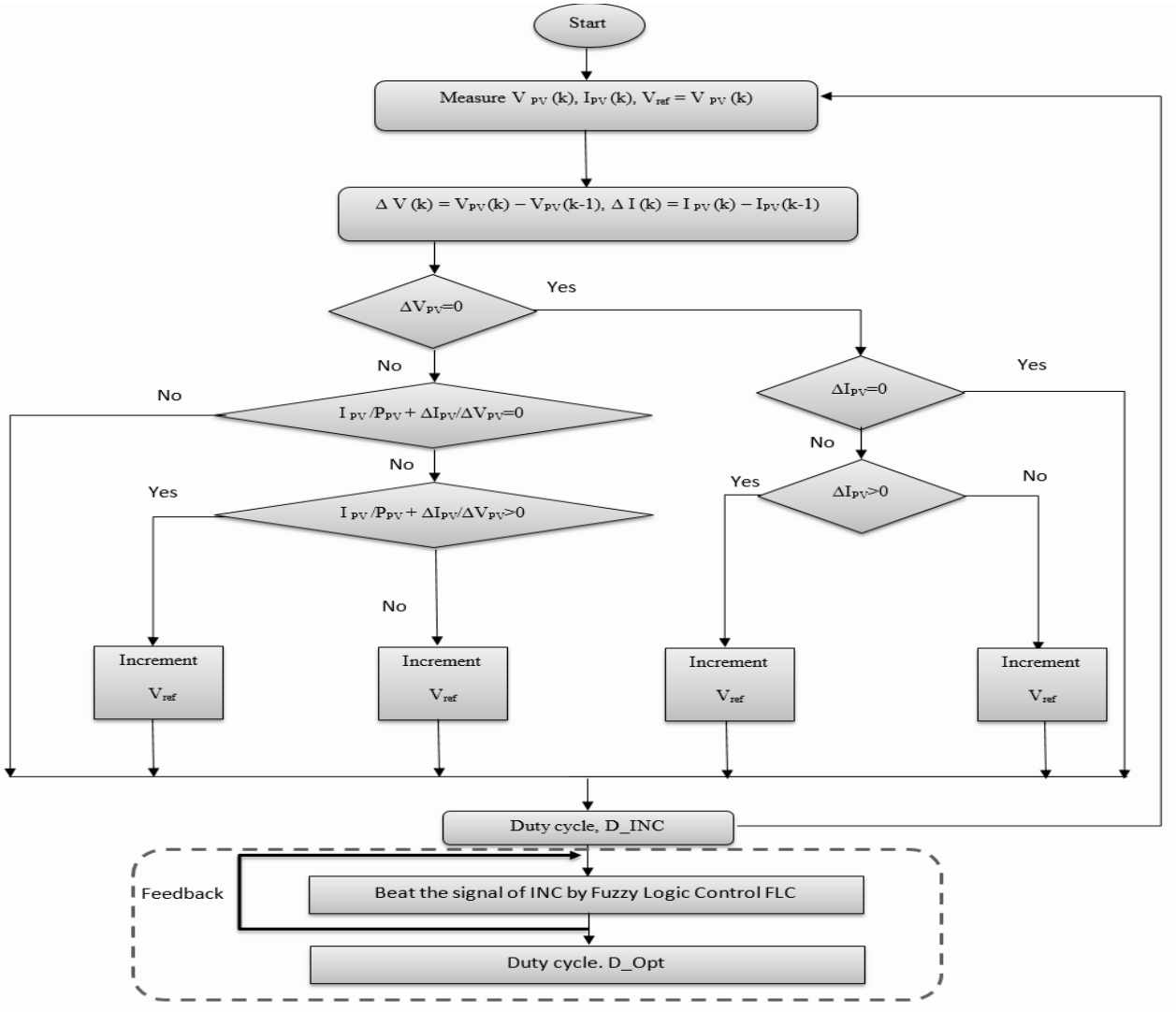


Figure IV. 15 Flowchart to the proposed combination of INC-FLC

IV.4.5 Result and Discussion

As in the first comparative simulation, we apply the same system with different methods. The optimization of the INC was compared with traditional. The use of fuzzy logic to amend and adjust the signal to get better results was successful.

Firstly, we show the choice of temperature and irradiation. Afterthought we appear in the result and explain that:

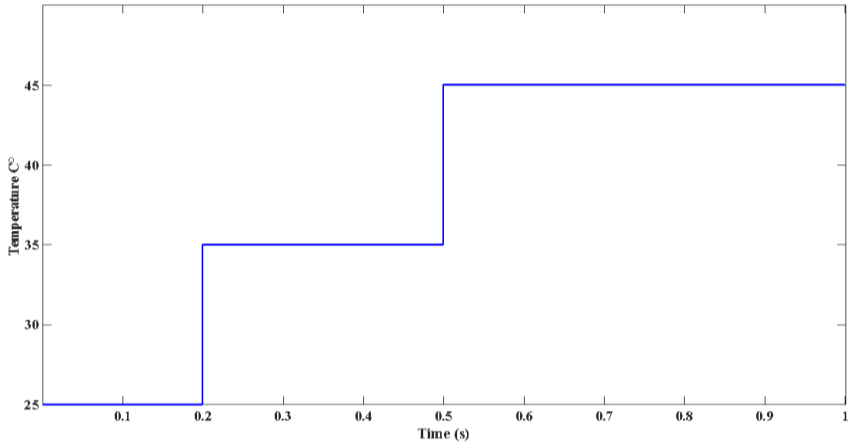


Figure IV. 16 Variation of temperature

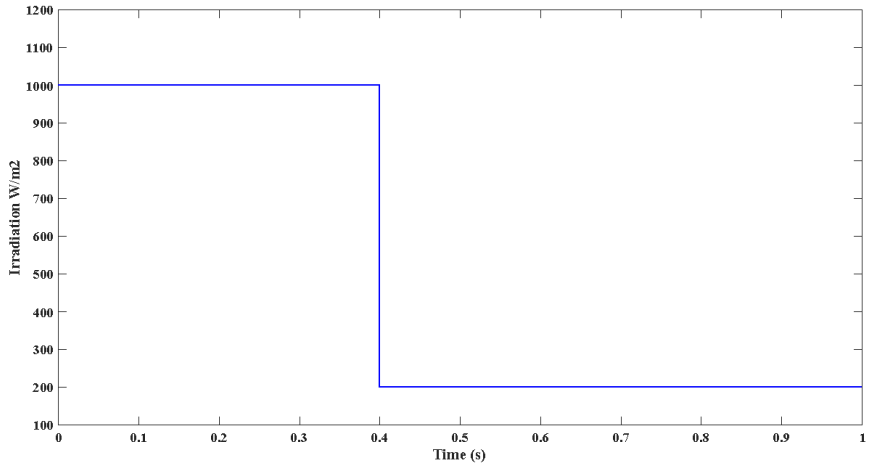


Figure IV. 17 Variation of Irradiation

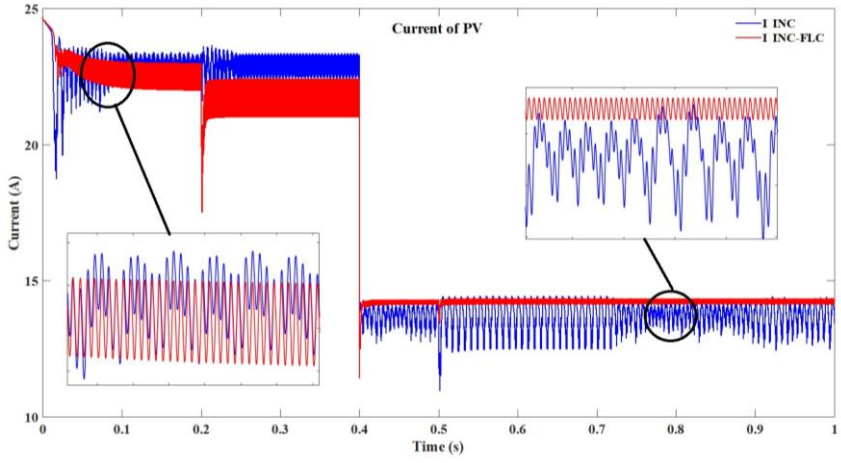


Figure IV. 18 Current of PV arrays by using the INC and INC-FLC

When the temperature increases and the irradiance diminish it will appear as follows. In Figure IV.18, the current outputs of the PV array are depicted. Both controllers experience a decrease in current. However, the INC-FLC controller demonstrates a superior response with minimal disturbance compared to the INC controller

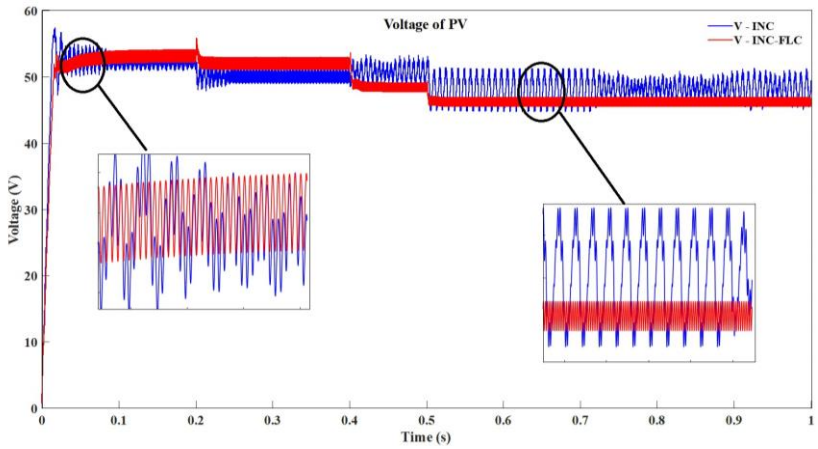


Figure IV. 19 Voltage of PV arrays by using the INC and INC-FLC

The INC-FLC control and INC simulation outcomes have unique characteristics due to the rapid variations in atmospheric conditions. Figure IV.19 illustrates the INC-FLC optimization's ability to effectively respond and demonstrate the ability to maintain the voltage at a level close to the desired value. The INC approach results in unstable performance due to more perturbation.

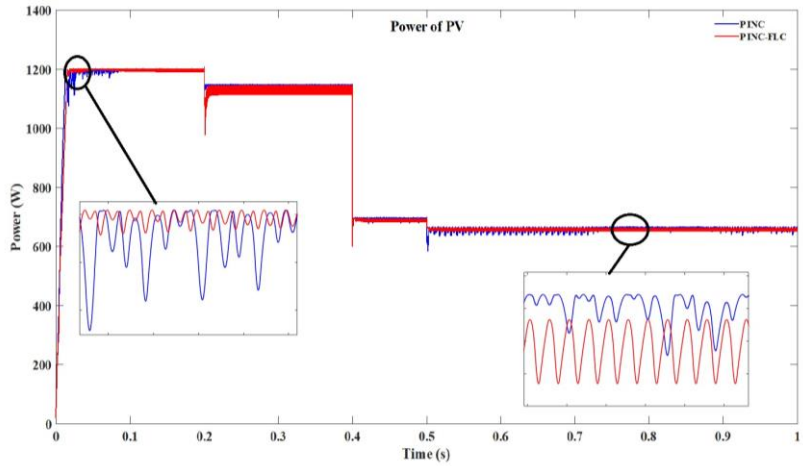


Figure IV. 20 Power of PV arrays by using the INC and INC-FLC

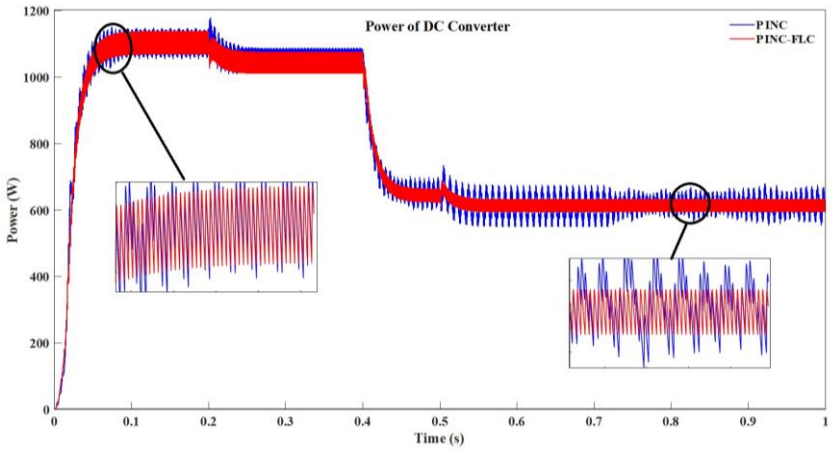


Figure IV. 21 Power of output DC convertor by using the INC and INC-FLC

When the temperature increases and the irradiance decreases. In Figures IV.20 and IV.21, the current outputs of the DC-DC converter are depicted. Both controllers experience a decrease in current. However, the INC-FLC controller demonstrates a superior response with minimal perturbation compared to the INC controller.

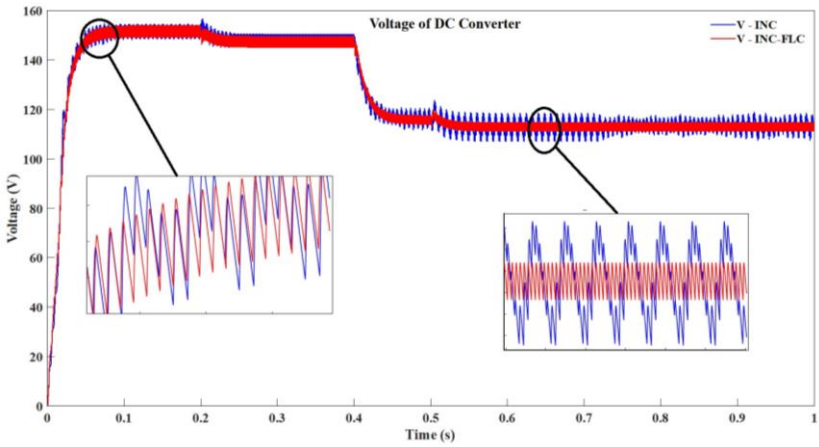


Figure IV. 22 Voltage of output DC convertor by using the INC and INC-FLC

Figure IV.22 illustrates the INC-FLC optimization's ability to effectively respond and demonstrate the ability to maintain the voltage at a level close to the value looked-for. The INC approach results in unstable performance due to more perturbation.

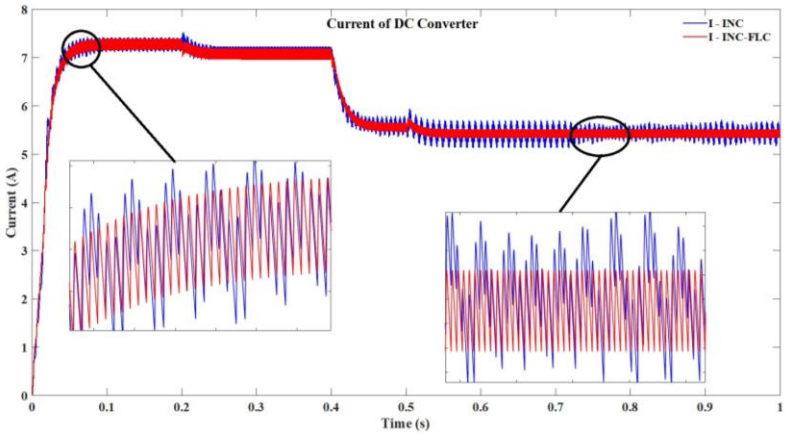


Figure IV. 23 Current of output DC convertor by using the INC and INC-FLC

When the temperature increases and the irradiance decreases it will present as follows. In Figure IV.23, the current of the DC Converter is shown. Both controllers experience a decrease in current. However, the INC-FLC controller demonstrates a good response with negligible disturbance compared to the INC controller.

IV.5 Conclusion

This section proposed an improved MPPT approach for standalone PV systems, which uses the PSO to select the best parameters to the PI controller and incorporates variable step sizes from the INC method. Additionally, we utilize the FL to enhance the INC method in order to maximize maximal power. Thus, the optimization methods appear a reliable tracker and provide quick response with less perturbation.

The simulation results indicate that the optimize method is better in the stand-alone PV array system. Moreover, it performs significantly better under high environmental conditions compared to conventional INC in terms of overshoot, ripple, speed, and accuracy. Furthermore, the proposal optimization efficiently enhances dynamic responsiveness. The simulation demonstrates the precise tracking of the proposed techniques.

V General conclusion

This work involves developing MPPT controllers that have two controls or one to enhance the classic Incremental Conductance INC and guarantee that the maximum power of the photovoltaic generator is reached regardless of environmental conditions. The purpose of these methods is to address the shortcoming of the classic INC method, including oscillations around MPP, imperfect MPPT, and slow follow-up of MPP…..ECT. The use of an INC algorithm alone to fix the ratio that does not disturb causes these disadvantages, especially when there are changes in weather conditions (temperature and irradiation) and with variable loads. To provide the reference voltage, power, the INC algorithm is utilized during the first phase and compared to Sliding Mode Control SMC, which proposed that approach at first. And the second is a nonlinear controller using PSO algorithm to compute the parameters of PI that installed into the INC for optimization, afterthought compared to the classic method as reference. Then combined the Fuzzy logic into INC in terms of optimization. Therefore, the proposed Sliding Mode, PSO-INC, and FLC-INC techniques were proven better than the conventional INC algorithm that scenario simulation results using the MatLab/ Simulink. In addition, the data sheet information of "**KC200GT**" is well matched by the modeling of the PV module using a simplified one-diode model.

The world's energy demand is changing rapidly today, but natural resources are decreasing due to demographic and industrial development. To solve this problem, the researchers focused on utilizing renewable energy sources. These include solar energy, which is found in most places of the world. However, its operation hindered by the high cost of solar cells, low efficiency, and intermittent power due to variation of weather conditions in certain regions. When designing a photovoltaic system, it is important to consider these problems.

We started in the first chapter with an overview of the various technologies used to produce electricity using renewable energies worldwide, and in Algeria in this context. Then we presented the evolution of solar photovoltaic energy, the renewable energy program in the world

and Algeria. Moreover, we went directly to explain the convert from sun to photocells and the component of it.

For the photovoltaic system to operate at its maximum power, it must have a good adaptation associated with an MPPT Algorithm, the main types of the systems presented in the literature and explain the advantages and disadvantages of each one in Chapter II, where the stand-alone system is clearly superior and its appeared less cost, can meet the consumption power, and easy to associate to the control.

The topic of chapter III was variable methods of MPPT controls, which were suggested in literature to solve the issues of fixed methods MPPT controls, like oscillations around MPP and slower response. The proposed technique, sliding mode control, is presented in the last section, which is comparable to INC when the SMC appeared with improved oscillations and response.

In chapter IV, an optimization of incremental conductance MPPT controller was proposed to address the well-known drawbacks of the conventional INC MPPT controller. These disadvantages include imperfect control of the MPP and oscillations around MPP. The first stage of the proposed optimization of the MPPT, which is based on INC, using the PSO algorithm optimization to provide a better duty cycle. And the second optimization of the INC via integrating the fuzzy logic, to ensure the stability and avoid the mentioned disadvantages. The simulation results using the MATLAB/Simulink showed that the proposed they both optimize incremental conductance techniques are better to the conventional INC, so that demonstrated by simulation results in all scenarios.

We contributed the MPPT controller in an autonomous PV system. Namely, SMC, PSO-INC, And INC-FLC each used the conventional INC as reference to confirm the performance. The simulation results demonstrate that this technique adheres to the MPP with a significant decrease in oscillations and has a high efficiency of up to 98.55%.

The results obtained in different scenarios reveal that these techniques are more efficient than SMC and the conventional INC that integrator to PSO or FL. Based in terms of efficiency, tracking speed, transient oscillation and steady-state performance. The MPP could be tracked by

the techniques proposed here, even if there were sudden changes in irradiation, temperature. These techniques are also characterized by its simplicity of implementation in the MPPT control.

These approaches are proven useful techniques for maximizing PV output power system based on different uniform weather condition

References Bibliographies:

[1] M. B. Shadmand, R. S. Balog, and H. Abu-Rub, “Model predictive control of PV sources in a smart DC distribution system: Maximum power point tracking and droop control,” *IEEE Trans. Energy Convers.*, vol. 29, no. 4, pp. 913–921, 2014.

[2] S. Maity and P. K. Sahu, “Modeling and analysis of a fast and robust module-integrated analog photovoltaic MPP tracker,” *IEEE Trans. Power Electron.*, vol. 31, no. 1, pp. 280–291, 2015.

[3] H. Islam *et al.*, “Performance evaluation of maximum power point tracking approaches and photovoltaic systems,” *Energies*, vol. 11, no. 2, p. 365, 2018.

[4] A. R. Reisi, M. H. Moradi, and S. Jamasb, “Classification and comparison of maximum power point tracking techniques for photovoltaic system: A review,” *Renew. Sustain. energy Rev.*, vol. 19, pp. 433–443, 2013.

[5] M. Ahmed, M. Abdelrahem, R. Kennel, and C. M. Hackl, “Maximum power point tracking based model predictive control and extended kalman filter using single voltage sensor for pv systems,” in *2020 IEEE 29th International Symposium on Industrial Electronics (ISIE)*, IEEE, 2020, pp. 1039–1044.

[6] O. K. Ahmed Hassen, *مباديء الطاقات المتجددة*. Hawija: Northern Technical University Iraq, 2010. [Online]. Available: https://www.researchgate.net/publication/315829748_mbady_altaqat_almtjddt

[7] “Renewables 2022 – Analysis - IEANo Title,” 2022. https://www.iea.org/reports/renewable-electricit (accessed Nov. 23, 2022).

[8] “Global Electricity Review 2022,” 2022. https://ember-climate.org/insights/research/global-electricity-review-2022/ (accessed Feb. 10, 2023).

[9] “Statistical Review of World Energy,” 2022. https://www.bp.com/en/global/corporate/energy-economics/statistical-review-of-world-energy.html (accessed Dec. 01, 2022).

[10] “Renewable electricity,” 2021. https://www.iea.org/reports/renewables-2021/renewable-electricity?mode=market&region=World&publication=2021&product=Total (accessed Dec. 01, 2022).

[11] K. Kaced and C. Larbes, “Study of MPPT techniques for photovoltaic systems under partial shading conditions,” Alger, Ecole Nationale Polytechnique, 2018. [Online]. Available: http://repository.enp.edu.dz/xmlui/handle/123456789/2199

[12] “Algeria Electricity Production,” *SONELGAZ*. https://www.ceicdata.com/en/indicator/algeria/electricity-production

[13] F. Sahnoune, K. Imessad, and D. M. Bouakaz, “Energy consumption renewable energy development and environmental impact in Algeria-Trend for 2030,” in *AIP conference proceedings*, AIP Publishing, 2017.

[14] “Algeria Powers Ahead with Huge Renewable Energy Plans,” 2021. https://www.ief.org/news/algeria-powers-ahead-with-huge-renewable-energy-plans (accessed

Dec. 01, 2022).

[15] "ENERGIES NOUVELLES ET RENOUVELABLES." https://www.energy.gov.dz/?rubrique=energies-nouvelles-renouvelables-et-maitrise-de-lrenergie

[16] Salim Abouda, "Contribution à la commande des systèmes photovoltaiques : application aux systèmes de pompages.," 2015. [Online]. Available: https://www.theses.fr/2015REIMS005

[17] "Reference Air Mass 1.5 Spectra," 2003.

[18] K. Djeriouat, "Optimisation Du Rendement Des Cellules Photovoltaiques À Heterojonctions Gainp/gaas," Université Abou Bekr Belkaid - Tlemcen, 2011. [Online]. Available: https://theses-algerie.com/1484651103986599/memoire-de-magister/universite-abou-bekr-belkaid---tlemcen/optimisation-du-rendement-des-cellules-photovoltaiques-à-heterojonctions-gainp-gaas

[19] "DE LA LUMIÈRE À L'ÉLECTRICITÉ." https://www.photovoltaique.info/fr/info-ou-intox/lenergie-solaire/de-la-lumiere-a-lelectricite/

[20] A. Einstein, "The Father of Solar Cells," 1933. https://www.greenmatch.co.uk/blog/2017/05/albert-einstein-father-of-solar-cells (accessed Oct. 27, 2023).

[21] M. Planck, "loi du rayonnement et l'idée de la quantité indivisible fondamentale d'énergie rayonnante appelée le quantum," 1927.

[22] H. N. Kadeval and V. K. Patel, "Mathematical modelling for solar cell, panel and array for photovoltaic system," *J. Appl. Nat. Sci.*, vol. 13, no. 3, pp. 937–943, 2021.

[23] Y. Cui, L. Hong, and J. Hou, "Organic photovoltaic cells for indoor applications: opportunities and challenges," *ACS Appl. Mater. Interfaces*, vol. 12, no. 35, pp. 38815–38828, 2020.

[24] R. A. Hmouda, Y. S. Muzychka, and X. Duan, "Experimental and Theoretical Modelling of Concentrating Photovoltaic Thermal System with Ge-Based Multi-Junction Solar Cells," *Energies*, vol. 15, no. 11, p. 4056, 2022.

[25] B. Salhi, "The photovoltaic cell based on CIGS: principles and technologies," *Materials (Basel).*, vol. 15, no. 5, p. 1908, 2022.

[26] W. Wang, A. C.-F. Liu, H. S.-H. Chung, R. W.-H. Lau, J. Zhang, and A. W.-L. Lo, "Fault diagnosis of photovoltaic panels using dynamic current–voltage characteristics," *IEEE Trans. Power Electron.*, vol. 31, no. 2, pp. 1588–1599, 2015.

[27] M. R. M. R. M. Boudia, "Modélisation électro-optique et optimisation des cellules solaires organiques.," 2016. [Online]. Available: https://www.semanticscholar.org/paper/Modélisation-électro-optique-et-optimisation-des-Boudia-Réda/c10137c8e03d724281b63e7b270d394e01e15d7e

[28] A. Feroz Mirza, M. Mansoor, Q. Ling, M. I. Khan, and O. M. Aldossary, "Advanced variable step size incremental conductance MPPT for a standalone PV system utilizing a GA-tuned PID controller," *Energies*, vol. 13, no. 16, p. 4153, 2020.

[29] Stéphane Petibon, “Nouvelles architectures distribuées de gestion et conversion de l’énergie pour les applications photovoltaïques,” Université Paul Sabatier, 2009. [Online]. Available: https://theses.hal.science/tel-00377788v1

[30] A. Lashab, D. Sera, J. M. Guerrero, L. Mathe, and A. Bouzid, “Discrete model-predictive-control-based maximum power point tracking for PV systems: Overview and evaluation,” *IEEE Trans. Power Electron.*, vol. 33, no. 8, pp. 7273–7287, 2017.

[31] TOUALBIA Asma, “Commande MPPT avancée d’un système de conversion d’énergie solaire,” Ecole Nationale Polytechnique - Alger, 2018.

[32] A. M. Othman, M. M. M. El-arini, A. Ghitas, and A. Fathy, “Realworld maximum power point tracking simulation of PV system based on Fuzzy Logic control,” *NRIAG J. Astron. Geophys.*, vol. 1, no. 2, pp. 186–194, 2012.

[33] N. H. Saad, A. A. El-Sattar, and A. E.-A. M. Mansour, “Improved particle swarm optimization for photovoltaic system connected to the grid with low voltage ride through capability,” *Renew. Energy*, vol. 85, pp. 181–194, 2016.

[34] A. Sheikholeslami, “Buck and Boost Converters [Circuit Intuitions],” *IEEE Solid-State Circuits Mag.*, vol. 13, no. 4, pp. 12–14, 2021.

[35] T. Bhattacharjee, M. Jamil, and A. Jana, “Designing a controller circuit for three phase inverter in PV application,” in *2018 International Conference on Electrical, Electronics, Communication, Computer, and Optimization Techniques (ICEECCOT)*, IEEE, 2018, pp. 882–886.

[36] M. Liang and T. Q. Zheng, “Synchronous PI control for three-phase grid-connected photovoltaic inverter,” in *2010 Chinese Control and Decision Conference*, IEEE, 2010, pp. 2302–2307.

[37] M. Zelba *et al.*, “A grid-tied inverter with renewable energy source integration in an off-grid system with a functional experimental prototype,” *Sustainability*, vol. 14, no. 20, p. 13110, 2022.

[38] I. Jamal, M. F. Elmorshedy, S. M. Dabour, E. M. Rashad, W. Xu, and D. J. Almakhles, “A comprehensive review of grid-connected PV systems based on impedance source inverter,” *IEEE Access*, vol. 10, pp. 89101–89123, 2022.

[39] P. C. Loh, D. M. Vilathgamuwa, C. J. Gajanayake, Y. R. Lim, and C. W. Teo, “Transient modeling and analysis of pulse-width modulated Z-source inverter,” *IEEE Trans. Power Electron.*, vol. 22, no. 2, pp. 498–507, 2007.

[40] J.-F. REYNAUD, “Recherches d’optimums d’énergie pour charge/décharge d’une batterie à technologie avancée dédiée à des applications photovoltaïques,” UNIVERSITE DE TOULOUSE, 2011. [Online]. Available: https://theses.hal.science/tel-00559630/document

[41] M. Abdel-Salam, M.-T. EL-Mohandes, and M. Goda, “History of Maximum Power Point Tracking,” *Mod. Maximum Power Point Track. Tech. Photovolt. Energy Syst.*, pp. 1–29, 2020.

[42] H. Abbes, H. Abid, K. Loukil, A. Toumi, and M. Abid, “Etude comparative de cinq algorithmes de commande MPPT pour un système photovoltaïque,” *J. Renew. Energies*, vol. 17, no. 3, pp. 435–445, 2014.

[43] M. Hammami and M. Hammami, “Improvement of RCC-MPPT in Case of Multiple DC-Link Voltage Harmonics,” *Lev. Doubling Netw. Ripple Correl. Control MPPT Algorithm Grid-Connected Photovolt. Syst.*, pp. 89–109, 2019.

[44] L. Zaghba, M. Khennane, A. Borni, and A. Fezzani, “Intelligent PSO-Fuzzy MPPT approach for Stand Alone PV System under Real Outdoor Weather Conditions,” *Alger. J. Renew. Energy Sustain. Dev*, vol. 3, pp. 1–12, 2021.

[45] M. Dehghani, M. Taghipour, G. B. Gharehpetian, and M. Abedi, “Optimized fuzzy controller for MPPT of grid-connected PV systems in rapidly changing atmospheric conditions,” *J. Mod. Power Syst. Clean Energy*, vol. 9, no. 2, pp. 376–383, 2020.

[46] D. B. B. S. BELHOUT and M. BOUCHAREB, “Optimisation énergétique de chaine de conversion d’énergie photovoltaïque,” UNIVERSITE MOHAMED BOUDIAF - M’SILA, 2021. [Online]. Available: http://dspace.univ-msila.dz:8080/xmlui/bitstream/handle/123456789/25472/161635095696.161635100090.pdf?sequence=1&isAllowed=y

[47] A. Eltamaly, “Performance of smart maximum power point tracker under partial shading conditions of photovoltaic systems,” *J. Renew. Sustain. Energy*, vol. 7, no. 4, 2015.

[48] H. Rezk and A. M. Eltamaly, “A comprehensive comparison of different MPPT techniques for photovoltaic systems,” *Sol. energy*, vol. 112, pp. 1–11, 2015.

[49] S. Lyden and M. E. Haque, “Maximum Power Point Tracking techniques for photovoltaic systems: A comprehensive review and comparative analysis,” *Renew. Sustain. energy Rev.*, vol. 52, pp. 1504–1518, 2015.

[50] A. M. Eltamaly, “Performance of MPPT techniques of photovoltaic systems under normal and partial shading conditions,” in *Advances in renewable energies and power technologies*, Elsevier, 2018, pp. 115–161.

[51] S. A. Mohamed and M. Abd El Sattar, “A comparative study of P&O and INC maximum power point tracking techniques for grid-connected PV systems,” *SN Appl. Sci.*, vol. 1, no. 2, p. 174, 2019.

[52] Ali GHELAM, “Non Linear Real Time Control of a Photovoltaic Conversion System,” Université Ziane Achour de Djelfa, 2020. [Online]. Available: http://dspace.univ-djelfa.dz:8080/xmlui/handle/123456789/3432

[53] Z. A. H. Al-Jawary, “Study and evaluation of distributed power electronic converters in photovoltaic generation applications,” 2022.

[54] A. Raj, S. R. Arya, and J. Gupta, “Solar PV array-based DC–DC converter with MPPT for low power applications,” *Renew. Energy Focus*, vol. 34, pp. 109–119, 2020.

[55] M. Lasheen, A. K. Abdel Rahman, M. Abdel-Salam, and S. Ookawara, “Adaptive reference voltage-based MPPT technique for PV applications,” *IET Renew. Power Gener.*, vol. 11, no. 5, pp. 715–722, 2017.

[56] T. Logeswaran and A. SenthilKumar, “A review of maximum power point tracking algorithms for

photovoltaic systems under uniform and non-uniform irradiances," *Energy Procedia*, vol. 54, pp. 228–235, 2014.

[57] J. A. Goguen, "LA Zadeh. Fuzzy sets. Information and control, vol. 8 (1965), pp. 338–353.-LA Zadeh. Similarity relations and fuzzy orderings. Information sciences, vol. 3 (1971), pp. 177–200.," *J. Symb. Log.*, vol. 38, no. 4, pp. 656–657, 1973.

[58] V. R. Kota and M. N. Bhukya, "A novel linear tangents based P&O scheme for MPPT of a PV system," *Renew. Sustain. Energy Rev.*, vol. 71, pp. 257–267, 2017.

[59] M. E. BAŞOĞLU, "An approximate short circuit strategy for transient MPPT performance of uniformly irradiated photovoltaic modules," *Balk. J. Electr. Comput. Eng.*, vol. 7, no. 1, pp. 88–93, 2019.

[60] T. R. Nath, "Solar Photovoltaic Power Generating System & Grid Integration-Modeling, Controller Design and Optimization," 2017.

[61] M. M. Rahman and M. S. Islam, "PSO and ANN based hybrid MPPT algorithm for photovoltaic array under partial shading condition," *Eng. Int*, vol. 8, no. 1, pp. 9–24, 2020.

[62] W. S. McCulloch and W. Pitts, "A logical calculus of the ideas immanent in nervous activity," *Bull. Math. Biophys.*, vol. 5, pp. 115–133, 1943.

[63] T. Obeidi, "Application des algorithmes génétiques dans la commande des hacheurs MPPT." Alger, Ecole Nationale Polytechnique, 2006.

[64] D. E. Goldberg, "Genetic algorithms in search, optimization and machine learning Addison Welssey Publishing company," *Reading, MA*, 1989.

[65] D. E. Goldberg, "Cenetic Algorithms in Search," *Optim. Mach. Learn.*, 1989.

[66] M. Birane, "Contribution à l'étude et à l'optimisation des chaines de conversion photovoltaïque." Université Amar Telidji de Laghouat, Département Electrique, 2017.

[67] S. D. Al-Majidi, M. F. Abbod, and H. S. Al-Raweshidy, "Design of an intelligent MPPT based on ANN using a real photovoltaic system data," in *2019 54th International Universities Power Engineering Conference (UPEC)*, IEEE, 2019, pp. 1–6.

[68] A. T. Azar and Q. Zhu, *Advances and applications in sliding mode control systems*. Springer, 2015.

[69] H. Mekki, D. Boukhetala, and A. T. Azar, "Sliding modes for fault tolerant control," in *Advances and applications in sliding mode control systems*, Springer, 2014, pp. 407–433.

[70] B. Tahar, M. Djillali, and H. Khaled, "Maximum Power Point Tracking under simplified sliding mode control based DC-DC boost converters.," *Prz. Elektrotechniczny*, vol. 97, no. 7, 2021.

[71] K. Nuortimo, J. Härkönen, and E. Karvonen, "Exploring the global media image of solar power," *Renew. Sustain. Energy Rev.*, vol. 81, pp. 2806–2811, 2018.

[72] A. El Hammoumi, S. Chtita, S. Motahhir, and A. El Ghzizal, "Solar PV energy: From material to use, and the most commonly used techniques to maximize the power output of PV systems: A focus on solar trackers and floating solar panels," *Energy Reports*, vol. 8, pp. 11992–12010, 2022.

[73] N. E. Zakzouk, M. A. Elsaharty, A. K. Abdelsalam, A. A. Helal, and B. W. Williams, “Improved performance low-cost incremental conductance PV MPPT technique,” *IET Renew. Power Gener.*, vol. 10, no. 4, pp. 561–574, 2016.

[74] T. Bouadjila, K. Khelil, D. Rahem, and F. Berrezzek, “Improved Artificial Neural Network Based MPPT Tracker for PV System under Rapid Varying Atmospheric Conditions,” *Period. Polytech. Electr. Eng. Comput. Sci.*, vol. 67, no. 2, pp. 149–159, 2023.

[75] V. K. Bhagat, K. Paul, R. Dutta, P. Sinha, and M. K. Debnath, “Performance Analysis of FLC & ANN Based MPPT Controller For Solar PV System,” in *2022 2nd Odisha International Conference on Electrical Power Engineering, Communication and Computing Technology (ODICON)*, IEEE, 2022, pp. 1–6.

[76] A. K. Podder, N. K. Roy, and H. R. Pota, “MPPT methods for solar PV systems: a critical review based on tracking nature,” *IET Renew. Power Gener.*, vol. 13, no. 10, pp. 1615–1632, 2019.

[77] R. Eberhart, “James. kennedy, particle swarm optimization,” in *Proceedings of the IEEE international conference on neural networks, Australia*, 1942.

[78] R. B. A. Koad, A. F. Zobaa, and A. El-Shahat, “A novel MPPT algorithm based on particle swarm optimization for photovoltaic systems,” *IEEE Trans. Sustain. Energy*, vol. 8, no. 2, pp. 468–476, 2016.

[79] O. F. Aje and A. A. Josephat, “The particle swarm optimization (PSO) algorithm application–A review,” *Glob. J. Eng. Technol. Adv.*, vol. 3, no. 3, pp. 1–6, 2020.

[80] M. Ez-Zghari, S. Chtita, N. El Youssfi, T. Zarrouk, K. El Khadiri, and A. Tahiri, “Optimized Energy Output from a PV System Using a Modified Incremental Conductance Algorithm for Rapidly Changing Insolation,” in *International Conference on Digital Technologies and Applications*, Springer, 2022, pp. 649–658.

[81] Y. Oubail, M. Boulakhbar, I. Aboudrar, M. R. Elmoutawakil Alaoui, and L. Elmahni, “Renewable energy sources integration in a microgrid control system: overview and perspective,” in *International Conference on Digital Technologies and Applications*, Springer, 2022, pp. 552–561.

[82] A. J. Attiya, Y. Wenyu, and S. W. Shneen, “Compared with PI, Fuzzy-PI and PSO-PI controllers of robotic grinding force servo system,” *TELKOMNIKA Indones. J. Electr. Eng.*, vol. 16, no. 1, pp. 65–74, 2015.